DEVELOPMENT OF COCRYSTALS OF WATER INSOLUBLE ACTIVE SUBSTANCES WITH INACTIVE EXCIPIENTS BY USING HOT MELT EXTRUSION

HIREN G. MORADIYA [B.Sc. (Hons)]

A thesis submitted in partial fulfilment of the requirements of the University of Greenwich for the Degree of Doctor of Philosophy

NOVEMBER, 2014

UNIVERSITY
of
GREENWICH

I

DECLARATION

"I certify that this work has not been accepted in substance for any degree, and is not concurrently being submitted for any degree other than that of Doctor of Philosophy being studied at the University of Greenwich. I also declare that this work is the result of my own investigations except where otherwise identified by references and that I have not plagiarised the work of others".

Hiren G. Moradiya (Candidate)

……………………………………………………………………………………………………

<u>PhD Supervisors</u>

Dr Dionysios Douroumis

Prof. Babur Z. Chowdhry

Date:

ACKNOWLEDGEMENTS

This thesis becomes a reality with the kind support and help of many individuals. I would like to extend my sincere thanks to all of them.

Foremost, I want to offer this endeavour to GOD almighty for the wisdom he bestowed upon me, the strength, peace of my mind and good health in order to carry out this research.

My deepest appreciation goes to principal advisor Dr Dionysios Douroumis for imparting his knowledge and expertise in this study as well as constant guidance, positive supports and providing necessary information regarding this research. The encouragement and supportive comments of my second supervisor, Prof. Babur Z. Chowdhry, has been invaluable on both an academic and a personal level, for which I am extremely grateful.

I would also like to acknowledge Dr Ian Slipper for all of his assistance in XRPD, Rietveld calculations and SEM analysis and Mrs Devyani Amin for her help with the HPLC experiments. I owe sincere and earnest thankfulness to all my colleagues and friends who have extended their support in a very special way for their suggestions at various points of my research programme.

I owe my deepest gratitude to my parents, elder brother, sister in-law and nephew, for their love and sacrifice to support me, without their encouragement it would not have been possible.

ABSTRACT

The major aim of the research reported herein was to develop and optimise hot melt extrusion (HME) as a robust technique for the cocrystallisation of poorly water soluble drugs and their coformers. Two pairs of cocrystals of a poorly water soluble drug, carbamazepine, with saccharin and *trans*-cinnamic acid, were produced by using single (SSE) and twin screw (TSE) hot melt extrusion. The optimum barrel temperature for TSE was chosen from various temperature profiles applied in the SSE experiments. Physicochemical characterisation of extrudates was undertaken by using differential scanning calorimetry (DSC) and X-ray powder diffraction (XRPD); it was found that the screw configuration in TSE plays an important role in the production of high quality cocrystals compared to cocrystals produced using SSE. Furthermore, samples collected from the three zones of the barrel of the extruder during CBZ-TCA extrusion, confirmed the gradual formation of cocrystals in TSE. The TSE extruded cocrystals exhibited faster dissolution rates compared to bulk CBZ, the prototype cocrystals and those produced by SSE. In a further study, a hydrophilic carrier, D-glucono-δ-lactone (DGL) was extruded with CBZ, at various molar ratios, by using HME processing. XRPD and HSM characterisation of extrudates revealed polymorphic transformation of bulk carbamazepine (form III) into polymorphic form I. DGL was shown to be a suitable carrier for CBZ in order to enhance its dissolution rate. The extrudates showed faster dissolution rates compared to the physical mixtures in the ascending order: 2:1<1:1<1.5:1 (CBZ:DGL molar ratio). Different HME variables were examined in order to optimise the formation of indomethacin-saccharin cocrystals by using TSE. Important HME processing parameters- screw speed and extruder barrel temperature -were found to have an influence on the production of the cocrystals. Indomethacin-saccharin cocrystals improved the dissolution performance of indomethacin. In-line NIR (near infrared spectroscopy) was used as a process analytical tool during the continuous manufacture of the cocrystals for further insight into the HME process. Scale-up of cocrystals was performed by increasing the throughput rate in the laboratory scale extruder without compromising the quality of the extrudates. Whilst scaling-up the HME process, the downstream process was operated in continuous mode in order to prepare the final dosage (capsule) form of the indomethacin-saccharin cocrystals. In-line particle size monitoring was performed during the extrusion and milling processes. Particle size had a significant influence on the dissolution properties of the milled compared to the non-milled cocrystals.

TABLE OF CONTENTS

LIST OF FIGURES

XIII

LIST OF TABLES

ABBREVIATIONS

Acronym	Meaning
API	Active pharmaceutical ingredient
BCS	Biopharmaceutics classification system
CBZ	Carbamazepine
CM	Continuous manufacturing
DSC	Differential scanning calorimetry
DGL	D-Glucono-δ-lactone
ΔH	Enthalpy
FDA	Food and Drug Administration
FTIR	Fourier-transform infrared spectroscopy
HME	Hot melt extrusion
HPLC	High pressure liquid chromatography
HSM	Hot stage microscopy
IND	Indomethacin
IPP	In-line particle size probe
MCC	Micro-crystalline cellulose
NIR	Near infra-red spectroscopy
NSAID	Non-steroidal anti-inflammatory drug
PAT	Process analytical tool

PCA	Principal component analysis
pKa	Acid dissociation constant
PM	Physical mixture
QBD	Quality by design
RH	Relative humidity
rpm	Revolution per minute
Rwp	Weighted profile R-factor value
SCH	Saccharin
SEM	Scanning electron microscopy
SMEDDS	Self-emulsifying drug delivery system
SSE	Single screw extruder
TCA	*Trans*-cinnamic acid
TSE	Twin screw extruder
XRPD	X-ray powder diffraction

PUBLICATIONS

Moradiya, H. G., Islam, M. T., Woollam, G. R., Slipper, I. J., Halsey, S., Snowden, M. J. and Douroumis, D. (2014) 'Continuous cocrystallization for dissolution rate optimization of a poorly water-soluble drug', *Crystal Growth & Design*, 14(1), 189-198.

Moradiya, H. G., Islam, M. T., Halsey, S., Maniruzzaman, M., Chowdhry, B. Z., Snowden, M. J. and Douroumis, D. (2014) 'Continuous cocrystallisation of carbamazepine and *trans*-cinnamic acid via melt extrusion processing', *CrystEngComm*, 16(17), 3573-3583.

Maniruzzaman, M., Islam, M. T., **Moradiya, H. G.**, Halsey, S. A., Slipper, I. J., Chowdhry, B. Z., Snowden, M. J. and Douroumis, D. (2014) 'Prediction of polymorphic transformations of paracetamol in solid dispersions', *Journal of Pharmaceutical Science*, 103(6), 1819-1828.

Moradiya, H. G., Nokhodchi, A., Michael, S. A., Bradley, R., Douroumis, D. (2015) 'Increased dissolution rates of carbamazepine – gluconolactone binary blends processed by hot melt extrusion', *Pharmaceutical Development and Technology*, 1-8. doi:10.3109/10837450.2015.1022783

Moradiya, H. G., Islam, M. T., Chowdhry, B. Z., Douroumis, D., 'Process optimization and scale-up of indomethacin-saccharin cocrystals: the effect of processing parameters', *Angewandte Chemie International Edition* (Submitted).

Islam, M. T., **Moradiya, H. G.**, Scoutaris, N., Halsey, S., Bradley, M., Chowdhry, B. Z., and Douroumis, D., (2014). 'Implementation of Transmission NIR as a PAT tool for monitoring drug transformation during HME processing', *European Journal of Phamaceutics and Biopharmaceutics* (Submitted).

CONFERENCE PRESENTATIONS

Moradiya, H. G., Chowdhry, B.Z., Douroumis, D. (2012), Cocrystallization of water insoluble actives by using hot melt extrusion, *United Kingdom & Ireland Controlled Release society (UKICRS)* at Aston University, Birmingham, UK (Poster Presentation).

Moradiya, H. G., Douroumis, D. (2012), Study of cocrystallisation in single and twin screw hot melt extrusion with model of carbamazepine and *trans*-cinnamic acid, *American Association of Pharmaceutical Science*, USA (Poster Presentation).

Moradiya, H. G., Chowdhry, B.Z., Douroumis, D. (2012), Study of cocrystallisation processes in hot melt extrusion, *Academy of Pharmaceutical Society* at Nottingham University, UK (Poster Presentation).

Moradiya, H. G., Slipper, I. J., Douroumis, D. (2013), Crystallinity determination of cocrystals by x-ray powder diffraction, *AAPS (American Association of Pharmaceutical Science) Student Chapter* at University of Greenwich, UK (Poster Presentation).

Moradiya, H. G., Chowdhry, B.Z., Douroumis, D. (2013), Continous cocrystallisation of poorly water soluble drug by using hot melt extrusion, *Academy of Pharmaceutical Society Pharmsci* at Heriot-Watt University, Edinburgh, UK (Oral Presenation).

Moradiya, H. G., Chowdhry, B.Z., Douroumis, D. (2014), Continous cocrystallisation of poorly water soluble drug by using hot melt extrusion, *AAPS (American Association of Pharmaceutical Science) Student Chapter* at University of Greenwich, UK (Oral Presenation).

Moradiya, H. G., Douroumis, D. (2014), Continuous solidification of self-micro emulsifying systems (SMEDDS) by using twin screw extrusion, *AAPS (American Association of Pharmaceutical Science) student chapter* at University of Greenwich, UK (Poster Presentation).

CHAPTER 1 : INTRODUCTION

1.1   OVERVIEW

Oral drug delivery has always been convenient and widely employed in drug development. Orally ingested drugs undergo first pass metabolism and, therefore, need to be fully dissolved in the gastric fluid to achieve the appropriate concentration of drug for the desired therapeutic effect (Qiu 2009). However, not all drugs possess the desired properties for oral formulations. For example, APIs with a low aqueous solubility display a limited rate of dissolution which can lead to inadequate and variable bioavailability. It is reported that around 40% of new drug entities exhibit poor water solubility (Merisko-Liversidge et al. 2003). The Food and Drug Administration (FDA) have categorized APIs according to the biopharmaceutics classification system (BCS) which relates to their solubility and permeability behaviour. According to the BCS classification, class I drugs are highly soluble and highly permeable, class II drugs have low solubility and high permeability, class III drugs exhibit high solubility and low permeability and class IV drugs show low solubility and low permeability (Amidon et al. 1995). In this classification system the drug is considered as being highly water soluble when the maximum dose is soluble in 250 ml of aqueous media over the pH range of 1 to 7.5 and, highly permeable when the extent of absorption in humans is determined to be 90% or more of an administered dose.

Noyes and Whitney (1897) established a quantitative description for dissolution:

$$\frac{dM}{dt} = \frac{D.A}{h}(c_s - c_t) \quad \textbf{Equation 1}$$

Where, dM/dt = rate of dissolution, D = diffusion coefficient in the diffusion layer, A = surface area of the drug particles, h = thickness of the diffusion layer, c_s = saturation concentration of the drug in the diffusion layer, c_t = the concentration of drug in bulk fluids solution at time *t*.

It is clear from the Noyes-Whitney equation that the rate of dissolution can be increased by simply increasing the surface area of the drug particles. However, this approach is ultimately limited by the solubility of the drug substance in the dissolving medium. Therefore,

improving the aqueous solubility of such compounds, even temporarily, can have a significant impact on *in vivo* performance (Otun 2011).

Alterations in molecular arrangement and/or interactions between molecules of crystalline materials can have an impact on their physicochemical properties (Schultheiss and Newman 2009). Salts, cocrystals, hydrates, solvates and polymorphs are modified forms of a drug and are widely used to alter the physicochemical properties of poorly water soluble APIs, Fig 1.1, (Blagden et al. 2014). However, other drug delivery systems are reported include, solid dispersions, self-emulsifying systems, micelles and nano-particles (Kolter et al. 2012).

Crsytalline Solid

Multicomponent Crystals

Cocrystals   Hydrates/Solvates   Salts   Polymorphs

Polymorphs
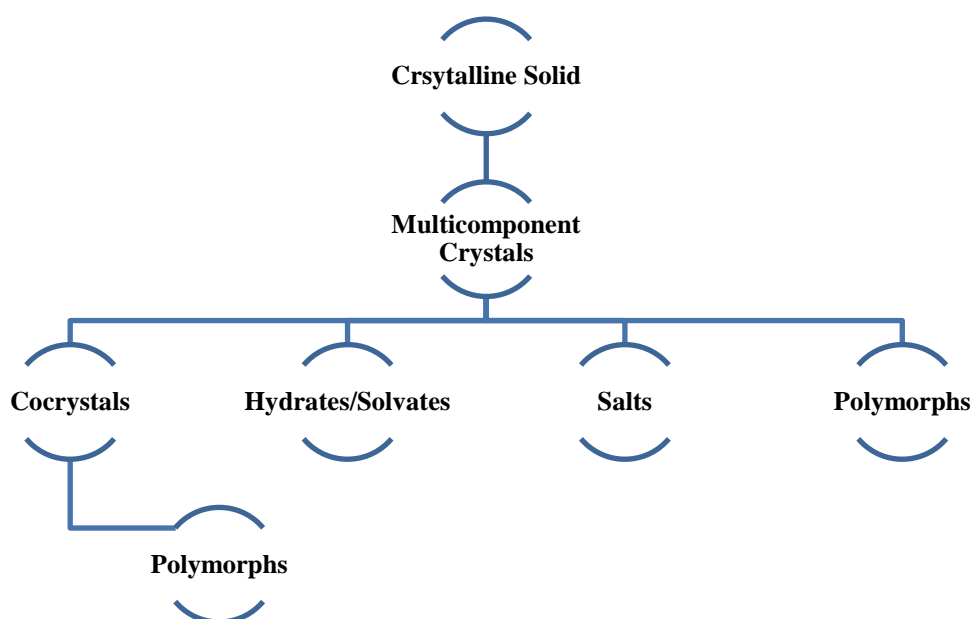
Fig. 1.1. Examples of solid state modification approaches to increase the solubility of an API.

1.2 PHARMACEUTICAL COCRYSTALS

Cocrystals have a long history; the first cocrystal of quinone and hydroquinone was reported by Friedrich Wöhler (1844). However, at that time the term cocrystal did not exist and was introduced in the 1980's by M.T. Etter (Stahly 2009). In the last decade, studies on cocrystals have achieved significant popularity and the focus has been on supramolecular chemical studies of intermolecular reactions in order to achieve the desired physicochemical and biological properties of the API.

It is common practice to screen for salt formation of new drug entities during the pre-formulation development stage (Serajuddin 2007), although when an ionisable site is

absent in the API and salts are difficult or impossible to form, cocrystals can be considered. The formation of a salt generally involves an acid-base reaction between the API and an acidic or basic substance. The difference between salts and cocrystals is that no proton transfer takes place in the formation of cocrystals (Elder et al. 2013). Cocrystals are bi-molecular entities which result in the formation of diverse crystals forms compared to the component molecules and have the ability to improve the physicochemical performance of the API. However, the distinct advantage which arises from the formation of cocrystals is that there should not be an alteration in the pharmacological properties of the API (Sekhon 2009). Cocrystals are formed with their molecular components (API and coformer; the coformer maybe another API) in a defined stoichiometric ratio such that the intermolecular interactions between the API and coformer are not covalent, but instead are formed via Van der Waals, hydrogen bond or π-π bond interactions (Vishweshwar et al. 2006). A wide range of coformers are available, e.g. those listed in GRAS (generally recognized as safe) substances by the FDA include sugars, food additives or, another API. Careful selection of the coformer is needed in order to achieve the drug's intended physicochemical properties as the coformer has a significant effect on cocrystals properties (Tomaszewska et al. 2013, Miroshnyk et al. 2009), and to avoid any toxic effects. Cocrystals are defined as: "Crystalline materials composed of two or more molecules within the same crystal lattice" (FDA 2013).

1.2.1 Properties of cocrystals

Cocrystals have different physicochemical properties because of their distinctive molecular structures and the nature of the intermolecular interactions between the API and coformer. A number of important properties of cocrystals-such as melting point, solubility, dissolution, stability, compressibility and bioavailability-differ from the individual molecular components. Moreover, a large number of different cocrystal systems has been reported in the scientific literature and each system is unique depending upon e.g. the nature of the molecular reaction, synthetic procedures used and the physicochemical properties of the coformers, including, of course, the API or APIs used. The following are some examples of cocrystals that have been demonstrated to show improvements in the properties of the APIs used compared to the individual (bulk) API's.

The melting point is important as it is directly related to the solubility with a higher melting point implying that the new material is thermodynamically stable (Blagden et al. 2008). One of the interesting studies with an API known as AMG 517 using dicarboxylic acids as

coformers showed a correlation between the melting of the coformer and the cocrystals (Stanton and Bak 2008). This might suggest the ability to predict the melting point of cocrystalline materials by choosing a higher or lower melting coformer. Although no generalization can be made of 50 cocrystals systems surveyed 90% of the cocrystals displayed melting points either lower or in between the API and coformer (Schultheiss and Newman 2009).

Solubility and dissolution behaviour are major concerns relating to the formulation of cocrystals and most of them are chosen in order to favour increased solubility. Bioavailability is a highly important pharmacokinetic factor to consider in the correct selection of the API during the drug development stage. There are certain parameters that influence solubility and/or dissolution behaviour of cocrystals, namely the solubility of the coformer, lattice energy, or intermolecular forces have a major impact on dissolution properties. General parameters such as particle size, chosen dissolution media and morphology of cocrystals can also influence dissolution (Tomaszewska et al. 2013).

- Carbamazepine-saccharin cocrystals produced via a solvent cooling method presented favourable dissolution (dependent on particle size) and physical/chemical stability compared to bulk carbamazepine. Oral administration of cocrystals in dogs indicated a higher drug absorption compared to the marketed product Tegretol® but there was no significant difference between pharmacokinetic parameters (Hickey et al. 2007).

- Traditional solvent cocrystallisation was performed on the hydrochloric salt of fluoxetine, an anti-depressant drug marketed as "Prozac®". Cocrystals of fluoxetine HCl were synthesized by using dicarboxylic acid coformers such as benzoic, fumaric or succinic acids (Childs et al. 2004). An intrinsic dissolution study in water at 10°C, showed 2:1 cocrystals of fumaric acid had a similar dissolution rate compared to fluoxetine HCl, but the dissolution rate for the benzoic acid 1:1 cocrystal was half that of fluoxetine hydrochloride. Fluoxetine HCl-succinic acid 2:1 complex had an, approximately, three times higher dissolution rate, but the dissolution was so fast that an accurate value was difficult to measure. This study suggested that the diverse solubility of cocrystals is related to the solubility of the coformer.

- Cocrystals of a BCS class II drug with glutaric acid demonstrated 18 times more drug release in stimulated gastric media and stability in aqueous media for up to 90 min compared to the bulk drug (McNamara et al. 2006). Capsules made only of cocrystal

powders were administered to 6 dog subjects at two different doses, 5 mg and 50 mg per kg; at both doses, cocrystals displayed an increase the area under the plasma concentration-time curve (AUC) values which were three times more than the bulk drugs.

- A low amount of poorly water soluble drug can have a higher bioavailability in the cocrystal form. Different solvents have been used, by employing the slurry method, to produce a stable cocrystal system of the free base AMG 57 and sorbic acid; the cocrystals displayed an increased dissolution rate compared to AMG 57 alone. In animal studies, using rats, the cocrystals displayed different pharmacokinetic compared to the bulk drug. A dose of AMG 57 cocrystals, 30 mg/kg, was found to result in the same bioavailability rate (Cmax) as bulk AMG 57 at 500 mg/kg and the AUC for bulk AMG 57 was halve that resulting from cocrystals of AMG 57-glutaric acid (Bak et al. 2008).

Moisture uptake from the atmosphere by drug formulations can convert a drug to its hydrate form and lead to undesirable properties and therefore the formulation needs to be stable in terms of potential hydration. Some cocrystal systems have proved resistance to hydrate formation. In a study carried out by Trask et al. (2005) to produce a stable form of caffeine, oxalic acid was used as the coformer; the resulting cocrystals were physically stable with no hydration occurring over a period of 7 weeks at 98% RH . Similarly, theophylline with a different carboxylic acid as a coformer was found to be totally stable with no hydrate formation (Trask et al. 2006). Theophylline-oxalic acid cocrystals were also stable at 98% RH for seven weeks. The researchers assumed that less availability of unreacted hydrogen bonds prevented the formation of hydrates in the crystalline lattice of cocrystals.
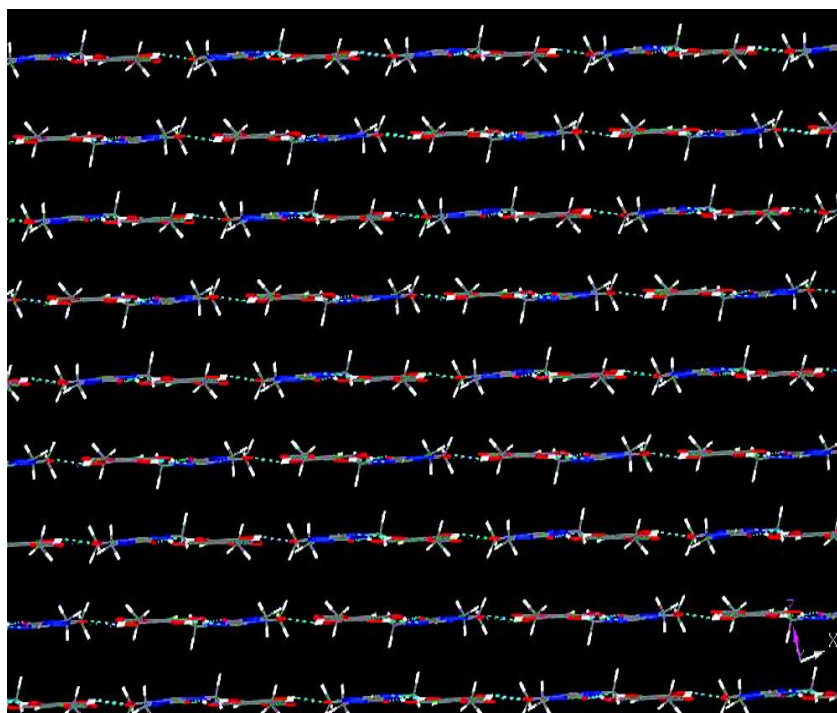
Fig. 1.2. Flat slip planar structural layers of caffeine-methyl gallate cocrystals result in better compaction properties compared to bulk materials. Broken lines indicate hydrogen bonds.

Some studies have also described the unique layer structure of cocrystals and conclusions have been drawn in relation to improved mechanical properties compared to the bulk materials. Specific compaction properties are required for ease of handling and manufacture of drug formulations. The presence of flat slip planes can be an effective criterion in selecting cocrystals with superior mechanical properties. For example, cocrystals of caffeine and methyl gallate (Fig. 1.2) were found to have good plasticity and the ability to form tablets without lamination even at high compaction force (Sun and Hou 2008). Paracetamol was screened against nine coformers (malonic acid, succinic acid, adipic acid, nicotinamide, ascorbic acid, saccharin, theophylline, theobromine, and caffeine), for a stable and mechanically improved form of the drug compared to polymorphs of paracetamol form II (having good compaction properties but not stable) (Karki et al. 2009). Further results have shown superior compaction properties of the cocrystals of paracetamol-theophylline compared to the form II polymorph. Similar results were reported for ibuprofen and flurbiprofen cocrystals formed by using nicotinamide as a coformer (Chow et al. 2012) which were more compressible and resistant to hydration compare to individual profens.

Formulation of two APIs into a single formulation is quite appealing for pharmaceutical development as it offers novelty, patent ability, patient compliance and therapeutic effectiveness (Sekhon 2012). Cocrystals of acetaminophen and theophylline show higher drug release when compared to a physical mixture of the two drugs. However, various pairs of cocrystals with two active substances have been reported, but careful studies are required to confirm that no deleterious physiological actions occur compared to the individual drugs (Lee et al. 2011). Drug-drug cocrystals of lamivudine and zidovudine, which are usually marketed as a physical mixture, were developed by a solvent evaporation method (Bhatt et al. 2008); however, solubility or dissolution studies for the foregoing system were not reported. Another example is the cocrystal of sildenafil and acetylsalicylic acid (Zegarac et al. 2014). It was claimed that such cocrystals could be used to treat patients with cardiac disease and that the cocrystals displayed significant improvements in intrinsic dissolution compared to bulk sildenafil and its salt (marketed as a Viagra®).

Recently, even after a large number of research publications and patents in the area of cocrystals, a novel drug-drug cocrystal has been registered; E-58425 was patented and entered phase II development ('Esteve R&D Portfolio' 2013). E-58425 was developed for mild to acute pain relief with a combination of two analgesic drugs, tramadol and celecoxib. Clinical trials on humans showed no adverse drug-drug physiological reactions. Different and superior effects were noted in relation to safety and tolerance of the cocrystals compared to simple co-administration of the individual drugs. This development indicates that it might not be too long before cocrystals will be available for clinical use.

1.2.2 Polymorphism in cocrystals

Polymorphism is the ability of a solid material to exist in more than one form or crystal structure and the different polymorphic forms have modified physicochemical properties. Similar to single crystalline compounds, cocrystals can also exist in different polymorphic forms and thus potentially display discrete physicochemical properties (Bond 2009). However, to date, all the reported studies have been limited to a single crystal determination in relation to supramolecular chemical properties of the cocrystal polymorphs and no other properties such as solubility, stability, dissolution and bioavailability have been reported (Aitipamula et al. 2014). Cocrystals of carbamazepine-saccharin (CBZ-SCH; Fig. 1.3) and carbamazepine-nicotinamide have been noted to have triclinic polymorphs with different molecular arrangements than the monoclinic form of the cocrystals (Porter III et al.

2008). Similarly polymorphism for cocrystals of caffeine-glutaric acid (Trask et al. 2004), caffeine-theophylline (Eddleston et al. 2013), 2:1 cocrystals of 4-hydroxybenzoic acid and 2,3,5,6-tetramethylpyrazine (Sreekanth et al. 2007), temozolomide with 4,4'-bipyridine-*N,N'*-dioxide (Babu et al. 2008) and ethenzamide with saccharin (Aitipamula et al. 2009) have been reported.
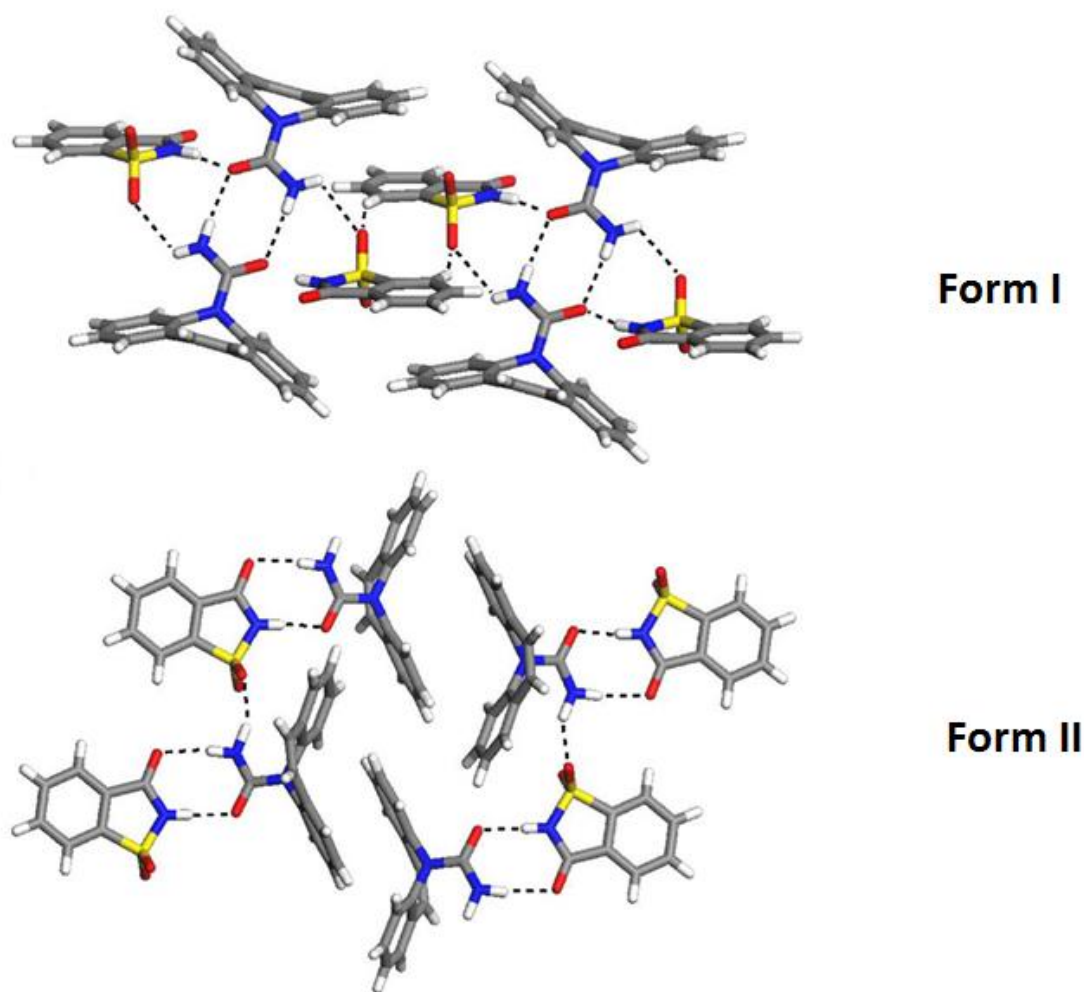
Fig. 1.3. Structure of CBZ-SCH cocrystal polymorphs verified by single crystal X-ray crystallography (Porter III et al. 2008).

1.2.3 Screening and preparation approaches

Relatively simple rules can be applied to make theoretical predictions about cocrystals by choosing molecules which are good hydrogen donors and acceptors. The formation of cocrystals between two components can also be predicted using Hansen solubility parameters (Mohammad et al. 2011), a theoretical approach to estimate drug miscibility with excipients or coformers. If the difference between the solubility parameters of two entities is less than seven, then they are miscible; the same approach was used to predict cocrystallisation between drug coformers. The Kofler method is widely used to screen new cocrystals. In practice, the component with higher melting point (A) is melted first then allowed to solidify, and then the other component (B) is melted and brought into contact with A. In the contact zone solidified A is dissolved in the liquid of B, producing a mixing zone when the sample is quenched and recrystallized. This mixing zone is flanked with pure component A at one side and pure B at the other side. When the sample is heated again until melting, under an HSM equipped with a polarizer, it is possible to observe the newly formed cocrystal, flanked by two eutectic mixtures, in the mixing zone. This cocrystal phase will retain birefringence and is usually clearly distinguishable from the eutectic and components A and B (Berry et al. 2008, Chadha et al. 2012). Raman spectroscopy can be employed, in combination with HSM, to record *in-situ* formation of cocrystals (Aina 2012). Differential scanning calorimetry is another useful tool to explore new cocrystal pairs by studying their phase behaviour (Lu et al. 2008). The physical mixture of the active with a suitable coformer is analysed via a DSC experiment. If they contribute two endothermic peaks, one peak is always attributed to the eutectic and the other is the melting point of the cocrystals. However, combining DSC and Fourier-transform infrared spectroscopy can also be useful tools to predict cocrystal formation (Lin et al. 2013a, Zhang et al. 2012).

Methods used to prepare cocrystals e.g., solvent or mechanochemical methods, which have the disadvantage of scalability, and others are described below.

Solvent evaporation

Solvent-based methods (such as evaporation of solvents, cooling crystallisation and the use of anti-solvents) are those that are mostly used for cocrystal formation. Successful cocrystallisation is dependent on the choice of different solvents and the solvent mixture (Jones et al. 2006). This technique involves the solubilisation of the API and the coformer, in

a stoichiometric ratio, in either one or a mixture of solvents. Both components should have the same/similar solubilities in the solvent(s); this is the major limitation of the method. A saturated solution is slowly evaporated to achieve super-saturation and this results in the formation of cocrystals. The solution is either evaporated at ambient temperature or at a specified temperature above the solvent boiling point to start the process. Even a combination of these two processes may help to accelerate the growth of cocrystals. Occasionally, the solvent used may lead to unexpected/undesired solvate formation (Trask and Jones 2005). The use of organic solvents can have a potentially harmful impact on the environment, and there maybe additional issues relating to the cost and disposal of the solvents.

Melting method

This technique is limited to thermo-resistant and stable active materials. A physical mixture of the API and coformer constituting the cocrystals is heated until it melts and is then slowly cooled to achieve crystallization. If the melting process is insufficient to form cocrystals, then seeding from the melts is used to grow cocrystals in combination with the solvent method (Liu et al. 2012).

Grinding method

This mechanical process involves grinding the compounds, by using either a mortar-pestle or a ball mill. Cocrystallisation depends on grinding time and choice of coformer (Braga et al. 2013). Wet grinding can be carried out to induce the process when there is no sign of the formation of a new phase, and can include the use of a small amount of solvent which acts as a catalyst for the crystallization process. The foregoing is referred to as solvent drop grinding or liquid assisted grinding (Friščić and Jones 2009). An issue relating to scale up of the grinding and a milling process is a key concern.

Super critical fluids

Recently, a new approach for cocrystallisation has been reported for screening and formation of cocrystals (Padrela et al. 2009, Padrela et al. 2010). Three cocrystallisation approaches were reported by using supercritical fluid technology: 1) supercritical solvent (CSS), 2) an anti-solvent and 3) atomizing fluid. The researchers successfully demonstrated an atomization process for screening of cocrystals with the coformer saccharin and six different

APIs, including indomethacin. The CSS technique was noted to be of limited use in the case of indomethacin, as this drug is poorly soluble in supercritical media. Theophylline-saccharin cocrystals at a previously unreported molar ratio of 2:1, were obtained; the foregoing has never been achieved using traditional techniques. The use of less solvent, compared to classical methods, is an advantage of this method; but drug solubility is still an issue when using supercritical fluids.

Ultrasound assisted cocrystallisation

Caffeine and maleic acid cocrystals have been synthesized by ultrasound assisted cocrystallisation (Aher et al. 2010). It was claimed that the ultrasound method is beneficial when the difference between the solubility of the two components is large/significant (non-congruently soluble pair). Super-saturation and the molar ratio of components were described as critical process considerations.

Thermal ink-jet printing

Recently thermal ink-jet printing of cocrystals has been demonstrated by Buanz et al. (2013). In this process a solution of desired cocrystals was prepared in a suitable organic solvent or using water. Evaporation was carried out by using a jet printer to formulate cocrystals. This approach has also been shown to be useful for synthesizing solid dispersions using polymer(s).

1.3 HOT MELT EXTRUSION (HME)

HME is an emerging engineering process that has been employed to overcome issues relating to the solubility and bioavailability of APIs. A technique adapted from the plastics and food industries, HME is now beginning to be extensively used in the development of pharmaceutical formulations and offers significant advantages compared to other approaches (e.g., spray drying, freeze drying, co-evaporation or grinding). HME is defined as the process of forming a new material (the extrudate) by forcing it through an orifice or die under controlled conditions such as temperature, mixing, screw and feed-rate.

The extrusion process was initially developed during the 18th century with the aim of building a single operating unit by combining the multiple tasks usually undertaken by different machines and/or instruments (Mollan 2003). Since the 19th century, HME has

mainly been utilised in the production of plastic bags, pipes, pasta and palletised veterinary foods (Andrews et al. 2009). Significant interest developed after the introduction of HME in the area of pharmaceutical research and it is now widely accepted in this area due to its versatility. The main applications of HME include the production of solid dispersions using polymer or lipid matrices which modify the drug release properties (sustained or enteric release, immediate release), taste masking of bitter APIs and the increased solubility and bioavailability of poor water-soluble-drugs (Singhal et al. 2011). With a number of applications (such as pellets, tablets, granules, topical or buccal films, implants and vaginal rings) having been developed by HME, its usefulness has been recognised (Crowley et al. 2007). In addition to being a proven manufacturing process, HME meets the goal of the US FDA's process analytical technology (PAT) scheme for designing, analysing and controlling the pharmaceutical manufacturing process via quality control measurements during active extrusion processing (Maniruzzaman 2012).

1.3.1 Advantages of HME

HME has the following (potential) advantages.

- The absence of organic solvents during processing makes HME beneficial for the environment (green technology).
- HME constitutes a quick, continuous operation and reduces the number of unit operations with optimal reproducibility.
- Ease of scale-up due to previously established techniques in the plastics and food industries.
- Short residence time; therefore time and cost effective
- Uniformity in the final product due to intense and dispersive mixing ability of the rotating screws.
- In-line process analysis tools available.
- Easy to clean instrument design when needing changes to different batches. (Almeida et al. 2012).

HME has potential limitations in regard to heat sensitive drugs, as there is more chance of them decomposing/degrading during processing using this technique. APIs should be thermally robust to avoid any undesired heat stress, but with a shrewd choice of carrier, low processing temperature, modification in screw design and reduced residence time effective

production can be achieved with improved efficiency (DiNunzio et al. 2010). A plasticizer can be added in the physical blend which decreases the glass transition temperature of the physical blend and allows the HME of the material at a lower processing temperature (Verreck 2012).

1.3.2 Process and instrumentation

The HME process entails the feeding, conveying-kneading of material by the screw, flow of molten mass through the die and exit from the die followed by downstream processing (Fig. 1.4). HME extrudates generally involve mixtures of an active drug with a thermoplastic polymer or lipid and/or other ingredients such as an antioxidant or plasticizer (Repka et al. 2007).
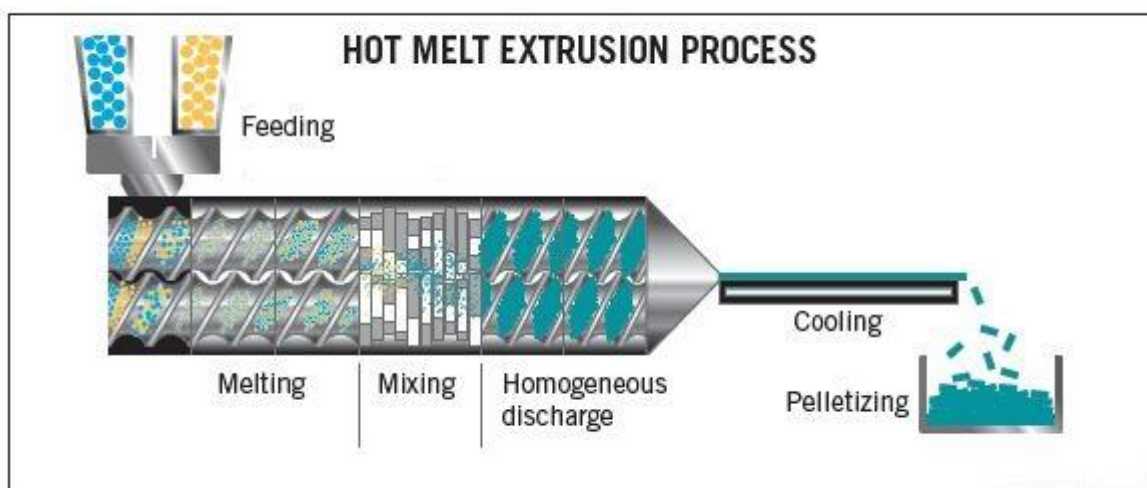
Fig. 1.4. Layout of a hot-melt extruder.

The extrusion process is carried out by using a hot melt extruder. The instrument is principally divided into extruder, auxiliary equipment for extruder, downstream processing equipment and monitoring tools (Madan and Madan 2012). The extruder itself has a conical shaped barrel consisting of a rotating screw or screws, feeder, die and a display unit for the control and display of instrument parameters. Input of material takes place through the feeder, transporting raw materials into the barrel. A pre-blended mixture or API carrier can be fed separately with the option of a single or multiple feeders. The temperature of each zone in the barrel is accurately maintained by a fixed thermostat and the screw is rotated using energy supplied by a motor unit. A die is attached to one end of the extruder to mould the processed

material(s) into the desired shape. Auxiliary equipment includes temperature/pressure gauges, torque and screw speed monitors.

Further processing takes place after the extrudates emerge from the extruder, using downstream equipment such as a conveyer belt to cool down the extruded materials to room temperature or under high-pressure air. A chilled roller is an additional option to convert the molten extrudates into a thin film shape using a cooling environment at the required temperature. Injection moulding is another means to form the extrudates into a mould array at high pressure and temperature. Injection moulding offers flexibility for the continuous production of tablets or implants (Quinten et al. 2009). A pelletiser, located after the conveyor belt, can be utilised to cut the strands into the required pellet size. Design optimization, analysis and control in real time of processes is possible by using PAT (process analytical tool) methodologies such as near infrared (NIR), Raman or ultrasonic probes.

Screw configuration, screw speed, temperature and feed rate are critical parameters for HME processing and can be controlled. Shear and torque are optional parameters that can be monitored and rely on processing parameters. Optimum temperature, screw speed and feed rate are all necessary to achieve good shear and run the process efficiently (Kolter et al. 2012).

1.3.3 Types of extruder

There are two types of commonly available extruders: single screw (SSE) and twin-screw (TSE). SSE consists of a single screw with a spiral shaped shaft and is a simple and cost effective option. In SSE, the amount of material the screw takes from the hopper depends on the screw speed, as the feeder is closely attached to the screw. The diameter of the screw increases along the length of the extruder barrel. The low screw pitch and smaller depth between the two patches at the head of the screw, near the feeder, gently mixes materials into a solid state. At the start of the first part of the barrel, dry materials first cause friction in the barrel, this is followed by melting of materials in the subsequent zones; the high pressure in the final zone of the extruder helps the material exit through the die (Luker 2012).

Fig. 1.5. Photograph of a commercially available twin screw extruder pharmalab-16 (Thermo-fisher) with chilled roller.

The TSE (Fig.1.5) is used more often than the SSE in pharmaceutical research due to its higher mixing capability, high throughput and reduced residence time compared to the SSE. The TSE can be either co-rotating (both screws rotate identically) or counter-rotating (opposite rotations), depending on the operating principle. Co-rotating TSE is the most beneficial due to its self-wiping properties, high throughput and intermeshed design (Chokshi and Zia 2010). Higher screw speed and more intense mixing can be achieved using co-rotating TSE compared with counter-rotating. A counter-rotating extruder is used when high shear is required; but high pressure, low output and air entrapment are limitations. Intermeshing and non-intermeshing are another design variable in TSE. Intermeshing is preferred as its conveying characteristic work on the "first in-first out" principle and minimizes the disadvantageous effect of localized overheating. A non-intermeshing screw is necessary to overcome problems relating to torque caused by highly volatile materials (Mollan 2003).

Fig. 1.6. Schematic diagram of screw elements a) mixing elements at 90°, b) mixing screws at 30°, and c) conveying screw.

TSE screws comprise a number of screw parts known as "conveying or mixing elements" which lie on the screw shaft with different geometry and can be interchangeable so that different screw configurations can be achieved, according to specific requirements. Conveying screws have a self-wiping geometry designed for easy transportation of material which helps to push material in a continuous manner, from feeding to discharge (Leister et al. 2012). Conveying elements are also used to prevent a vacuum, so that the flow of the melt, to the following sections, is not affected. Mixing elements are also known as kneading discs. Each mixing element has the same shape, but can be used at different angles (i.e. 30°, 60° or 90°; Fig.1.6) to achieve distributive or dispersive mixing (Wildi and Maier 1998). Screw configuration can have an effect on the mixing ability of the extruder, shear or pressure during the extrusion process, and the properties/characteristics of the final product.

1.3.4 HME in pharmaceutical research

The exceptional flexibility and extensive use of HME is validated by the number of publications in this area. A number of applications have proved that HME is a more significant and beneficially productive tool for several pharmaceutical applications compared to traditional techniques. Some of the literature in the pharmaceutical area, covering a range of HME applications is reviewed in Table1.2.

Furthermore, some HME developed drug formulations, such as Rezulin®, KALETRA®, NORVIR®, ONMEL® and medical devices such as NuvaRing®, IMPLANON®, OZURDEX® , have gained approval from the FDA (Lang et al. 2014).

16

Table 1.1. Examples of pharmaceutical applications of HME with different APIs and excipients reported in the scientific literature.

Application/Purpose	API	Excipients	Final Dosage form/Remarks
Taste masking	Paracetamol	Eudragit® EPO	Granules (Maniruzzaman et al. 2012a)
	Cetirizine	Kollidon VA64	Orally disintegrating tablets (Douroumis et al. 2011). Showed masking of bitter taste of API which were supported by *in vivo* and electronic tongue studies.
Combination of immediate and sustained release	Hydrochlorothiazide: immediate release Releasemetoprolol tartrate: sustained release	Ethyl cellulose Polyethylene oxide	Multi-layered tablets in one step process by using two extruders simultaneously. Good adhesive between two layers (Dierickx et al. 2012).

Sustained release	Diclofenac sodium	Caprtiol-888	Granules, tablets (Vithani et al. 2013)
	Chlorpheniramine maleate	Polyethylene oxide/ Chitosan and xanthan gum	Matrix tablets (Fukuda et al. 2006, Zhang and McGinity 1999)
	Paracetamol	Ethyl cellulose and Compritol® 888 ATO	Powder, Granules (Islam et al. 2014) QBD approach was employed to develop formulations by using NIR as a PAT tool.
Orally disintegrating tablets	Ibuprofen	Methacrylate copolymer (Eudragit® E PO)	Granules (Gryczke et al. 2011)
Enteric coating	5-Aminosalicylic acid	Eudragit® L100-55	Tablets prepared from API-polymer extrudates showed excellent resistance to dissolution in gastric media (Andrews et al. 2008)

Controlled release	Metoprolol tartrate	Polyethylene oxide	Fixed dose mini-tablets (Vynckier et al. 2014)
Prolonged-release swellable matrices	Theophylline or ketoprofen	Hydroxypropyl cellulose	Tablets (Loreti et al. 2014)
Injection moulding	Metoprolol tartrate	Ethylcellulose and hydroxypropylmethylcellulose (HPMC)	Injection moulded sustained release tablets (Quinten et al. 2009)
Inclusion complex	Ketpofrofen	β-Cyclodextrin and SBE$_7$-β-CD	HME was found to have a better mixing capacity and the HME extrudates displayed more favourable dissolution characteristics compared to conventional techniques (Fukuda et al. 2008)

Nanoparticles	No description of drug	Compritol® 888 ATO and Tween- 80	Extruded combination of surfactant and lipid were directly fed into the high pressure homogenizer to produce solid lipid nanoparticles (Patil et al. 2014)
	Lopinavir and Ritonavir	Kollidon® VA64, Span® 20 and Hydrophilic fumed silica (Aerosil® 200)	Preparation of *in situ* silica nanoparticles by HME (Kanzer et al. 2010)
Solid SMEDDS (self-micro emulsifying drug delivery system)	Indomethacin	Capryol (lipid), Labrasol (surfactant) and Transcutol (co-surfactant)	One step, continuous solidification using "green methods" for liquid-SMEDDS to obtain microparticles upon dilution in aqueous media (Moradiya and Douroumis 2014)
Implants	Bovine serum albumin	Poly(d,l-lactide-co-glycolide)	A syringe-die device was used as a downstream attachment to make implants (Ghalanbor et al. 2012)

Processing of thermally unstable drug	Carbamazepine	Soluplus and Eudragit® E PO	Combination of two miscible polymers with thermally unstable drug can be easily processed by using HME (Liu et al. 2013)
Supercritical fluid as a plasticizer and foaming agent	No API	Polyvinylpyrrolidone-vinyl acetate/Eudragit® E100 PO/ Ethyl cellulose	Foam-like extrudates obtained and surface area was increased in some cases. CO_2 was used as a plasticizer (Verreck et al. 2006).
Metastable polymorphs	Artemisinin	-	Possible by optimisation of screw speed, extrusion temperature and screw configurations (Kulkarni et al. 2013a, Kulkarni et al. 2013b).

Films	Ketoconazole	Hydroxypropyl cellulose, Polyethylene oxide	Thin films for local application on the nail (Mididoddi and Repka 2007, Trey et al. 2007). The films produced had good adhesiveness, suitable for the desired application; tested on human nail samples.
	Itraconazole and alpha-tocopherol	Hydroxypropylcellulose	

1.4 COCRYSTALS AND HME

Medina, et al. (2010) first introduced HME technology for cocrystallisation using the model drug AMG 517 and caffeine. They found that a high mixing screw configuration provided a standard environment for manufacturing cocrystals. Subsequently, Dhumal and et al. (2010) reported the use of HME for the production of agglomerated cocrystals of ibuprofen and nicotinamide. By applying a quality based design (QBD) approach, various temperatures and screw configurations were examined using TSE. Daurio et al (Daurio et al. 2011) attempted cocrystallisation of four model cocrystal systems using TSE: caffeine-oxalic acid, nicotinamide-*trans* cinnamic acid, carbamazepine-saccharin (only 95% conversion confirmed by solid state NMR), and theophylline-citric acid. They applied a combined traditional solvent drop approach with HME; however, a very small amount of solvent did not induce cocrystallisation as noted for the grinding process, possibly due to temperature restrictions caused by the solvent.

Co-extrusion of cocrystals of carbamazepine and nicotinamide with polymers such as soluplus, PVP/VA or HPMC using HME has been reported. Solid dispersions made with cocrystal have a significantly increased dissolution rate compared to bulk CBZ, bulk cocrystals, physical mixtures of cocrystals-polymers and solid dispersions of CBZ-polymers (Liu et al. 2013). In another study, it was also reported that the presence of a certain amount (20% w/w) of soluplus results in carbamazepine being more stable (prevents the formation of CBZ dihydrate form) in aqueous media compared to bulk cocrystals which aids dissolution (Boksa et al. 2014). Only a few studies have been reported on the use of HME for cocrystallisation and a detailed study of HME is needed to understand the crucial parameters of the extrusion process that can establish HME as a robust, continuous cocrystallisation process.

1.5 STATEMENT OF DISSERTATION RESEARCH

The overall objective of the studies reported herein was the implementation of HME in order to enhance the dissolution rate of poor water-soluble drugs using a cocrystal approach. The primary aim of the research was to optimize a) the purity of the different cocrystals produced by using two types of HME extruders and b) the role of the mixing zones in TSE. Furthermore, a study was included in order to understand the cocrystallisation process in

HME by using PAT and altering the external HME parameters to make the process faster, reliable and scalable with a high through-put rate without compromising the purity of the cocrystals. After production of the cocrystals a further objective was to characterise the cocrystals produced using XRPD, DSC, HSM, SEM and dissolution studies.

CHAPTER 2 : CONTINUOUS COCRYSTALLISATION FOR DISSOLUTION RATE OPTIMISATION OF A POORLY WATER-SOLUBLE DRUG

2.1   INTRODUCTION

The oral route of drug administration is the most preferable as it is convenient, inexpensive, patient friendly and easier to administer than other routes. However, with poorly water-soluble drugs, i.e. class II drugs in the BCS system, traditional formulations can result in low bioavailability of the drug. Around 60% of drugs that are screened during industrial research are poorly water soluble (O'Donnell and Williams 2012). Therefore the solubility enhancement of poorly soluble drugs is becoming increasingly important in both industry and academia.

Cocrystallisation is an emerging approach to modify the physicochemical properties of poorly soluble active pharmaceutical ingredients (APIs) where chemical modification of the constituents occurs between components and results in a unique structural composition (Good and Rodríguez-Hornedo 2009, Alhalaweh and Velaga 2010, Sanphui et al. 2011, Alhalaweh et al. 2011, Schultheiss and Newman 2009). Such modification can result in greater solubility, enhanced stability and dissolution rate and thus bioavailability of the API without affecting its pharmacological action (Friscic and Jones 2007, Almarsson and Zaworotko 2004). Further studies also noted that the multi-layered structure of cocrystals resulted in improved mechanical properties, gave better compressibility, which could be helpful in dosage form preparation (Karki et al. 2009, Chattoraj et al. 2010). Pharmaceutical cocrystals are normally formed between an API and coformer; the latter should not interact with the drug entity to produce an unacceptable product. Cocrystals can be defined as crystalline complexes of two or more molecular components which interact together (bond) via non-covalent interactions within a single crystal lattice (Miroshnyk et al. 2009, Vishweshwar et al. 2006).

Conventionally, cocrystals have been obtained by various solvent methods or by grinding. Solvent methods include slurry conversion, solvent evaporation, crystallisation via slow cooling and precipitation (anti-solvent method). The grinding method involves grinding of

two or more components by hand or by using milling techniques (Yadav et al. 2009). Grinding is carried out by using a small amount of solvent, such that the solvent acts as a catalyst. However, scale up of such conventional methods is a major challenge. Recently, thermal ink-jetting has been reported as an alternative approach for the manufacture of cocrystals, where the coformers were dissolved in water and/or water-ethanol solutions (Buanz et al. 2013). The use of toxic solvents during processing is an additional burden to overcome as it is a costly process and requires special disposal systems. In addition, solvent methods usually require equal solubility of the components in order to avoid precipitation.

Hot melt extrusion (HME) is a relatively novel technique in the pharmaceutical industry which has been adapted from the plastic and polymer industries. Growing attention has been paid to HME as it is widely utilised for various pharmaceutical applications. HME is a continuous process that draws materials towards a die at a constant screw speed and elevated temperature in order to obtain uniformly shaped pellets or strips (Andrews et al. 2009). Some major advantages of HME include the following. It is a continuous process, easy to scale up and quality assurance can be monitored by following process analytical technology (PAT) procedures. In addition, HME is considered a green technology as processing of materials does not require the usage of organic solvents or water.

In this work carbamazepine, a Class II BCS active, was used with saccharin as a coformer in order to form cocrystals (Fig. 2.1). Carbamazepine is a widely used anti-convulsant drug which displays poor aqueous solubility and high intestinal permeability. Single screw extruders (SSE) and twin screw extruders (TSE) were employed to produce carbamazepine and saccharin cocrystals by investigating HME processing parameters. The cocrystals produced by HME were compared with prototype cocrystals developed by a solvent method (Hickey et al. 2007).
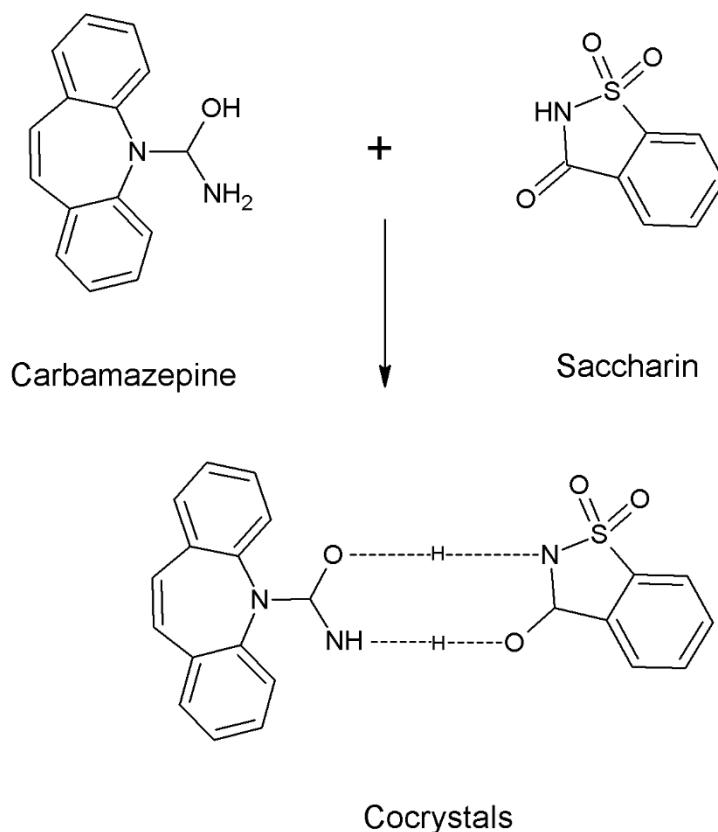
Fig. 2.1. Chemical structures of CBZ, SCH and H-bonding in CBZ-SCH cocrystals.

2.2 MATERIALS AND METHODS

2.2.1 Materials

Carbamazepine (CBZ) and saccharin (SCH) were purchased from Sigma Aldrich (Gilingham, UK) and used without any further treatment. Ethanol and methanol used for HPLC analysis and solvent cocrystallisation were of analytical grade and purchased from Fisher scientific (UK).

2.2.2 Hot Melt Extrusion

Carbamazepine and saccharin were accurately weighed and blended, at a molar ratio of 1:1, in a Turbula mixer for 10 min for uniformity. The powder blends were fed into the single screw extruder (RCP 0625, Randcastle, USA) or co-rotating twin screw extruder (TSE) of an HME (Eurolab-16, Thermo Fisher, Germany) using a screw speed of 10 rpm. Screw speed was set to 5 and 10 rpm for TSE. Extrusion was carried out without the use of a die. Typical temperature profiles used within different zones of the extruder from hopper to extruder were:70/95/110/120/120/120/120/120/115°C. However, the maximum temperature was

27

adjusted in order to optimize the quality of the cocrystal produced and was varied from 120 to 140°C.

2.2.3   Cooling cocrystallisation process

CBZ-SCH cocrystals (prototype) were prepared according to Hickey et al. (2007). Briefly, the solids were dissolved in 280 ml of a 62.5/37.5% (v/v) ethanol/methanol mixture and heated to 70°C for 1 hr under reflux. The temperature was decreased in 10°C increments to induce precipitation in the un-seeded system. The appearance of the cocrystal solid phase was first observed in the range of 60–50°C. The temperature was further decreased to 30°C in order to drive additional precipitation. Following equilibration at 30°C, the solids were isolated using a Buchner funnel and rinsed with cold ethanol.

2.2.4   Differential scanning calorimetry (DSC)

The thermal behaviour of bulk CBZ, the physical mixture (PM) of CBZ-SCH, the prototype and extruded cocrystals were examined by employing a differential scanning calorimeter (Mettler Toledo 823e, Greifensee, Switzerland). Samples (3-5 mg) were placed into an aluminium pan and crimped. Each pan was heated from 0°C to 200°C at 10°C/min heating rate under an atmosphere of nitrogen gas using a flow rate of 50 ml/min. Star evaluation software was used for the analysis of the data.

2.2.5   Hot stage microscopy (HSM)

The HSM experiments were conducted by using a Mettler Toledo FP82HT (Leicester-UK) hot stage microscope instrument. Powder cocrystals were sprinkled on a glass slide, covered with a coverslip and heated from ambient room temperature to 220°C at 10°C per min. Changes in morphology were collected as a video recording by using a PixeLINK PL-A662 camera (PixeLINK, Ontario, US).

2.2.6   X-Ray powder diffraction (XRPD)

XRPD experiments were performed by using a D8 Advance X-ray Diffractometer (Bruker, Germany) in theta-theta geometry using both reflection and foil transmission modes. A Cu anode X-ray tube was powered at 40 kV and 40 mA with a 0.2 mm exit slit. Sample rotation was set at 15 rpm. Data collection was between 2-55° 2θ in reflection and 4-55° 2θ in transmission mode, with a step size of $0.02°\ 2\theta$ and a counting time of 0.3 s per step. Rietveld refinements were performed using TOPAS V4.2 software (Bruker). Crystal structures were

retrieved from the Cambridge Crystal Structure Database: CBZ pure form III CSD (Cambridge structure database) code CBMZPNO1 (Reboul et al. 1981), CBZ-SCH form I CSD code UNEZAO (Fleischman et al. 2003). The March-Dollase model for preferred orientation was used on plane (001) for CBZ pure form III and CBZ-SCH form I. The background was modelled by using a Chebychev function with five coefficients. All peak shapes were modelled using fundamental parameters based on the geometry of the D8 instrument.

2.2.7 Dissolution studies

The dissolution studies were conducted by using a Varian 705 DS dissolution paddle apparatus (Varian Inc., North Carolina, US). Extrudates equivalent to 200 mg of CBZ were placed in 900 ml of 0.1 M hydrochloric acid solution (pH 1.2) at a set bath temperature of $37 \pm 2°C$ at 100 rpm for 2 hr. Samples were collected and filtered at pre-determined time intervals. Furthermore the GraphPad Instat® software (GraphPad Software Inc.) was used to analyse and compare the dissolution profiles between the cocrystals and the bulk drugs.

2.2.8 HPLC analysis

The content of CBZ in all dissolution samples was confirmed by HPLC analysis. The experiments were performed by using an HPLC system (Aligent Technologies, 1200 series) equipped with a quaternary pump. A Hypersil 200 mm×4.6 mm (5 μm) BDS C18 column was employed. Column temperature and retention time were set at 40°C and 4 min, respectively. The mobile phase was 70:30 (v:v) methanol:water. The sample volume was 20 μl injected by using auto sampler and scanned at a wavelength of 285 nm using a flow rate of 0.9 ml/min.

2.2.9 Scanning electron microscopy (SEM)

The morphology of all the extruded samples, including bulk CBZ and SCH, was examined by using SEM (Hitachi SU8030, Japan). Samples were placed on an aluminium stub and coated with a thin layer of chromium using argon gas at room temperature. SEM images were obtained using an accelerating electron beam voltage of 1-2 kV.

2.2.10 Particle size measurements

The particle size distribution was measured by laser diffraction (Mastersizer 2000, Malvern,UK), whereby 5 gm of powders were placed in the dry powder feeder. Each sample was measured three times.

2.3 RESULTS AND DISCUSSION

2.3.1 Hot melt extrusion continuous processing

In this study HME, a continuous manufacturing process, was explored for the development of cocrystals by processing CBZ/SCH blends at a 1:1 molar ratio. The processing of the cocrystals was optimized by using single screw (SSE) and twin screw (TSE) extruder in parallel, as processing parameters play a key role in the quality of the materials obtained. The screw type, configuration and temperature profile were the critical processing parameters as previously reported (Dhumal et al. 2010). The prototype cocrystal was produce by a solvent method for comparison with the HME extruded cocrystals.

Initially HME cocrystals were developed using SSE at three different temperatures (120°C, 135°C, and 140°C) in order to identify the optimal extrusion temperature. It was found that 135°C provided high crystallinity cocrystals with improved dissolution compared to other SSE extruded cocrystals (120°C and 140°C).

Based on these results TSE was further employed to improve the cocrystallisation process. In both SSE and TSE studies the die was removed from the extruder as the extrudates were not produced in the form of strands or melted material but rather as granular powders.

The morphology of the bulk materials, the prototype and the extrudates was examined by using SEM (Fig. 2.2). The crystal shape of bulk CBZ was flaky or thin plate-like; this observation was in agreement with previously published studies (Nokhodchi et al. 2005), whereas the cocrystals obtained via the solvent process were polyhedral prismatic. In contrast, the shape of the extruded cocrystals was block shaped. The change in the shape of the samples can be explained by the interaction between CBZ and SCH molecules, which results in the modification in crystal morphology.
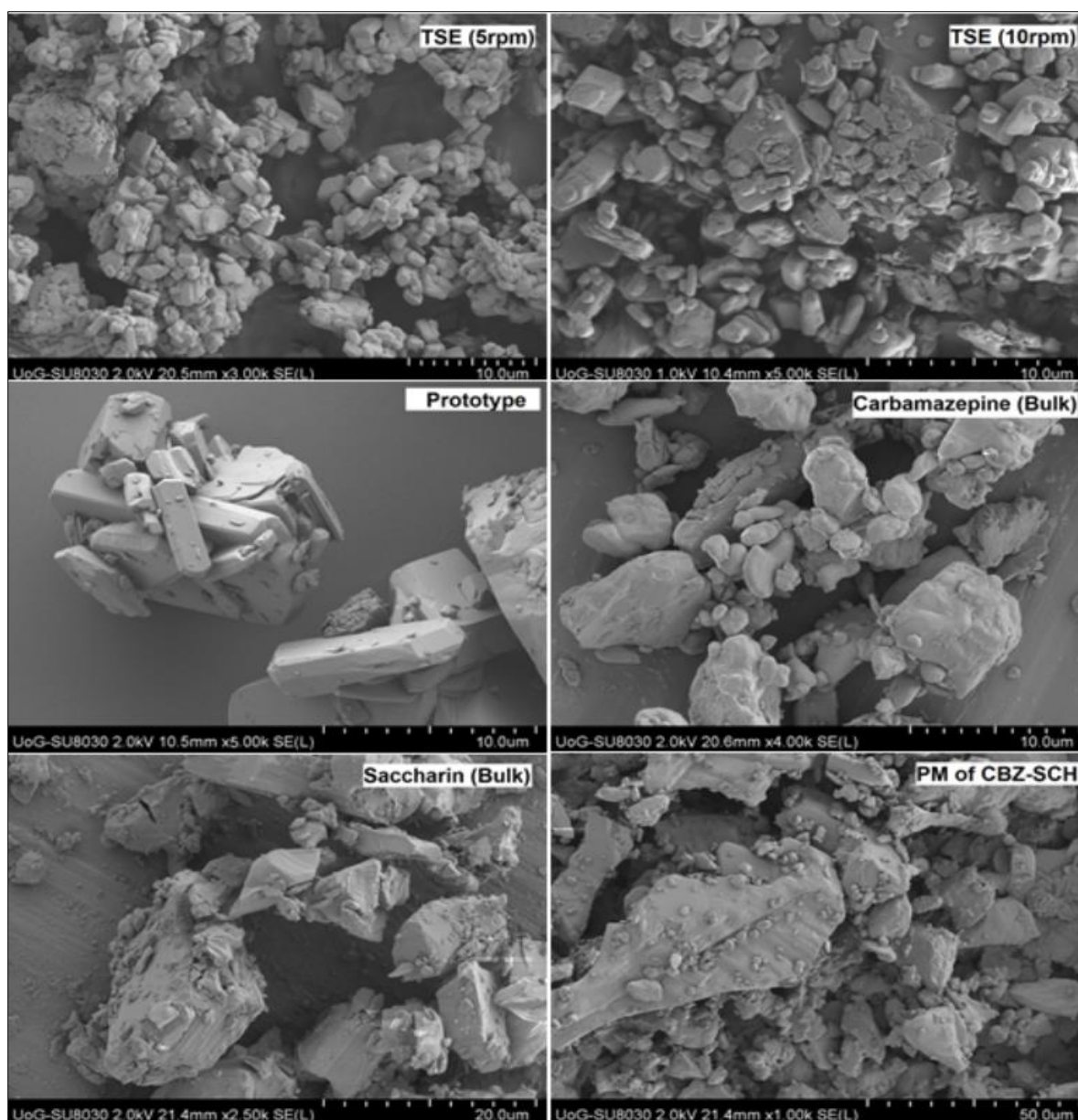
Fig. 2.2. SEM images of bulk CBZ, SCH, physical mixture, CBZ-SCH prototype, TSE (5 rpm) and TSE (10 rpm) cocrystals.

2.3.2 Thermal analysis

CBZ exhibits enantiotropic polymorphism i.e., a transition temperature is observed below the melting point of either of the polymorphs at which both these forms have the same free energy. Above the transition temperature, the higher melting Form I has the lower free energy and is more stable. In contrast, the lower melting Form III is more stable below the transition temperature since it has a lower free energy (Behme and Brooke 1991).

The thermophysical properties of the bulk powders, the prototype and the extruded materials, were analysed using DSC (Figs. 2.3-2.5). The thermogram of bulk CBZ showed a melting endothermic peak at 175.31°C followed by a second peak at 191.50°C. The thermogram for bulk saccharin showed a sharp melting peak at 227.1°C. Two endothermic transitions were detected in the thermogram for the PM at 155.65°C and 173.56°C (Fig. 2.3). The first endotherm in the physical mixture, at 155.65°C, represents a eutectic melt and the endotherm at 173.56°C represents the melting of the cocrystals (Lu et al. 2008). In contrast, for the samples prepared by SSE only a single melting endotherm was detected which varied according to the extrusion temperature, as shown in Fig. 2.4. The endothermic peaks ranged from 168.5°C to 171.63°C, which is below the melting endotherm of the bulk CBZ or SCH. All of the extruded cocrystals using SSE had endotherms which were relatively broad with varying melting enthalpy values (ΔH), depending on the HME processing temperature (at constant screw speed) and the quality of the cocrystals. A comparison of the melting endotherms revealed that the optimal SSE processing temperature occurred at 135°C. At this temperature a narrow melting endotherm with a high ΔH value was obtained.
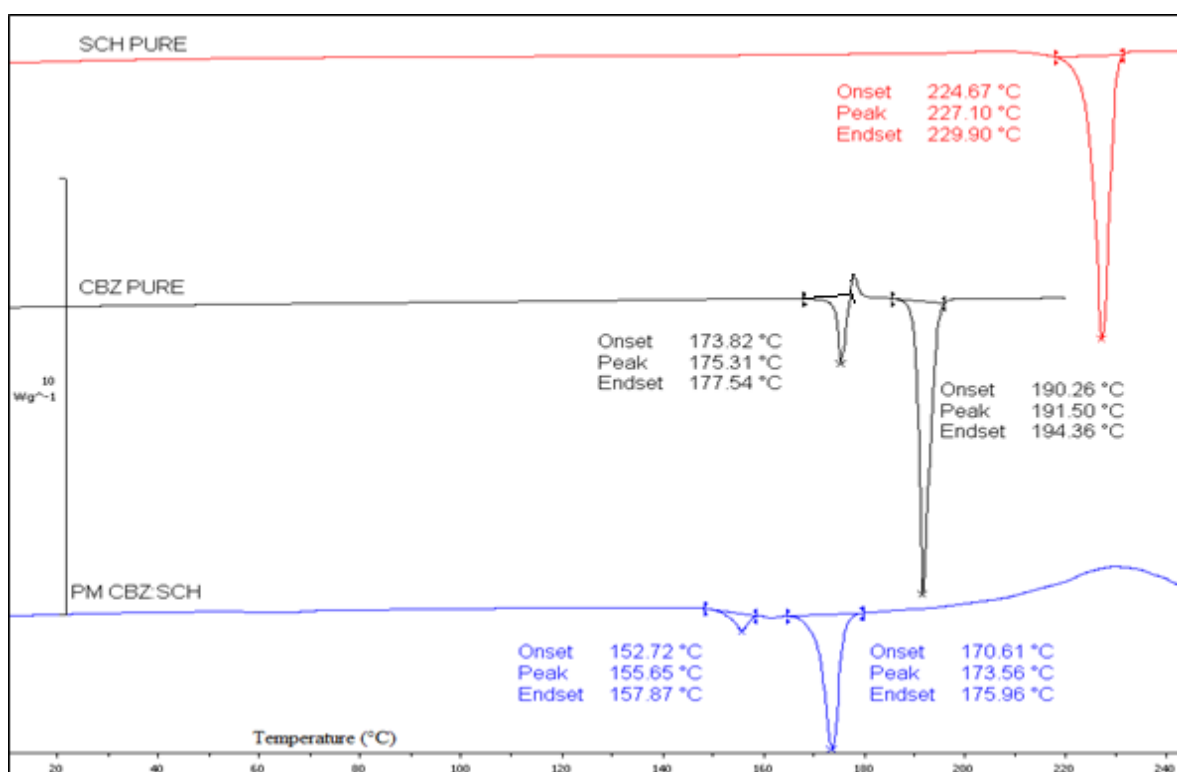
Fig. 2.3. DSC thermograms of bulk CBZ, SCH and PM.
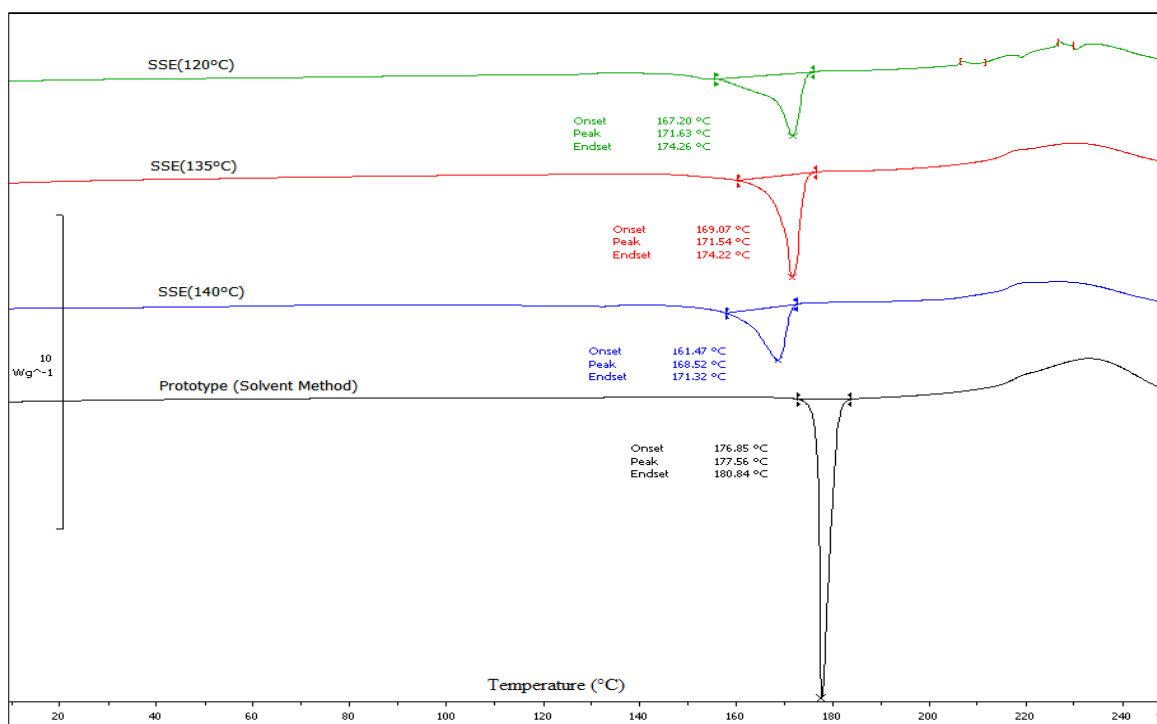
Fig. 2.4. DSC thermograms of CBZ-SCH cocrystals processed using SSE at 120°C, 135°C, 140°C and the prototype.
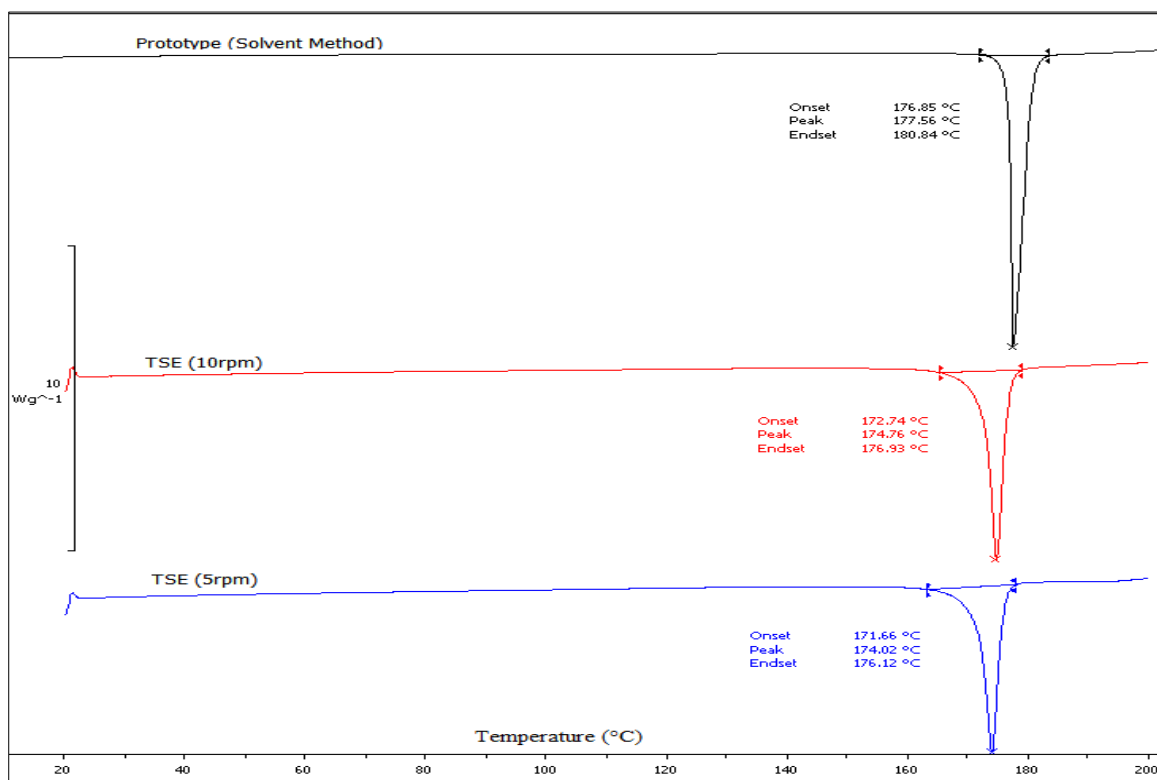
Fig. 2.5. DSC thermograms for CBZ-SCH prototype and CBZ-SCH cocrystals processed by TSE (5 and 10 rpm).

33

Powder blends extruded using the twin-screw extruder at low screw speed (5 rpm) presented a single melting endotherm at 174.02°C (ΔH= -107.89 J/g). Similarly the extruded blends at higher screw speed (10 rpm) showed a single melting peak at 174.76°C (ΔH= -119.80 J/g), as shown in Fig. 2.5 Interestingly, for both TSE screw speeds the melting endotherms were shifted closer to the endotherm of the prototype indicating a more effective mixing process compared to the SSE. In addition, for cocrystals produced by TSE an increase in the melting enthalpy and narrow melting peaks were observed. The suppression of the CBZ-SCH melting points and the presence of a single melting endotherm suggest the formation of a new entity with a new structure. In addition, the DSC thermogram of the prototype produced by the solvent process, showed a slightly higher, sharp melting peak at 177.56°C (ΔH= - 144.91 J/g). The higher melting endothermic peaks for the produced cocrystals were accompanied by increased ΔH values (Table 2.1). This data suggests a higher purity and crystallinity for the CBZ-SCH prototype and r the TSE extruded cocrystals.

Table 2.1. Melting endothermic peaks and normalized ΔH values for the bulk, extruded and prototype cocrystals.

Material	Peak endotherm (°C)	Enthalpy (ΔH, J/g)
SCH bulk	227.1	-162.62
CBZ bulk (2nd peak)	191.5	-102.5
SSE 120°C	171.6	-76.4
SSE 135°C	171.5	-85.5
SSE 140°C	168.5	-71.2
TSE 135°C (5 rpm)	174.0	-107.9
TSE 135°C (10 rpm)	174.8	-119.8
Prototype	177.6	-144.9

As shown in Fig. 2.6, HSM was used to investigate the thermal events associated with bulk CBZ and the optimized TSE cocrystals. The bulk CBZ showed the formation of needle shaped crystals (form I) after melting at 175°C followed by a complete melting at 191.7°C, in good agreement with the DSC thermograms.
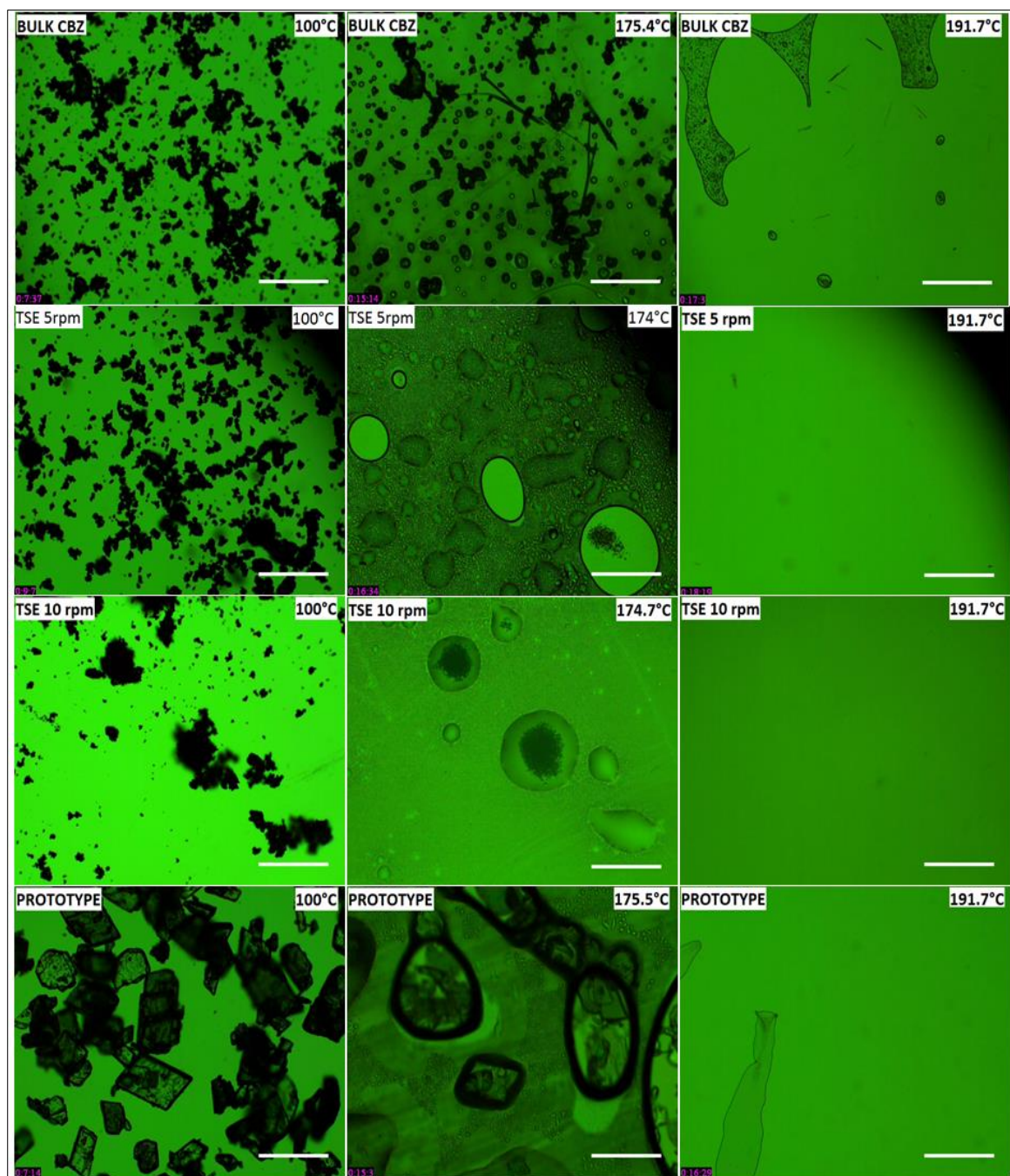
Fig. 2.6. HSM images of bulk CBZ, prototype and TSE cocrystals (135°C, 5 rpm and 10 rpm).

The TSE samples showed complete melting of the cocrystals at 174°C and 174.7°C, respectively. These results confirmed the DSC studies and only a single melting event was detected for both HME and solvent method cocrystal samples.

2.3.3 X-ray powder diffraction (XRPD)

Samples were further analysed by XRPD to identify the diffraction patterns of the cocrystals formulated by HME and the solvent method. As shown in Fig. 2.7 the intense peaks for CBZ form III appear at 13.07°, 15.31°, 19.49°, 24.96° and 27.24° 2θ (Rustichelli et al. 2000) while for bulk SCH the intense peaks occur at 9.56°, 16.02°, 19.13°, 25.14° 2θ values. In contrast, the diffraction peaks for the CBZ-SCH prototype (Fig. 2. 8) appear at 7.03°, 13.67°, 14.02°, 14.95°, 20.14°, 21.45°, 21.74°, 23.43°, 25.79° and 28.29° 2θ values and as it can be seen they are completely different than those of the individual bulk substances. The XRPD diffractograms are in agreement with those reported by Porter III et al. (2008) where the distinctive XRPD peak at 6.9° 2θ is related to the CBZ-SCH form I cocrystals.
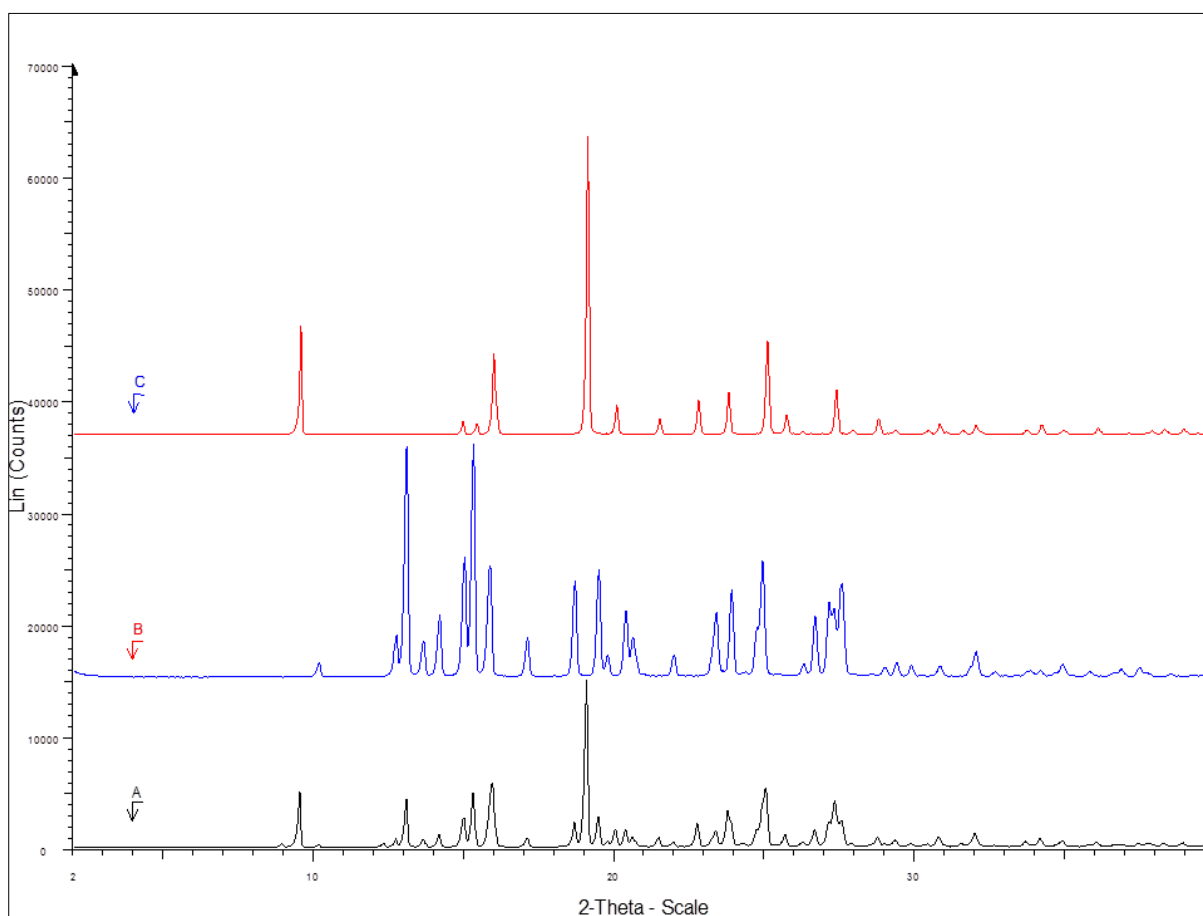
Fig. 2.7. XRPD diffractograms for bulk PM (A) bulk CBZ (B) and bulk SCH (C).
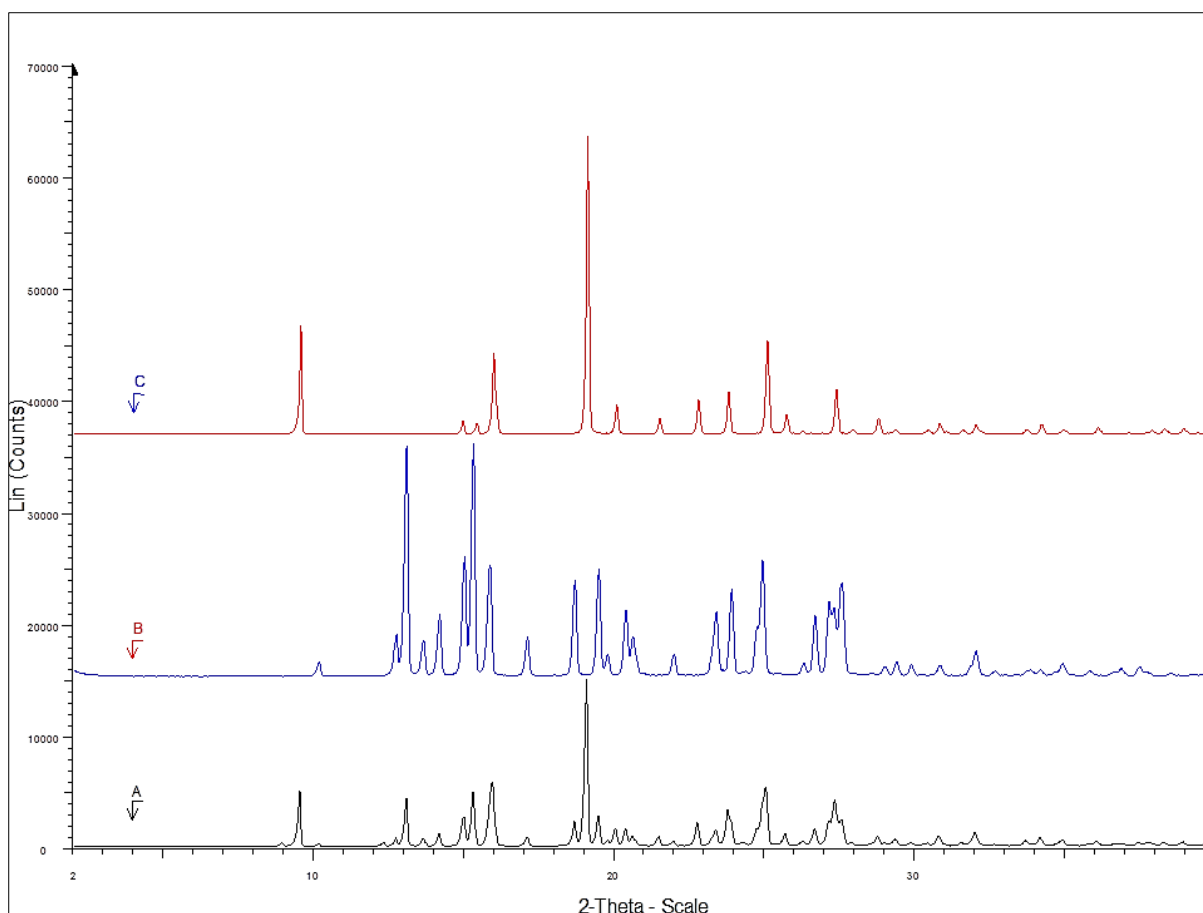
Fig. 2.8. XRPD diffractograms of cocrystals processed by SSE at120°C (D), SSE at 135°C (E), SSE at 140°C (F) and the prototype (G).

Diffraction peaks for extruded cocrystals by using SSE, irrespective of the screw rate of the extruder, appear to be identical to those of the prototype. However, the characteristic XRPD diffraction peaks of the extrudates are, in intensity, indicating a lower fraction of crystallinity compared to the prototype. The samples of bulk CBZ (form III) and the two TSE samples of CBZ-SCH cocrystals at the operating conditions of 135°C and screw speeds of 5 and 10 rpm were analysed in reflection mode (Fig. 2.9). However, the prototype sample demonstrated significant preferred orientation, such that a good refinement was not possible in reflection mode. This was subsequently run in transmission mode in Mylar foil, where the preferred orientation was reduced and a better fit obtained. In this case the use of spherical harmonics in the Rietveld refinement further reduced the effect of preferred orientation and lowered the Rwp (weighted profile R-factor value) to 9.4%.
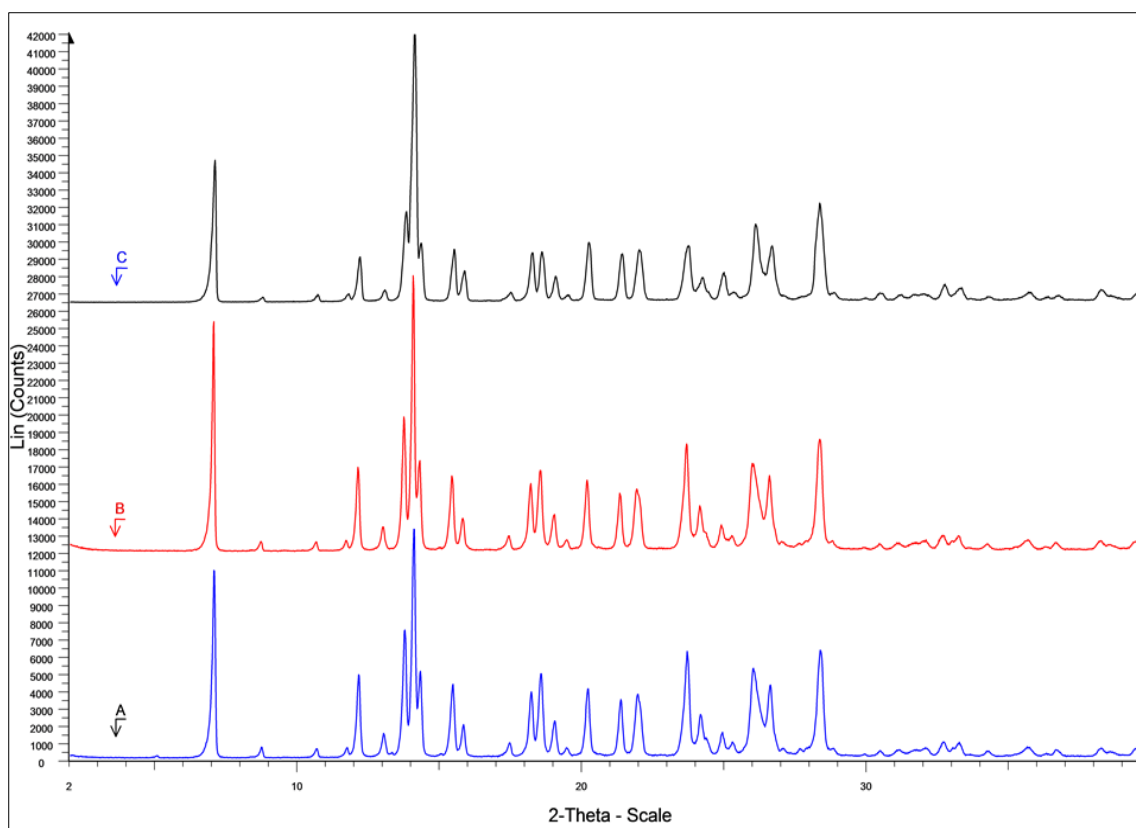
Fig. 2.9. XRPD diffractograms of cocrystals processed by TSE (5 rpm), TSE (10 rpm) and prototype (A, B and C, respectively).

In Rietveld analysis, the t total weight fractions of all the included crystalline phases sum to 1 and the quantity of the amorphous component is not known. However, it can be estimated by using an internal standard of a known crystal structure, in this case a corundum spike. If a significant proportion of amorphous material is present in the sample, then the amount of the spike standard will be overestimated in the normalised Rietveld result since the amorphous component is not measured. The program TOPAS can be used to calculate the content of amorphous material if the weight fraction of the added spike (W_S) is known, since it measures the normalised weight fraction of the spike in the Rietveld refinement (R_S) (see appendix, Figs. S.1-4). The fraction of amorphous material (A) is then calculated from the weight fractions:

$$A\% = \frac{(R_s - W_s)}{R_s(1 - W_s)} \times 100 \quad \textbf{Equation 2}$$

The estimated values of amorphous material for bulk CBZ, prototype and two TSE cocrystals are given in Table 2.2. The prototype presented high crystallinity (99.96%) compared to the TSE cocrystals produced using 5 rpm and 10 rpm (97. 5%). The difference between the

38

prototype and the TSE CBZ-SCH cocrystals was attributed to the optimized solvent process compared to the continuous extrusion processing which can be developed further (e.g. by altering the screw configuration).

Table 2.2. Weight percent values for the calculation of amorphous component, (error in parentheses).

		Rietveld (%)	**Spiked (%)**	**Original (%)**
CBZ bulk	Amorphous	0	0.55 (0.32)	0.92 (0.54)
	CBZ-III	59.78	59.45	99.08
	corundum	40.22	40	0
CBZ-SCH (5 rpm)	Amorphous	0	1.52 (0.36)	2.53 (0.61)
	CBZ-SCH-I	59.38	58.48	97.47
	corundum	40.62	40	0
CBZ-SCH(10 rpm)	Amorphous	0	1.49 (0.5)	2.48 (0.8)
	CBZ-SCH-I	59.4	58.51	97.52
	corundum	40.6	40	0
CBZ-SCH (solvent)	Amorphous	0	0.02 (0.51)	0.04 (0.86)
	CBZ-SCH-I	59.99	59.98	99.96
	corundum	40.01	40	0

2.3.4 Dissolution studies

Dissolution studies of the cocrystals produced is one of the main criteria used to assess their performance compared to the bulk CBZ. For this reason the dissolution patterns of all extrudates were compared to those of the bulk CBZ and the prototype. As expected, the bulk CBZ showed a slow dissolution rate, with approximately 60% after 2 hr (Fig. 2.10). A PM of CBZ:SCH (1:1 molar ratio) showed a low dissolution profile similar to bulk substance suggesting that only SCH does not affect the dissolution rates of CBZ. The cocrystal extrudates processed by SSE demonstrated faster dissolution rates depending on the extrusion temperature; increasing in the order 135°C > 120°C > 140°C. The SSE 135°C extrudates showed a rapid dissolution rate with about 77% of CBZ being dissolved in 30 min, whilst almost 90% was dissolved in 120 min. Increased dissolution rates were also observed for the SSE120°C extrudate compared to the bulk CBZ (60% in 30 min). For the SSE140°C extrudates dissolution was slightly higher than the bulk CBZ due to the low quality of the cocrystals. It is obvious that the quality of the cocrystals affected their dissolution behaviour and confirmed that the optimized SSE135°C cocrystals were of the best quality. A Kruskal-Wallis non-parametric test followed by the Dunn *post hoc* multiple comparison test, was used to investigate the differences between the three dissolution profiles. This showed a significant difference ($p < 0.05$) for the cocrystals processed at SSE (120-135°C) but not for those processed at 140°C using SSE.

As shown in the data in Fig. 2.11, the TSE processed cocrystals also gave increased dissolution rates compared to the prototype. For the TSE (5 rpm) extrudates, 75% of drug release was achieved after 30 min. Interestingly, the CBZ-SCH cocrystals processed at 10 rpm showed a slower dissolution rate (65% in 30 min) compared to those processed at 5 rpm (TSE) suggesting that the screw rate is a critical process parameter (Dhumal et al. 2010). The dissolution performance of the CBZ-SCH prototype was also a key element of this study and it was compared to those of the extruded cocrystals. The data in Fig. 2.11 shows clearly that the dissolution rate was faster than the bulk CBZ with 40% dissolving in 30 min and 65% after 60 min. However, the prototype showed significantly lower dissolution rates in comparison to the SSE (135°C) and TSE processed cocrystals.
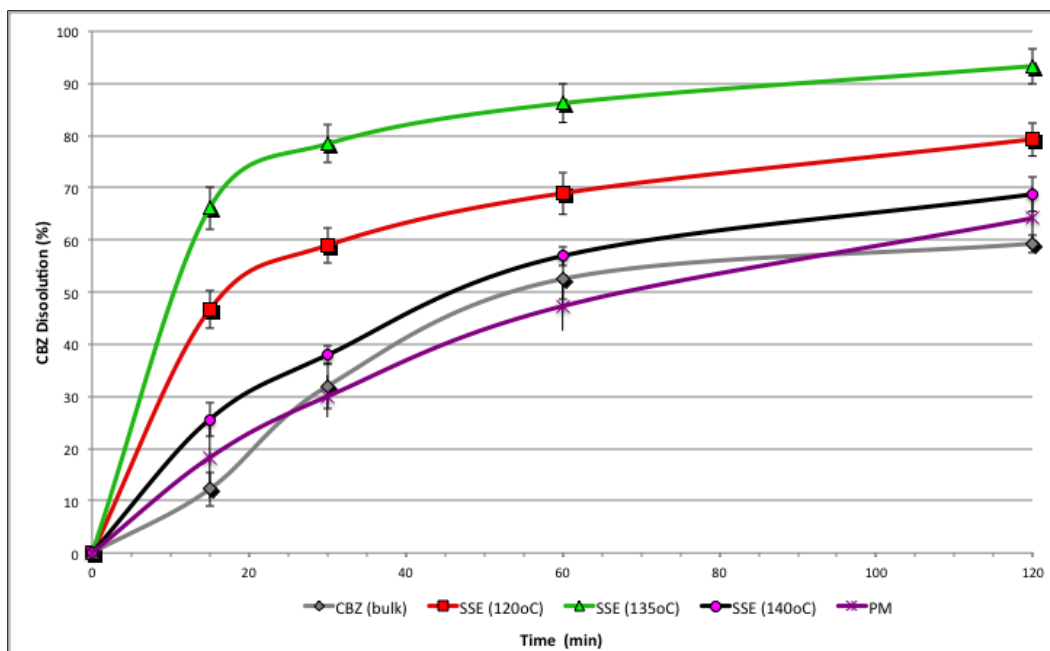
Fig. 2.10. Dissolution profiles (pH 1.2) of bulk CBZ, physical mixture (PM) and CBZ-SCH cocrystals (processed using SSE (120°C), SSE (135°C) SSE (140°C)).
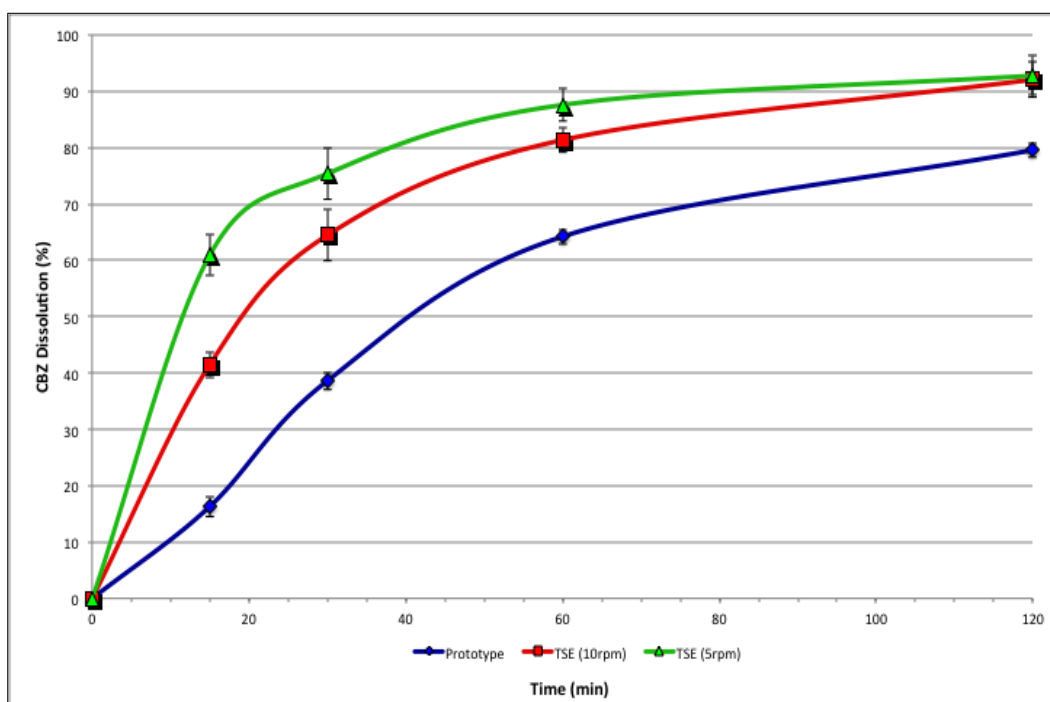
Fig. 2.11. Dissolution profiles (pH 1.2) of CBZ-SCH prototype and cocrystals processed by using TSE (5 and 10 rpm).
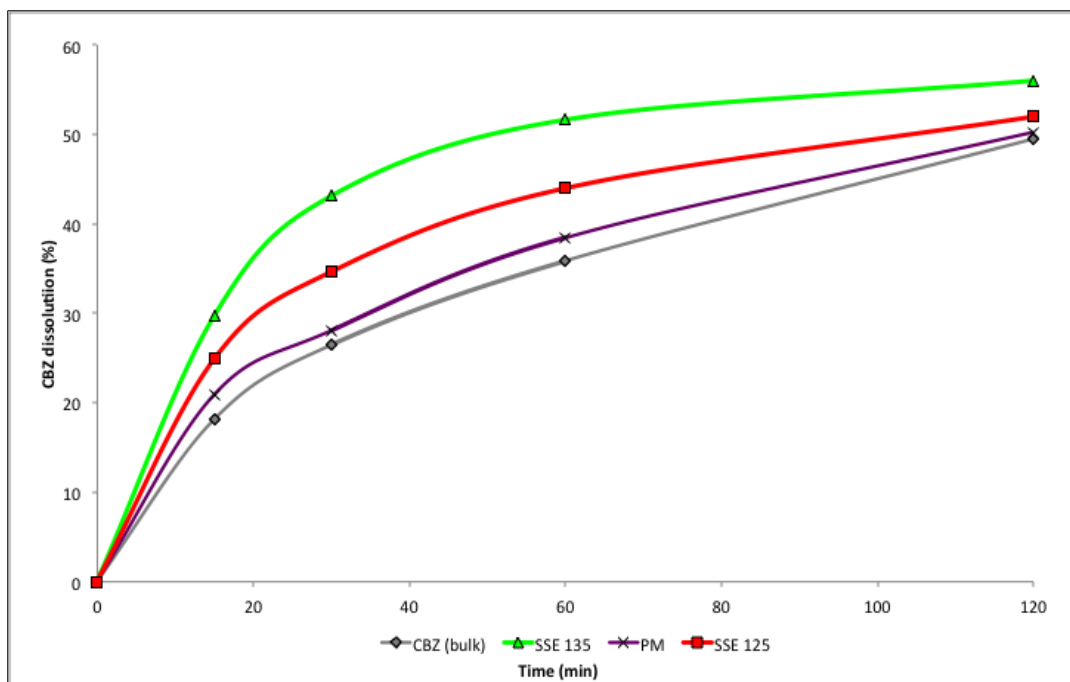
Fig. 2.12. Dissolution profiles of bulk CBZ, physical mixture (PM), CBZ-SCH cocrystals processed with SSE (120°C and 135°C) at pH 6.8.
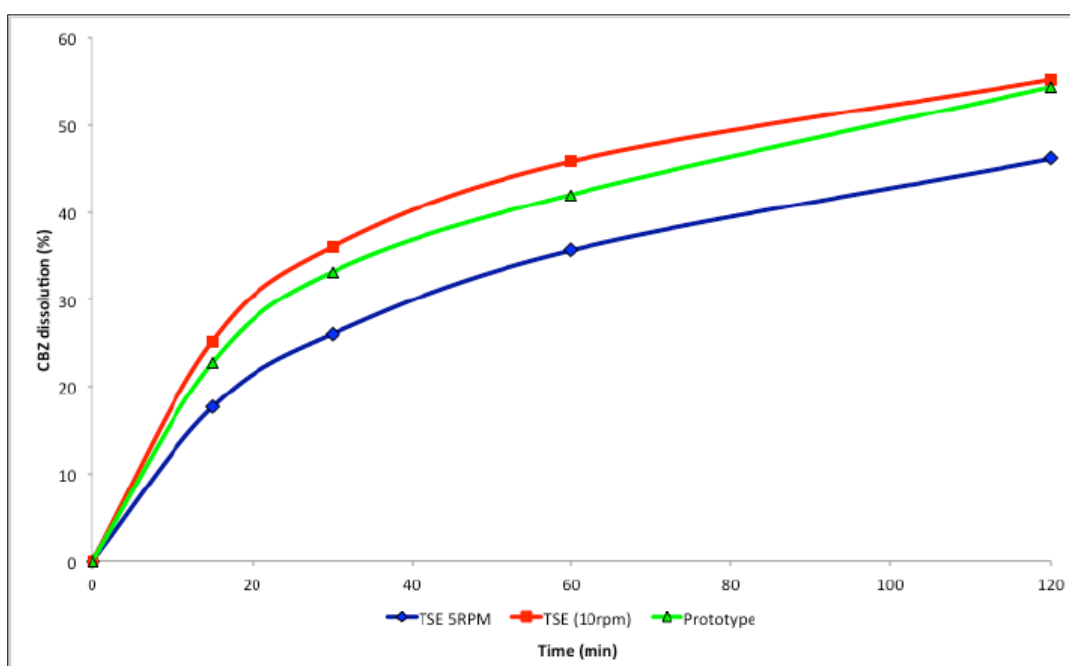
Fig. 2.13. Dissolution profiles of CBZ-SCH prototype and cocrystals processed with TSE 135°C (5 rpm and 10 rpm) at pH 6.8.

In Table 2.3 the particle size distribution is depicted where the d[v, 0.5] and d[v, 0.9] are recorded for the bulk CBZ, the prototype and the extruded formulations. The results showed a smaller particle size distribution for bulk CBZ but quite larger particles for the prototype and the extruded batches. It is obvious that the particle size distribution of the extrudates and the prototype does not favour the dissolution patterns and thus their faster dissolution rates cannot be attributed to the particle size. Finally, as shown by XRPD analysis the prototype presents higher crystallinity (~2.5%) compared to the TSE batches and a small amorphous content could affect the dissolution rates. However, it is unlikely that such a small amorphous trace would result significant increase in the dissolution rates (Fig. 2.11). In addition, the SSE batches at 120°C and 135°C (Fig. 2.10) suggesting that only high purity cocrystals can provide increased dissolution rates. The dissolution studies carried out in phosphate buffer at pH 6.8 showed slower dissolution rates compared to acidic media but the order of the dissolution pattern was similar (Figs. 2.12-13).

Table 2.3. Particle size analysis of bulk CBZ, prototype and extrudates.

	d[0.5] (μm)	d[0.9] (μm)
CBZ bulk	48.31	88.59
SSE	114.65	433.76
TSE (5 rpm)	105.73	481.69
TSE (10 rpm)	103.79	369.8
prototype	122.18	419.47

Physical stability studies of the produced HME cocrystals (both SSE and TSE) under accelerated conditions (40°C and 75% RH) showed excellent physical stability without any changes in the crystallinity. Further XRPD analysis provided identical diffractions peaks of cocrystals without the appearance of any new peaks. These finding were also in a good agreement with similar studies conducted by Hickey et al. (2007).

2.4   CONCLUSIONS

In conclusion, HME, a continuous manufacturing process, was employed to produce high quality CBZ-SCH cocrystals. The study revealed that the extrusion temperature and screw configuration (single or twin screw) were critical processing parameters for the manufacture of high quality cocrystals. DSC evaluation of SSE extrudates showed a broad and blunt peak compared to TSE extrudates and the prototype indicated less purity/ incomplete formation of cocrystals in the SSE process. Rietveld refinement showed similar crystallinity of TSE extruded cocrystals using different screw speeds (97.5 & 97.5) compared to the prototype (100%). The TSE extruded CBZ-SCH cocrystals when compared to a CBZ-SCH prototype proved to be of similar quality (high crystallinity) but with faster dissolution rates. However, all the extrudates (including SSE, TSE and prototype cocrystals) were found to have higher dissolution rates compared to bulk CBZ. Continuous cocrystallisation has been shown to be a novel approach for the production of pharmaceutical cocrystals of water insoluble drugs with enhanced performance compared to conventional methods.

CHAPTER 3 : STUDY OF COCRYSTALLISATION PROCESS IN HOT MELT EXTRUSION WITH COCRYSTALS OF CARBAMAZEPINE AND *TRANS*-CINNAMIC ACID

3.1   INTRODUCTION

The development of novel drug formulations and processing technologies has been traditionally explored by the pharmaceutical industry and still remains a strong focus of research in both industry and academia. This is of significant importance for the development of poorly water-soluble active pharmaceutical ingredients (APIs) as approximately 40% of drugs in the pipeline have low water solubility. The lack of efficient formulation and processing technologies can reduce the commercial potential of such drugs.

To date, cocrystals are an emerging formulation approach in pharmaceutical drug development with the aim of improving the solubility, dissolution, bioavailability and stability (Hickey et al. 2007, McNamara et al. 2006, Trask et al. 2006, Steed 2013b, Blagden et al. 2007) of various poorly water soluble drugs. In addition to improvements in the physicochemical properties of the drug molecules, cocrystals can be highly patentable as completely new drug entities. Cocrystals have been viewed from a supramolecular perspective, which involves understanding the intermolecular interactions between the API and the coformer candidates (Desiraju 1995, Aakeroy et al. 2010). The molecular components in cocrystals are held together by non-covalent interactions such as hydrogen bonds, van der Waal forces or π-bonds without altering the chemical and physiological action of the drug(s) compound(s). Cocrystals are formed as homogenous phases between two or more molecular components in the crystalline lattice which usually consist of a drug substance and a cocrystal coformer (Lu et al. 2008). Moreover, according to the FDA guidelines pharmaceutical, "cocrystals are crystalline materials composed of two or more molecules in the same crystalline lattice" (FDA 2013).

The solvent method and mechanical grinding are the two most common processes that are conventionally used to produce pharmaceutical cocrystals (Yadav et al. 2009) but in reality both of these techniques are time consuming and difficult to scale-up. Excessive use of organic solvents can be environmentally harmful, costly and a small residue of the solvent

can be toxic which can raise regulatory issues. The solubility of the active compounds in organic solvents can lead to the formation of undesired solvates (Trask et al. 2005). Other techniques such as spray drying (Alhalaweh and Velaga 2010), ultra-sonication (Aher et al. 2010), and supercritical fluid techniques (Padrela et al. 2009) have been reported for the development of various pharmaceutical cocrystals.

HME has been introduced in the pharmaceutical industry and it is now widely utilised as a highly versatile and robust processing methodology. HME has found several applications in formulation development including solubility and bioavailability enhancement or taste masking of bitter APIs via the manufacture of amorphous solid dispersions. Recently, HME has gained significant interest in pharmaceutical research for the manufacture of cocrystals (Dhumal et al. 2010, Daurio et al. 2011). HME is considered a continuous process with excellent scalability, high throughput efficacy, strong mixing capacity and low residence time compared to traditional technologies.

Cinnamic acid is an excellent coformer for the formation of cocrystals; interact via hydrogen bonds with its hydroxyl and /or carbonyl group. Carbamazepine (CBZ) has been reported as a model drug for the formation of cocrystals due to the presence of the amide functional group, which interacts with a range of cocrystal formers. Recently published research showed that cocrystals of carbamazepine-cinnamic acid can effectively prevent the conversion of CBZ to its dihydrate form, which could be attributed to the relatively lower solubility of the coformer and explains the greater stability of cocrystals in aqueous media (Shayanfar et al. 2013). Author also mentioned that highly water soluble coformers are thermodynamically unstable and could transform CBZ to its dihydrate form when placed in aqueous medium.

Herein, a solvent free cocrystallisation process for carbamazepine and *trans*-cinnamic acid is reported by using both single screw (SSE) and twin screw extrusion (TSE) processing via HME. In addition the role of screw configuration in the formation of cocrystals during twin-screw extrusion is examined.

3.2 MATERIALS AND METHODS

3.2.1 Materials

Bulk carbamazepine Form III (CBZ) and *trans*-cinnamic acid (TCA) were purchased from Sigma Aldrich (Gillingham, UK) and used as received. Acetonitrile and ethyl acetate were analytical grade and purchased from Fisher scientific (UK).
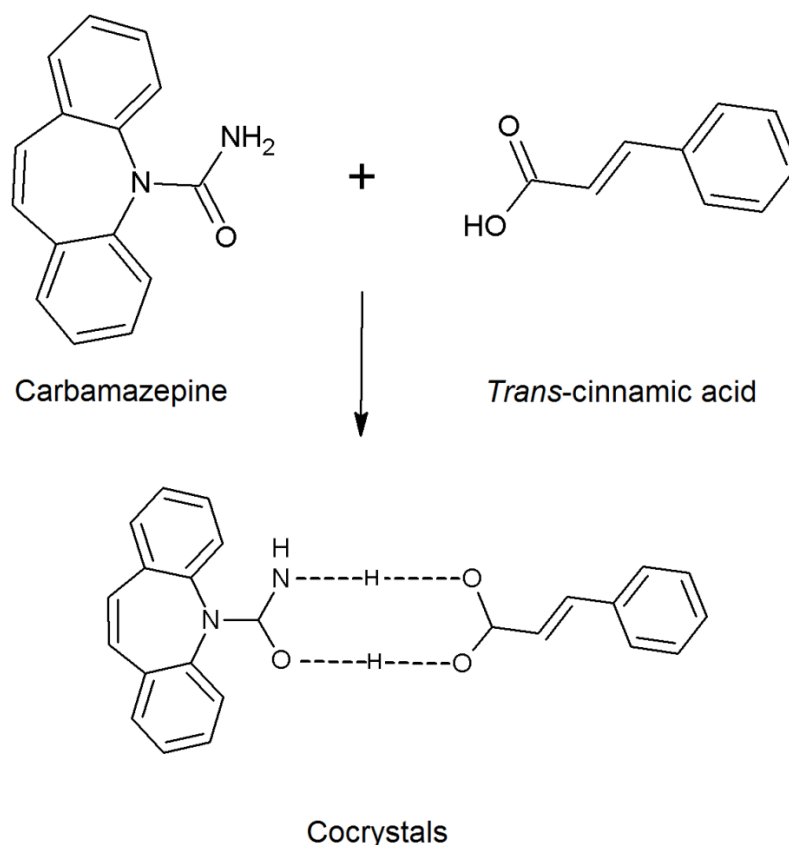
Fig. 3.1. Chemical structures of CBZ, TCA and H-bonding in CBZ-TCA cocrystals (Mcmohan 2006).

3.2.2 Solvent evaporation of CBZ-TCA cocrystals

Cocrystals of CBZ -TCA were produced by the traditional solvent evaporation method and used as reference (prototype) (Mcmohan 2006). Briefly, CBZ and TCA, at a 1:1 molar ratio, were dissolved in ethyl acetate followed by heating for 5 min at 75°C. The prepared solution was left to evaporate for 72 hr and subsequently the dried cocrystals were collected for further evaluation.

3.2.3 HME processing

HME extrusion was performed by using both single screw (RCP 0625, Randcastle, USA) and Eurolab 16 twin-screw extruders (Thermofisher, Germany) without the die. Equimolar amounts (1:1) of CBZ and TCA were accurately weighed and blended thoroughly in a T2F Turbula mixer (Willy A. Bachofen AG, Switzerland) for 10 min. The blend was directly fed into the hot-melt extruder. The temperature of the individual zones of the HME was set up according to the requirements and the screw speed was kept at 10 rpm. During TSE processing samples from different zones of the extruder barrel were collected.

3.2.4 Scanning electron microscopy (SEM)

The morphology of all extruded samples including the bulk CBZ and TCA was examined by SEM (Hitachi SU8030, Japan). Samples were placed on double sided carbon tape sticks on an aluminium stub and coated at room temperature with a thin layer of chromium under an atmosphere of argon. The accelerating voltage of the electron beam used was 2 kV.

3.2.5 Differential scanning calorimetry (DSC)

DSC was used to evaluate the thermal state of the samples including bulk substances, the physical blend and the extruded formulations collected from different barrel zones of the hot-melt extruder. The samples were weighed in crimped aluminium pans and heated from 25°C to 200°C in the DSC (Mettler Toledo 823e, Greifensee, Switzerland) at a heating rate of 10°C/min. Pure nitrogen gas was used as a purge gas, at a flow rate of 50 ml/min. Star software was used for post-experimental analysis of the DSC data.

3.2.6 Hot stage microscopy (HSM)

The HSM analysis was conducted by using a Mettler Toledo FP82HT (Leicester-UK) hot stage instrument together with a microscope (Leica microsystems, China). Samples were scattered on a glass slide and heated from ambient temperature to 200°C at a heating rate of 10°C/min. Thermal events for all samples were collected as a video recording by using a PixeLINK PL-A662 camera (PixeLINK, Ontario, US).

3.2.7   X-ray powder diffraction (XRPD)

XRPD was used to determine the solid state of the bulk materials, physical mixtures and extrudates using a Bruker D8 Advance (Germany) in theta-theta mode. For study purposes a Cu anode at 40 kV and 40 mA, parallel beam Goebel mirror, 0.2 mm exit slit, LynxEye position sensitive detector with a 3° opening (LynxIris at 6.5 mm) and sample rotation of 15 rpm were used. Each sample was scanned from 2 to 40° 2Θ with a step size of 0.02° 2Θ and a counting time of 0.3 sec per step; 176 channels active on the PSD making a total counting time of 52.8 sec per step.

3.2.8   Dissolution studies

Dissolution studies were carried out using a USP II paddle apparatus (Varian 705, US). Samples equivalent to 200 mg of bulk CBZ, CBZ-TCA extruded powders and prototype were placed into 900 ml of 0.1 M (pH 1.2) HCl in each dissolution vessel (n=3). The temperature of the media was maintained at 37°C with a paddle rotation of 100 rpm. About 2-3 ml of samples were withdrawn at 15, 30, 60 and 120 min intervals and filtered using a 200 μm filter prior to HPLC analysis.

3.2.9   HPLC analysis

HPLC analysis was carried out by using an AGILENT 1200 series HPLC (USA) instrument equipped with an auto sampler. The mobile phase was prepared with 60:40 (v/v) ratios of Na mono-phosphate buffer (pH 7.3) and acetonitrile. A Zorbex Eclipse C8 (4.6 mm×150 mm, 5 μm) column from Agilent, USA was used at a flow rate of 1 ml/min using detection at 254 nm wavelength. A calibration curve was constructed by varying the concentration of standard solutions between 10 and 50 μg/ml.

3.2.10 Physical stability

Bulk CBZ and extruded cocrystals were placed in open glass vials and exposed to pre-equilibrated accelerated conditions (75% RH ± 5%) created by using a supersaturated solution of sodium chloride (Sigma Aldrich, Germany) at 40°C ± 2°C for six months.

3.2.11 Particle size distributions

The particle size distribution was measured by laser diffraction (Mastersizer 2000, Malvern, UK), whereby 5 gm of powders were placed in the dry powder feeder. Each sample was measured three times.

3.3 RESULTS AND DISCUSSION

3.3.1 HME processing

Cocrystals were collected in powder form as the die (which is usually placed at the end of extruder to shape the extrudates) was removed. HME temperature profiles were found to play a key role in SSE extrusion and influenced the properties of the cocrystals.

Fig. 3.2. Schematic of the screw in TSE indicating the mixing zones in the HME.

Extrusion trials carried out using SSE revealed that the temperature profile set at a maximum of 135ºC formed extruded cocrystals of better quality compared to those at 125°C. As the spiral screw design of SSE was unable to provide better material mixing (Luker 2012), further optimization of the extruded cocrystals was carried out with TSE equipment by optimizing the temperature. During TSE processing the screw configuration was adjusted to achieve good mixing by assembling the kneading elements in three separate "mixing zones" (Fig. 3.2). Extruded samples were collected from each zone in order to investigate the effect of the kneading elements and provide a better understanding of the cocrystallisation process.
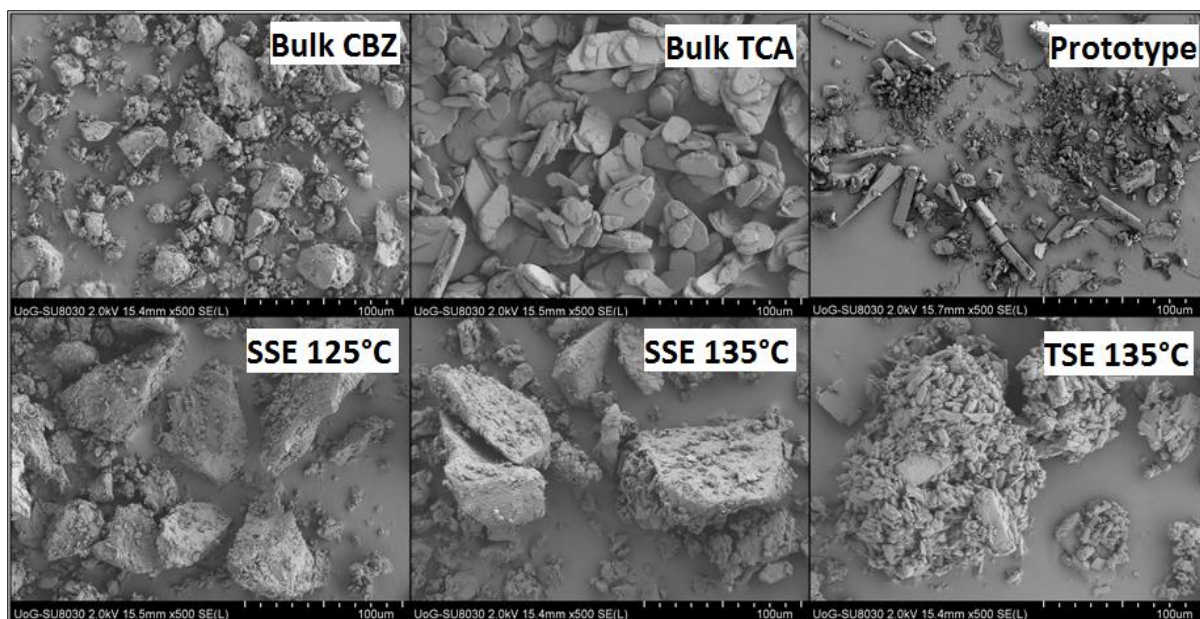
Fig. 3.3. SEM micrographs of bulk CBZ, bulk TCA and cocrystals manufactured by using SSE at 125ºC, SSE at 135ºC and TSE at 135ºC.

SEM analysis revealed differences in the shape and size between extruded cocrystals and bulk components which is a strong indication of the formation of a new phase between the parent components. Bulk CBZ consisted of flaky or thin plate liked materials whilst TCA displayed disc shaped crystals (Fig. 3.3). All HME treated cocrystals were found to be clumped with undistributed geometry, as they did not undergo further particle size reduction. The TSE cocrystals were more clustered compared to those produced via SSE, where several micro-crystals packed together to form larger particles. This could be possibly attributed to the effect of the mixing zones of the twin-screw extruder. The prototype cocrystals were found to be polyhedral prismatic with a smaller particle size distribution compared to the extrudates.

3.3.2 Thermal analysis

DSC was employed to evaluate the thermal properties of the pure components as well as the extruded cocrystals. Analysis of the thermal transition of bulk CBZ indicated the existence of polymorphic form III as the melting peak appeared at 175.14°C (ΔH 15.40 J/g) followed by a subsequent phase transformation leading to the melt at 192.39°C (ΔH 99.93 J/g) (Fig. 3.4). The thermogram of bulk TCA showed an endothermic thermal transition due to its melting at 134.55°C (ΔH 145.47 J/g) (Fig. 3.4). The physical blend of CBZ-TCA, at a 1:1 molar ratio, showed one minor endotherm at 93.92°C (ΔH 4.90 J/g) and two main endotherms at

121.81°C (ΔH 25.49 J/g) and 141.69°C (ΔH 99.40 J/g) as shown in Fig. 3.4. The thermal transition in the PM at 121.81°C corresponds to a eutectic melt and that at 141.69°C represents the melting of cocrystals (Lu et al. 2008).

Cocrystals processed by SSE at 125°C and 135°C showed a single endothermic blunt peak at 137.72°C (ΔH 58.79 J/g) and 138.46°C (ΔH 61.67 J/g), respectively. The endothermic peak suggests a single structured system while the blunt shape of the peak points to the presence of amorphous or unreacted crystalline portion of the material left in the SSE extruded products. Despite the fact that SSE produced high torque, sufficient to form cocrystals, the lack of dispersive mixing resulted in low quality (reduced crystallinity) cocrystals.
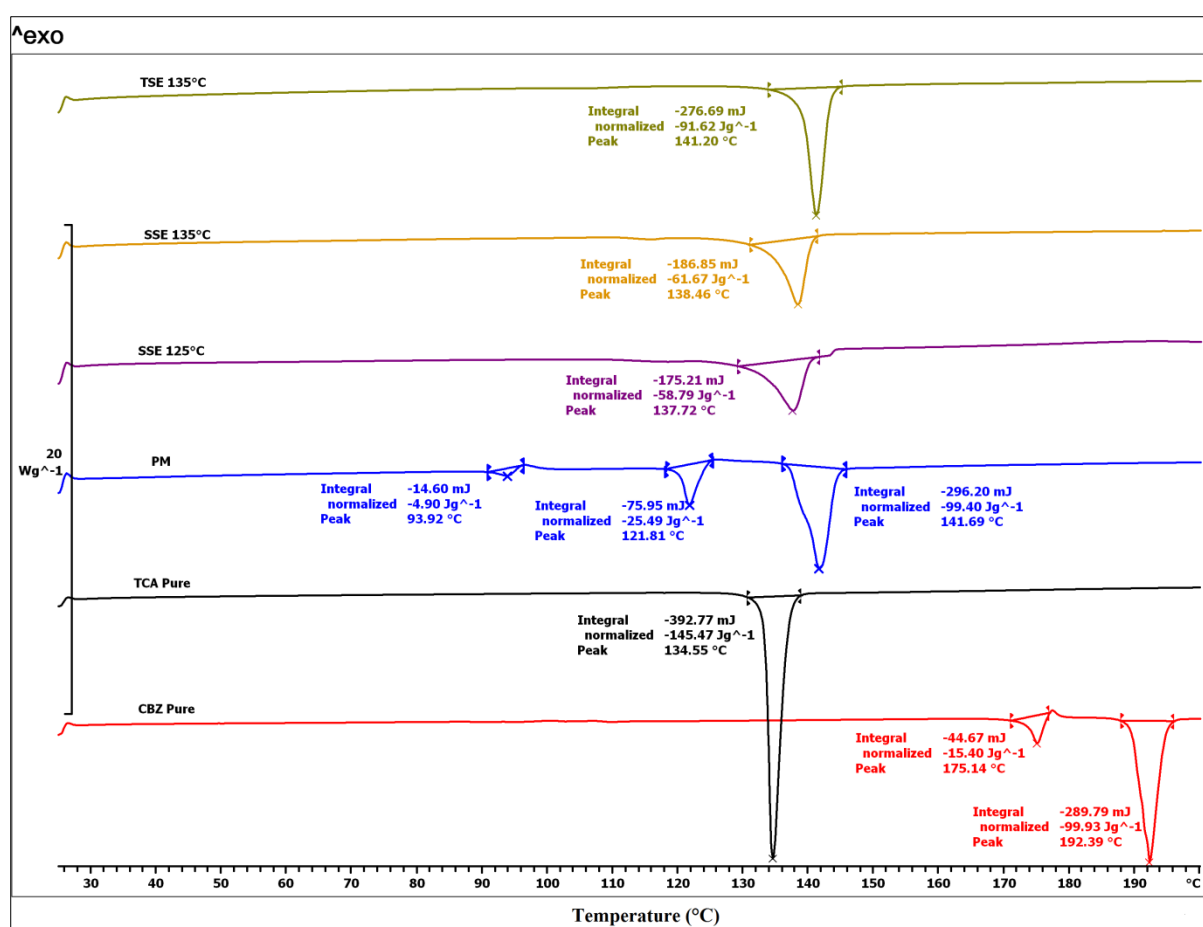
Fig. 3.4. DSC thermograms of bulk CBZ, bulk TCA, cocrystals processed with SSE125ºC, SSE135ºC, TSE135ºC and the PM.

A single, sharp endothermic peak was observed in the thermogram (Fig. 3.4) of the extruded cocrystals processed using TSE135°C, which is quite similar to that of the prototype cocrystals obtained by the solvent crystallization process. The thermogram of the CBZ-TCA

52

cocrystal processed via TSE showed a sharp melting transition at 141.20°C (ΔH 92.62J/g) while the prototype at 143.08°C (ΔH 114.46 J/g).
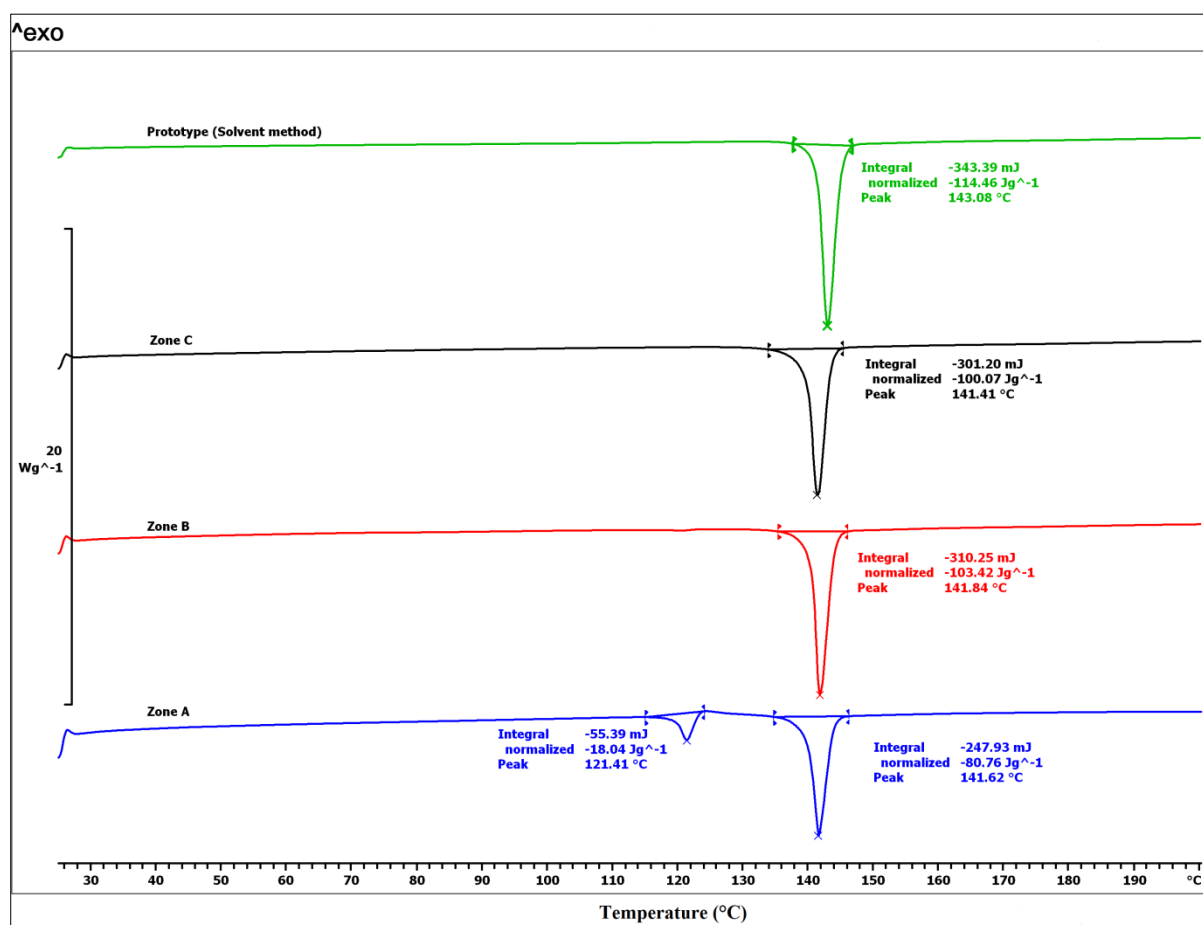
Fig. 3.5. DSC thermograms of samples collected from different mixing zones in TSE with the prototype prepared by the solvent method.

Furthermore, the data in Fig. 3.5 shows the DSC thermograms of the materials collected from three different mixing zones during TSE processing. By comparing the thermograms of the samples collected from zone-A and the PM (Fig. 3.4) it can be seen that they are almost identical (except the peak at 93.92°C) suggesting no major cocrystal transformation of the processed blends.

In contrast, the thermal transitions of the processed materials collected from zone B presented a sharp melting peak at 141.84°C which corresponds to the final melting point of the stable cocrystals but with some evidence of unreacted material at 121.41°C. The complete formation of CBZ-TCA cocrystals occurred in zone C where the absence of the small endothermic peak is evident.
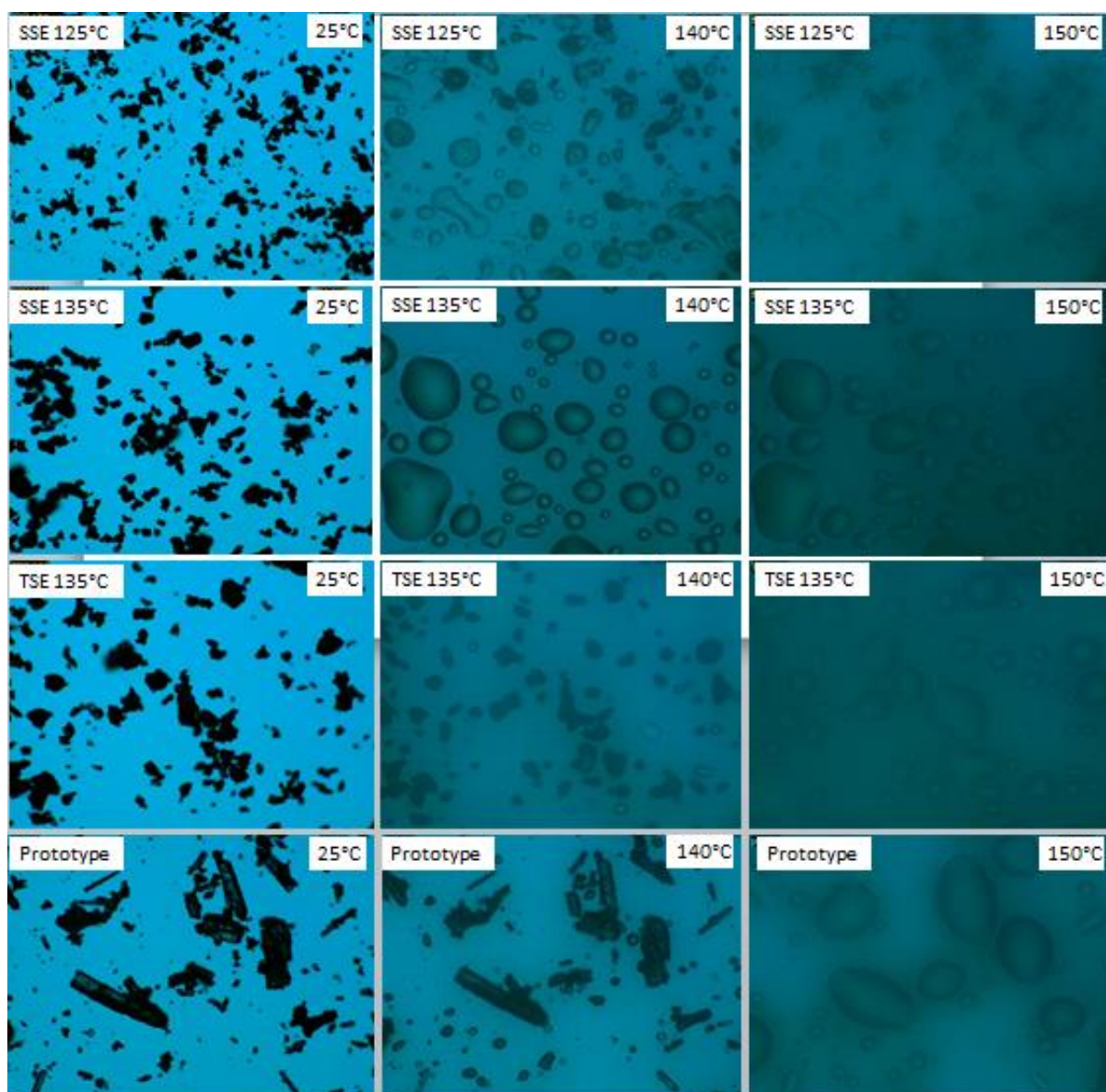
Fig. 3.6. HSM images of cocrystals manufactured by using SSE, TSE and the prototype.

HSM studies were conducted to visually determine the thermal transitions at different stages of heating. DSC results were in good agreement with HSM findings. Cocrystals processed by SSE (125°C) melt at 138°C in HSM; nevertheless, some untreated materials were observed even above 150°C. However, vapour produced from the sample made the image a bit darker which eventually cleared at around 185°C. It was assumed that the evaporation is related to the melting of the remaining CBZ in the cocrystal. Interestingly, this was not the case for the extruded cocrystals processed both by SSE and TSE at 135°C. As shown in Fig. 3.6 cocrystals extruded at 135°C presented different melting behaviour, depending on the

extrusion processing whereas for SSE and TSE melting occurred at 138.46°C and 141.20°C, respectively.

3.3.3 XRPD analysis

XRPD diffractograms of pure components, the physical blend, cocrystals (SSE, TSE and solvent method) and materials collected from different mixing zones of the hot-melt extruder are illustrated in Figs. 3.7 and 3.8. In the data in Fig.3.7 it can be seen that cocrystals processed by using SSE at 125°C and 135°C showed lower intensity peaks indicating the presence of unprocessed cocrystals. In contrast, cocrystals processed via SSE at 135°C presented higher intensity diffraction peaks compared to SSE at 125°C.
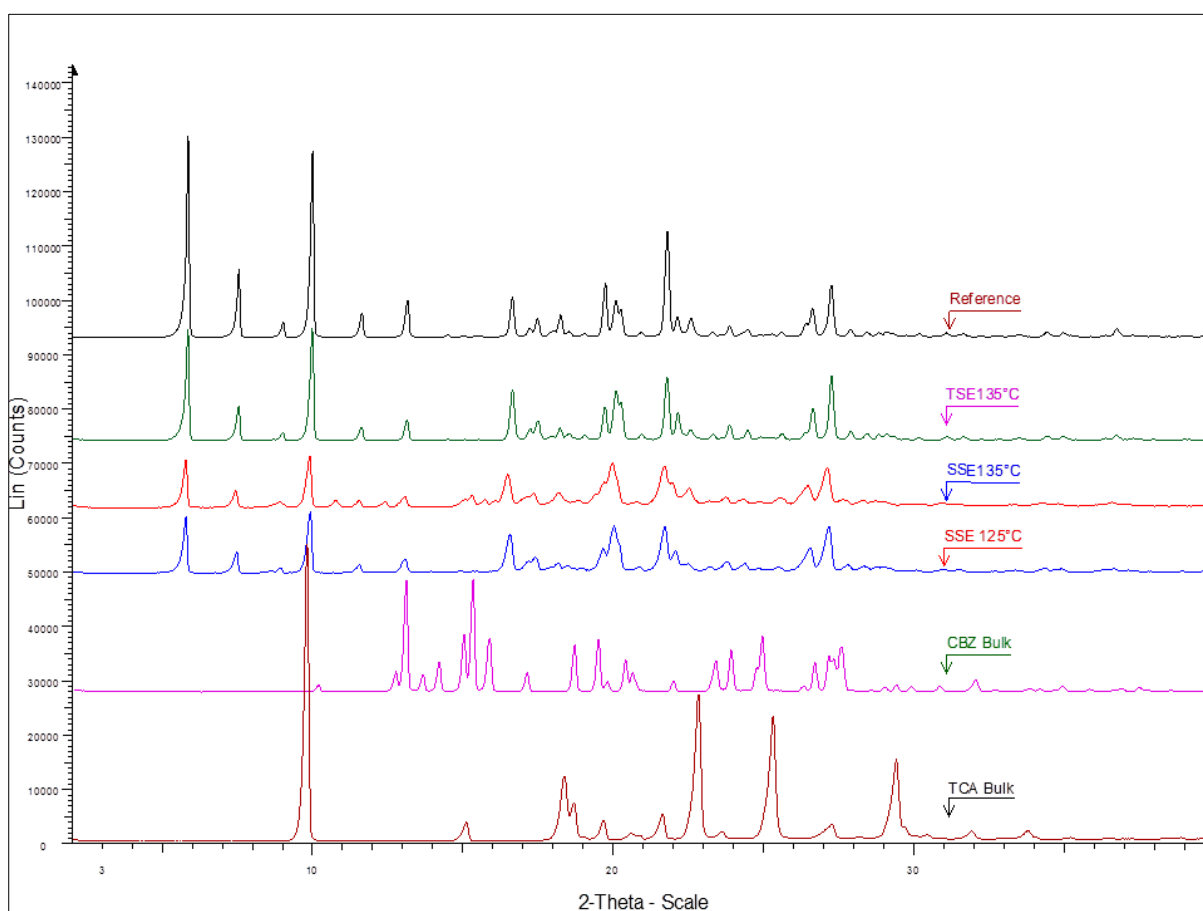
Fig. 3.7. X-ray powder diffractograms of bulk CBZ, bulk SCH, SSE125ºC, SSE135ºC, TSE135ºC and reference cocrystals.

In Fig. 3.8 it can clearly be seen that the formation of cocrystals started in the 2nd mixing zone (zone-B) and new intensity peaks appeared at 5.78° and 7.57° 2θ values. The same peaks with very low intensity were observed in zone-A including identical XRPD peaks that

correspond to bulk CBZ and TCA. It is obvious that both components started to interact at a molecular level in zone-A whilst in the 2nd mixing zone (zone-B), the peaks at 15.30°, 15.87°, 24.94° 2θ are eliminated. Finally, the formation of cocrystals was completed in zone 3 with the appearance of diffraction peaks at 5.83°, 7.57°, 9.91°, 16.66°, 21.82°, and 27.33° 2θ values which are identical to those of the prototype. Apparently, the screw configuration in zone-B played a crucial role for the initiation of the cocrystallisation process while the placement of the mixing elements at 60° and 90° angles in zone 3 resulted in cocrystals with improved crystallinity.
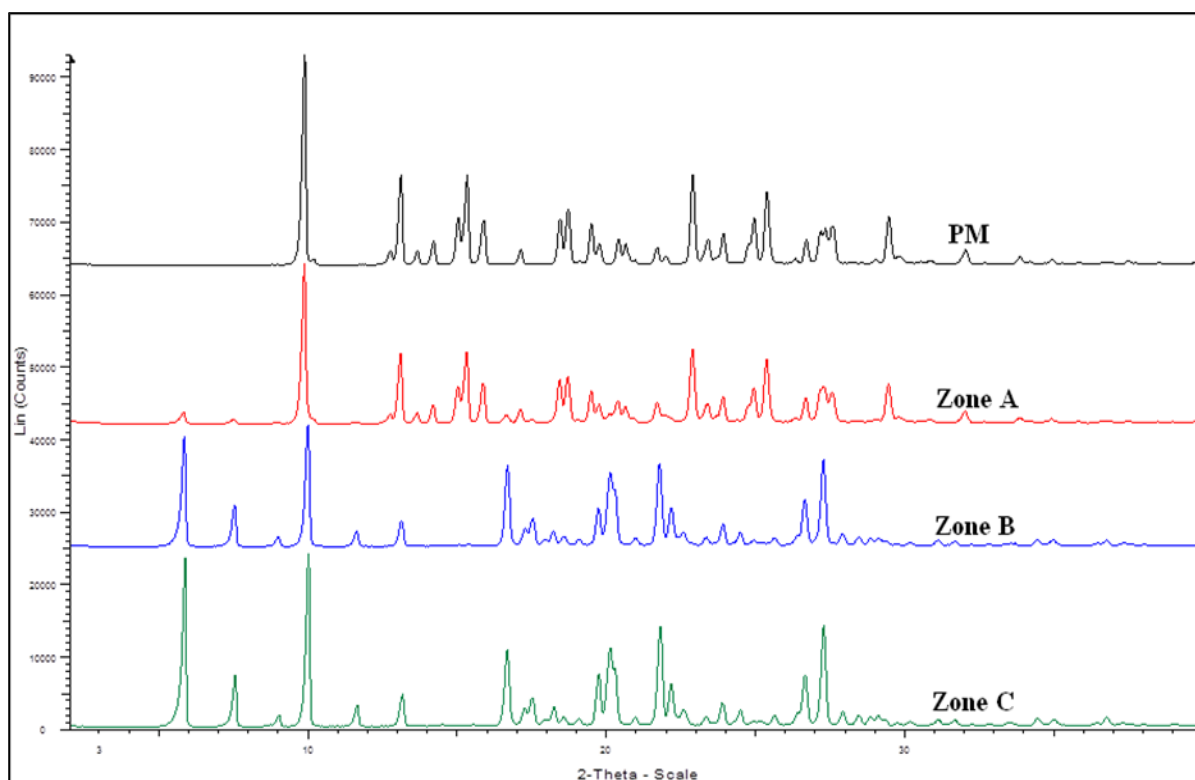
Fig. 3.8. X-ray powder diffractograms of the PM and samples collected from the TSE barrel zones (A, B and C).

3.3.4 Dissolution studies

Dissolution studies were conducted in order to assess the performance of the cocrystals produced compared to bulk CBZ. A slow dissolution rate of 49% after 2 hr was observed for bulk CBZ (Fig. 3.9). In contrary, SSE processed cocrystals at 125 and 135°C showed significant enhanced dissolution rate with more than 50% after 1 hr. However, the dissolution of the SSE125°C cocrystals was limited to 60% after 120 min, while the SSE135°C samples

reached a maximum of 76% dissolution after 120 min. Nevertheless, the TSE135°C cocrystals presented the higher dissolution rates with 50% drug release within the first 10 min and 70% after 1 hr. TSE and prototype cocrystals showed 80% drug release after 120 min but overall drug dissolution of TSE cocrystals was higher than prototype. The SSE cocrystals showed fast dissolution rates especially for the first 60 min in comparison to the prototype, but slower compared to the TSE135°C. Nevertheless, Dissolution study suggested the faster dissolution rates are related to the higher purity of the developed cocrystals. In addition, as shown in Fig. 3.10 the influence of the particle size distribution was excluded as bulk CBZ presented smaller particle size while the extruded samples and the prototype consisted of larger particles.
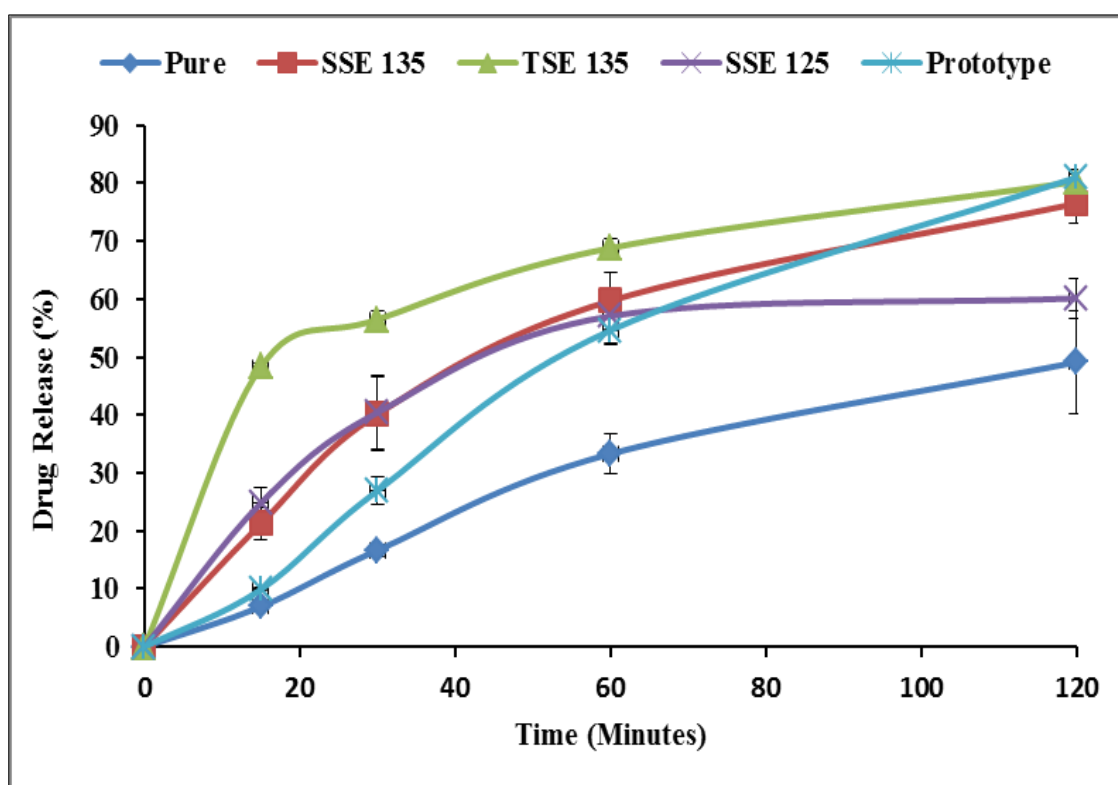
Fig. 3.9. Dissolution profiles of bulk CBZ, prototype cocrystals (solvent evaporation method), extruded cocrystals of SSE (processed at 125°C and 135°C) and TSE processed cocrystals at 135°C.
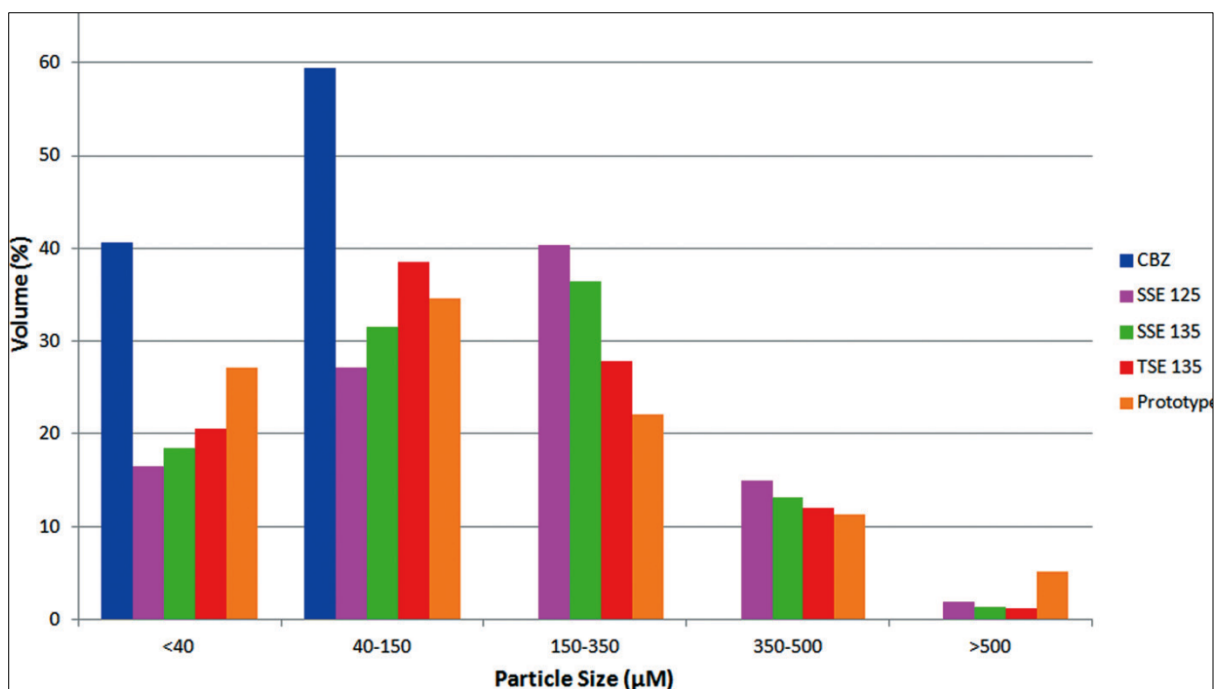
Fig. 3.10. Particle size distribution of bulk CBZ, extrudates (SSE125ºC, SSE135ºC and TSE135ºC) and prototype.

3.3.5 Physical stability

Stability studies of the cocrystals produced by HME (SSE and TSE) under accelerated conditions (40°C and 75% RH) showed excellent stability without any changes in crystallinity after 6 months. Furthermore XRPD analysis showed identical peak intensities of the cocrystals as a result of crystal integrity. In addition, no visual alterations in morphology or colour of cocrystals were observed.

3.4 CONCLUSIONS

In this study, cocrystals of CBZ-TCA were extruded by using SSE and TSE. A small amount of cocrystals was extruded first in the primary study by using SSE, two temperature profiles were chosen and an appropriate temperature from those SSE experiments was further applied in the TSE. For comparative purposes, prototype cocrystals were prepared by using a solvent evaporation method. SEM, DSC, HSM and XRPD analysis were performed on all the extruded cocrystals including the prototype. By SEM, a different shape of cocrystals were seen for extrudates compared to prototype due to the different processing technique used to prepare the cocrystals. In DSC, SSE extrudates gave a single endotherm; however, the low intensity and broad shape of the endotherm for SSE cocrystals indicated unprocessed

cocrystals due to an unreacted traces of the PM. HSM results of SSE125ºC cocrystals showed an unreacted CBZ from PM which was melting at around 185ºC. Cocrystals prepared by TSE at 135ºC barrel temperature, showed a sharp, single endothermic peak which was similar to the prototype cocrystals. XRPD analysis (performed on all extruded cocrystals, bulk components and prototype cocrystals) showed similar XRPD profiles for the TSE and prototype cocrystals. SSE cocrystals were found to have less intense diffraction peaks compared to TSE and prototype cocrystals indicating less crystallinaty of SSE cocrystals compared to the TSE and prototype cocrystals. One of the aims of formulating the cocrystals was to increase the solubility of CBZ. Dissolution carried out at pH 1.2 showed lower to higher rate of dissolution as per purity of cocrystals. The dissolution rates of the cocrystals were found to increase in the ascending order of bulk CBZ< SSE< prototype < TSE. Twin screw extrusion processing produced cocrystals with a faster dissolution rate compared to both single screw extrudates and the prototype.

Off-line DSC and XRPD performed on samples collected from different zones of the barrel during twin screw extrusion showed gradual formation of cocrystals along the side of the barrel. Mixing zone B in the middle of the extruder barrel was found to play a major role in the production of the cocrystals. Cocrystal formation started in zone A which was similar to the PM; however, the major diffraction peaks for the cocrystals were found in zone B and final cocrystal formation occurred in zone C.

Overall, continuous approaches for the manufacture of CBZ-TCA cocrystals was established by using hot melt extrusion with an increase in the rate of dissolution of CBZ.

CHAPTER 4 : INCREASED DISSOLUTION RATES OF CARBAMAZEPINE-D-GLUCONO-δ-LACTONE BINARY BLENDS PROCESSED BY HME

4.1 INTRODUCTION

Increasing the aqueous solubility and thus the dissolution rate of poorly water soluble drugs has always been a concern for pharmaceutical and formulation scientists as the majority of drug molecules fall into the low solubility class. To achieve the desirable bioavailability, the drug molecule must be dissolved in gastric fluid so that it can permeate and be easily absorbed in the intestine (Rubinstein 2010). Therefore, it is essential to achieve the desired solubility and thus dissolution rate of water insoluble APIs in order to achieve a better pharmacological effect.

The proper selection of suitable drug carriers for an API using different formulation strategies can be used to increase the dissolution rate of poorly water soluble APIs. Hydrophilic carriers dissolve more rapidly in aqueous media and thus facilitate faster dissolution rates of drugs (Prajapati et al. 2007). However, various physicochemical properties of the carrier (such as porosity, hydrophobicity; particle size and surface area) can significantly influence the dissolution properties of the API (Talukder et al. 2011, Fang Tian et al. 2007). It has been reported that various carriers such as superdisintegrants, polymers, sugars and lipids can be used in order to enhance the dissolution of poorly water-soluble drugs (Saharan et al. 2009). Numerous reported research studies on carbamazepine (CBZ) with various carriers - such as D-glucosamine, β-cyclodextrin complex, lactose or microcrystalline cellulose, hydrophilic swellable polymers, polyethylene glycol, and others - have shown an effect on dissolution of the poorly water soluble CBZ (Javadzadeh et al. 2007, Kou et al. 2011, Moneghini et al. 2002, Rane et al. 2007)

Polymorphism has always been an interesting area of research, as in many cases it has been found to occur unexpectedly during e.g. different manufacturing processes (e.g. solvent methods or mechanical manufacturing process like grinding, milling, compression, and granulation or even during the storage period of drying process) (Lefebvre and Guyot-Herman 1986, Otsuka et al. 1997, Davis et al. 2004, Guo et al. 2011). Polymorphism is

known as the ability of a compound to be arranged in different structures in a crystalline lattice by changing molecular orientation and position. Being different in crystalline structure, lattice energy and molecular conformation the polymorphs present differences in melting point, physical and chemical stability, solubility, dissolution and bioavailability of the parent API polymorphic form (Allen et al. 2009, Vippagunta et al. 2001); all the foregoing properties may vary among the polymorphs of the same active substance. Modifications in crystal habit and packaging of polymorphs may also have an effect on their mechanical properties (Sun and Grant 2001)

CBZ is a poorly water soluble antiepileptic drug which has four known polymorphic forms: the triclinic (form I), the trigonal (form II), the P-monoclinic (form III) and the C-monoclinic (form IV) (Grzesiak et al. 2003). Form III has the lowest free energy and is considered as the most stable but exhibits low aqueous solubility. CBZ exhibits enantiotropic polymorphism which implies the transition temperature is below the melting point of either of the polymorphs at which both these forms (I & III) have the same free energy (Behme and Brooke 1991).

Studies of tablets prepared using different CBZ polymorphs have been compared with the marketed product Tegretol™ and showed variability in dissolution rates which did not correlate precisely in human trials (Elqidra et al. 2004). These findings were also supported by using an artificial stomach-duodenum model (Carino et al. 2006) but, most importantly, revealed an increased initial dissolution rate of CBZ form I compared to those of form III and the dihydrate form (Kobayashi et al. 2000, Otsuka et al. 1999). According to Kobayashi et al. (2000) the solubility of Form I and III has been reported as 500 and 460.2 µg/ml, respectively at 37°C. Furthermore, Nair et al. (2002) showed that CBZ-PEG formulations with increased amounts of PEG resulted in the transformation of CBZ form III into CBZ form I.

Hot melt extrusion (HME) has been adopted as an emerging approach in pharmaceutical research and development. HME is considered as an economic, continuous processing methodology which is easy to scale up and solvent free. It has successfully been applied in various pharmaceutical applications such as taste masking of bitter drugs, sustained release, production of drug incorporated films, cocrystallisation and implants (Almeida et al. 2012, Dhumal et al. 2010). In the current study, for the first time, CBZ was extruded with D-glucono-δ-lactone (DGL) at various molar ratios in order to enhance the dissolution rate of

the drug. DGL is a Food Standard Agency listed additive (FSA 2013) and is hydrophilic. Previous investigations revealed that DGL in solid dispersion formulations containing CBZ was able to improve the dissolution rate of CBZ (Al-Hamidi et al. 2010). The aim of the present study is to explore the potential use of DGL to enhance the dissolution rate of CBZ processed via HME. The molar ratio of drug: carrier and the solid state properties of CBZ in hot-melt extrudates were also investigated.
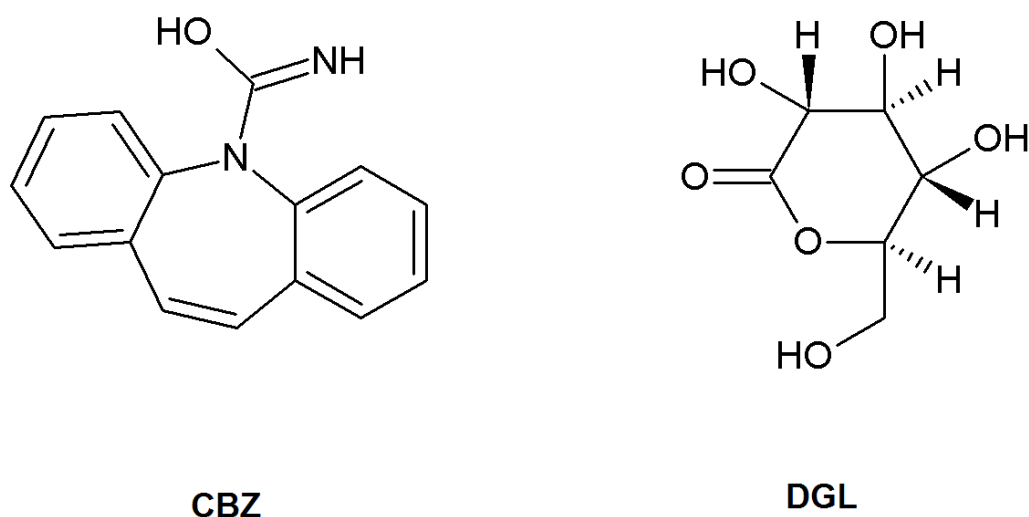
Fig. 4.1. Chemical structures of CBZ and DGL.

4.2   MATERIALS AND METHODS

CBZ and DGL were purchased from Sigma Aldrich, UK and used as received without any further treatment.

4.2.1   HME process

Three different batches of CBZ and DGL at molecular ratios of 1:1, 1.5:1 and 2:1 were accurately weighed. All prepared mixtures were then mixed for 10 min using a T2F turbula blender (Willy A. Bachofen AG, Switzerland). Physical blends were extruded by using a co-rotating twin screw hot melt extruder (Pharmalab-16, Thermo Fisher, Germany). The highest temperature in the barrel was set at 140°C with a screw speed of 10 rpm. The extruded material was directly collected from the extruder and analysed in terms of thermal, physical and dissolution behaviour. The preferred elevated temperature profile, applied throughout the HME barrel was 30/90/125/140/140/140/140/140/130°C.

4.2.2 Particle size measurements

The particle size distribution of all the formulations was obtained using a dry powder dispersion unit (Scirocco 2000) incorporated in a Malvern Mastersizer 2000 (Worcestershire, UK) laser diffraction particle size analyser. Three particle size distribution measurements were made in continuous sequence for reproducibility of each batch. Calculations of particle size were received automatically from the Mastersizer 2000 software.

4.2.3 Scanning electron microscopy (SEM)

The morphology of all extruded samples, bulk CBZ and DGL were examined by SEM (Hitachi SU8030, Japan). Samples were placed on a thin layer of Mikrostik non-conductive adhesive (Agar scientific, UK) on an aluminium stub and coated with chromium under an atmosphere of argon at room temperature. The accelerating voltage of the electron beam used was 2 kV in order to obtain SEM images.

4.2.4 Differential scanning calorimetry (DSC)

All three batches of extruded material, the physical mixture (PM), pure CBZ and DGL were analysed using DSC (Mettler-Toledo 823e, Greifensee, Switzerland). Around 4-6 mg of sample were weighed and loaded in sealed aluminium pans. The pans were heated from ambient temperature to 220°C at a heating rate of 10°C/min and compressed nitrogen gas was used to purge the samples.

4.2.5 Hot stage microscopy (HSM)

Visual thermal analysis was conducted by HSM using a Mettler Toledo FP82HT instrument, (Leicester, UK) supplied with a microscope (Leica microsystems, China). Small amounts of samples were placed on glass slides and heated from ambient temperature to 220°C at 10°C per min heating rate. Changes in morphological behaviour were recorded in a video format by using a Pixelink PL-A662 camera (PixeLink, Ontario, US).

4.2.6 X-Ray powder diffraction (XRPD)

XRPD data for all samples was performed in theta-theta scanning mode with reflection mode by using a Bruker D-8 Advance (Germany) XRPD instrument. All samples were scanned with step size of 0.02 degrees and 0.3 sec per step counting time. All samples were packed into low background SI - sample holders in order to reduce background noise and scanned

from 2 to 40 °2θ by employing a Cu anode X-ray tube (40 kV and 40 mA). The sample holder was rotated at 15 rpm.

4.2.7 Dissolution studies

Dissolution studies were conducted by using a USP dissolution apparatus I. Samples equivalent to 200 mg of CBZ, including bulk CBZ and PMs were placed in the basket of the dissolution apparatus with 900 ml of 0.1 M HCl at pH 1.2 as a dissolution medium at 100 rpm rotation and 37°C temperature. Samples were withdrawn every 10 min from the dissolution vessels via a peristaltic pump attached to the apparatus and evaluated at 285 nm with a UV spectrometer connected to the dissolution device.

4.3   RESULTS AND DISCUSSION

4.3.1   HME process

All samples extruded from the hot-melt extruder were collected in solid, ground form without attaching the die at the end of the hot-melt extruder. Slow screw rotation rates (10 rpm) were employed, which resulted in increased residence times and excellent mixing of the materials. The highest temperature used along the extruder barrel was fixed at 140°C, as the aim of this study was to examine the effect of the molar ratio of the drug:carrier on the extrusion process and, subsequently, dissolution of the materials obtained.

The morphology of extrudates and bulk materials was studied using SEM. In the case of bulk CBZ flaky, micronized, thin plate like crystals were obtained, whilst bulk DGL presents block shaped particles (Fig. 4.2). The hot-melt extruded samples displayed completely different particle morphologies compared to the bulk materials. Batches of hot-melt extruded CBZ presented elongated (needle shape) crystals which could be an indication of the presence of a different CBZ polymorphic form compared to the untreated CBZ (F. Tian et al. 2007), and they appeared to be stacked together. It is possible that due to the applied shear, temperature and the mixing effect of the extrusion screws inside the barrel of the hot-melt extruder a polymorphic transformation of CBZ is facilitated (Fig. 4.2). It has been previously proved that the temperature profile, screw speed and configuration play a key role in CBZ transformation and more specifically in the formation of cocrystals (Dhumal et al. 2010, Moradiya et al. 2014a).
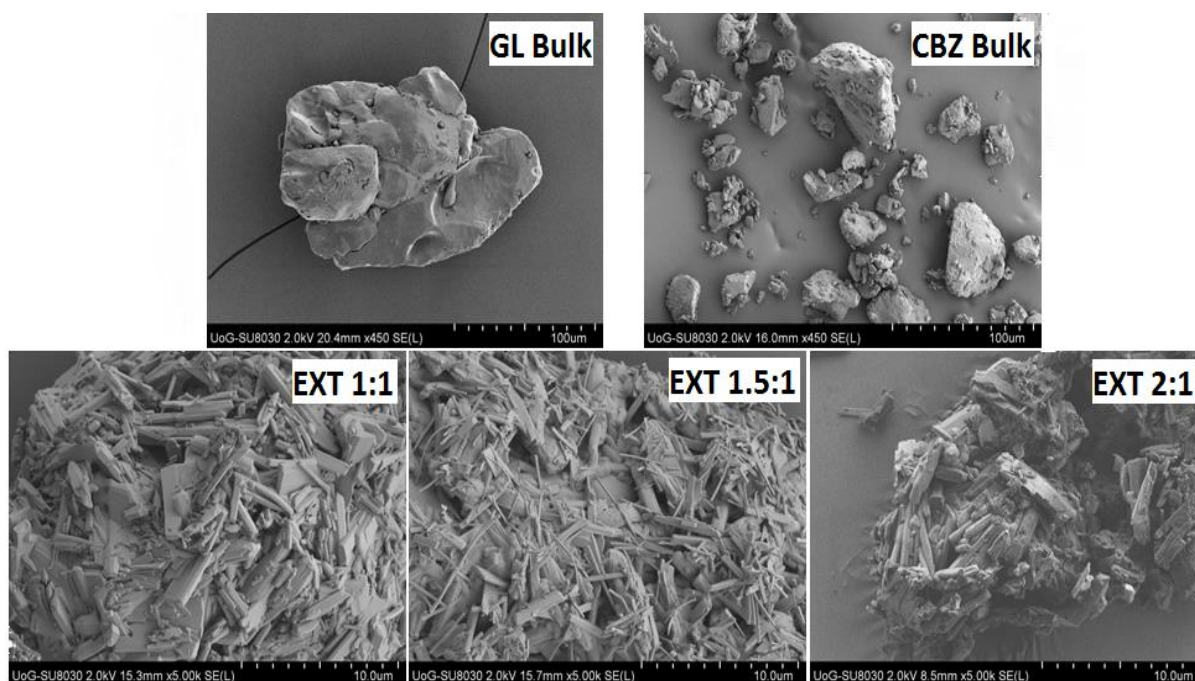
Fig. 4.2. SEM images of bulk CBZ, DGL and different molar ratios of CBZ:DGL HME processed extrudates.

4.3.2 Thermal analysis

DSC was employed to evaluate the solid state of the pure components as well as the extrudates. The thermogram of CBZ showed a small endothermic peak at 175.5°C followed by any exothermic event while a sharp endotherm occurs at 191.6°C indicating the melting of form I CBZ. This small exothermic peak is characteristic of the transition of the anhydrous monoclinic b-form (form III) to the polymorphic form I and occurs via a solid-solid transformation. The thermogram of DGL showed a sharp endothermic peak at 168.0°C (Fig. 4.3).
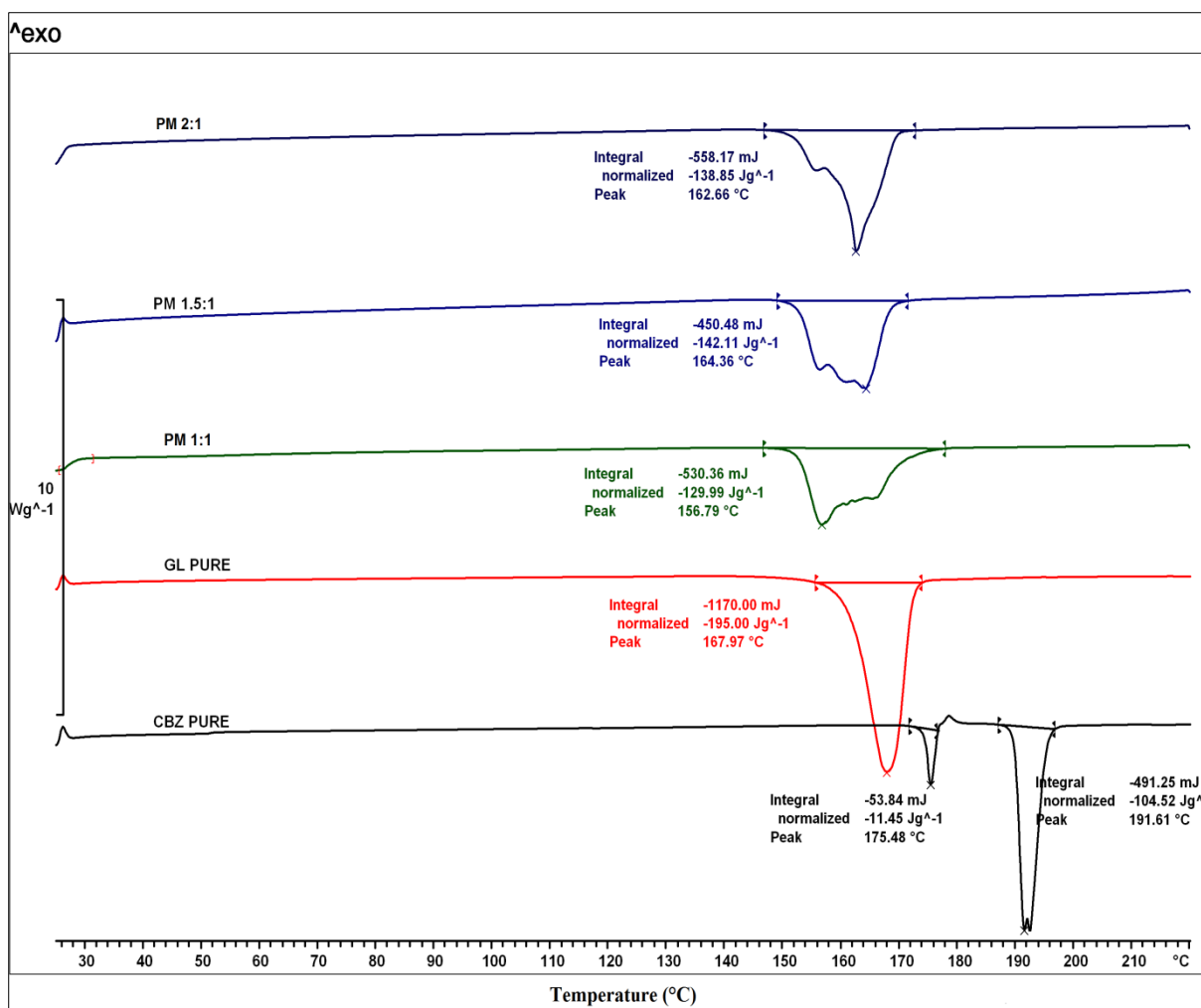
Fig. 4.3. DSC thermograms of bulk CBZ, DGL and PMs of CBZ/DGL at molar ratios of 1:1, 1.5:1 and 2:1.

In contrast, the absence of CBZ peaks at 175.48°C and 191.61°C in all the physical blends pointed to the melting of all the components in a single lattice during the DSC heating cycle. The melting endotherms of all PMs showed irregular patterns suggesting the presence of more than one melting peak in close proximity, and varied from 156.79°C to 164.36°C (Fig. 4.3). Similarly, the DSC thermograms of the extruded batches at 1:1 and 2:1 ratios presented double endothermic peaks at 159.61°C and 156.94°C, respectively. Interestingly, the extruded batches at a ratio of 1.5:1 showed a single endothermic peak at 155.68°C. However, DSC analysis did not reveal the type of CBZ polymorph in the hot-melt extruded blends (Fig. 4.4).
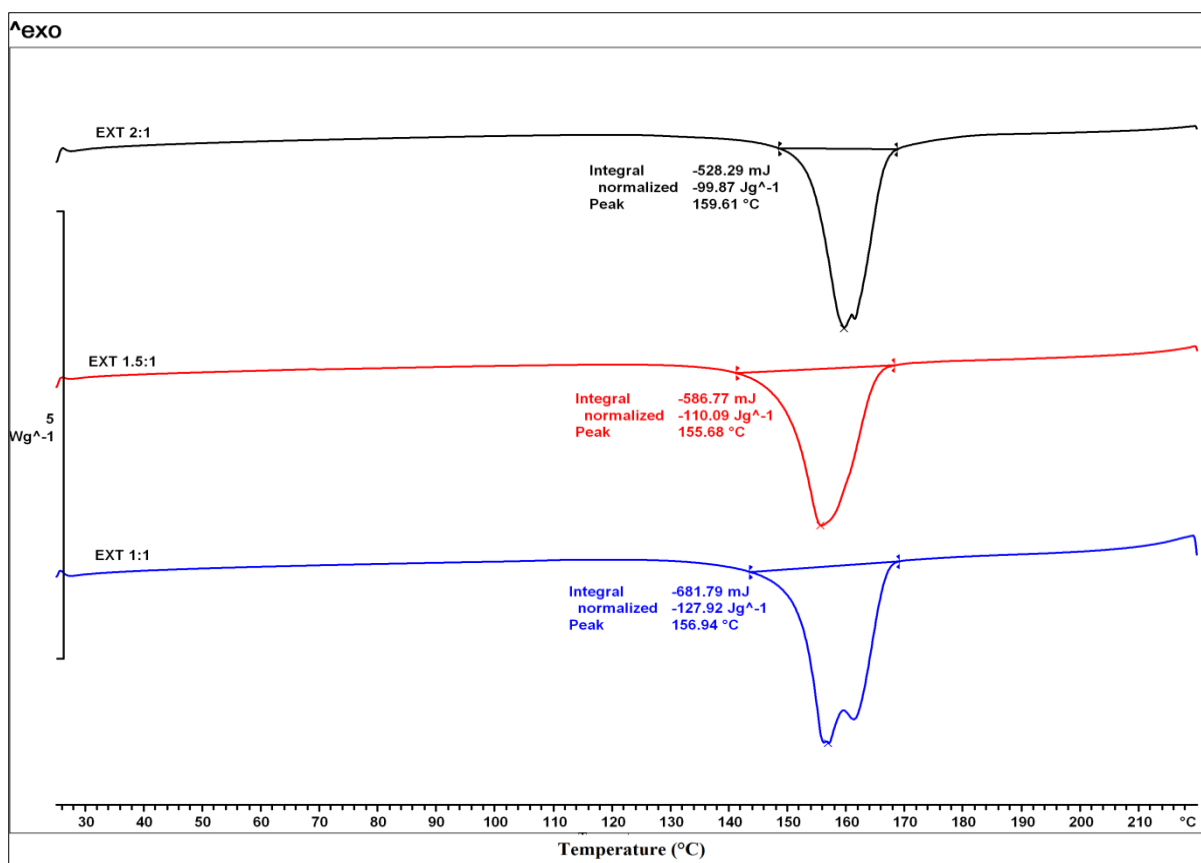
Fig. 4.4. DSC thermograms of hot-melt extruded samples at molar ratios of 1:1, 1.5:1 and 2:1 CBZ:GNL.

In order to attain a better understanding of the transformation of CBZ due to HME processing the samples were further analysed by using HSM. For all PMs, initial CBZ crystallisation was observed around 159°C and needle shaped crystals were observed indicating the presence of form I polymorph. The sample crystallisation continued leading to melting of the extrudates between 172-183°C, depending on the CBZ-DGL ratio. However, it is still impossible to distinguish the melting of individual components in the PMs or the extrudates via HSM. In contrast to the PMs the HSM analysis of the extrudates did not show the formation of CBZ needle shaped crystals but only the melting of the samples. Thus, we assumed that any CBZ transformation took place during HME. Nevertheless, it is obvious that the presence of DGL plays an important role in CBZ polymorphic transformations facilitating the formation of polymorph form I.
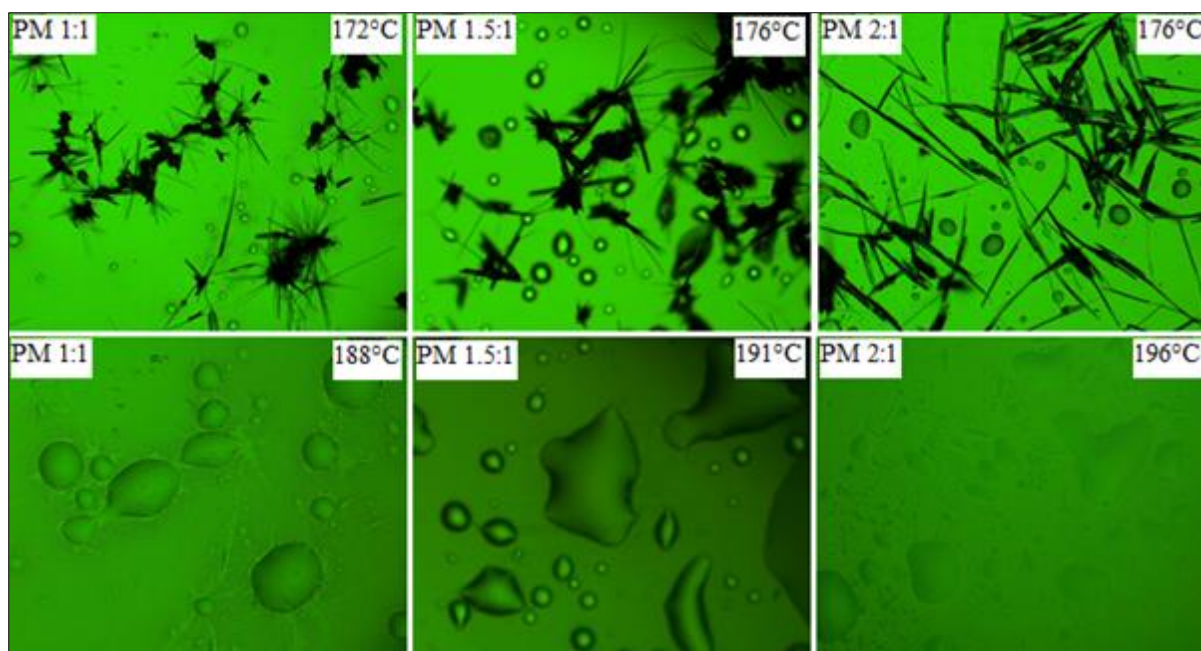
Fig. 4.5. HSM images of PMs of CBZ/DGL at different temperatures.
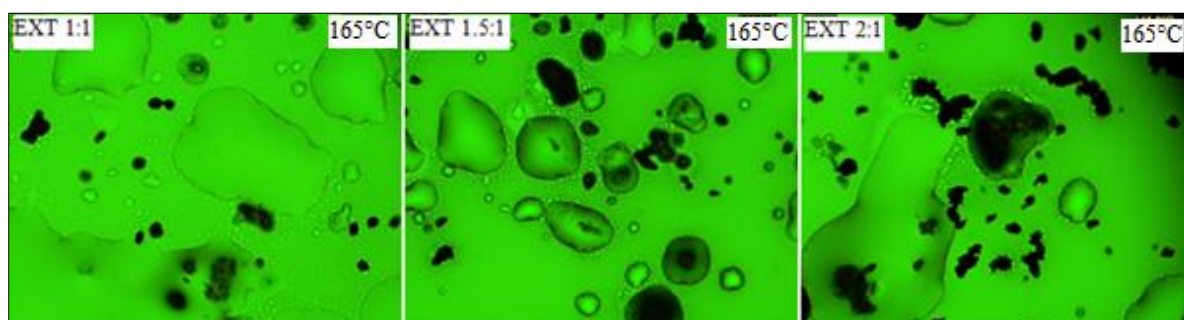
Fig. 4.6. HSM images of hot-melt extruded materials at ratios of 1:1, 1.5:1 and 2:1 CBZ/DGL at 165°C.

4.3.3 XRPD analysis

XRPD analysis was carried out for all the extruded formulations as well as the physical mixtures and pure (bulk) substances to determine the polymorphic state of CBZ. The data in Fig 4.7 illustrates the diffractograms for bulk CBZ, DGL and their PMs at different molar ratios. Pure CBZ showed distinct XRPD peaks at 13.07°, 15.31°, 19.49°, 24.96° and 27.24° 2θ values which are typical of form III while for DGL peaks were observed at 17.88°, 23.87°, 26.72°, 27.28° 2θ values. Fig 4.7 shows the presence of typical drug and carrier intensity peaks for the PMs indicating that no solid transformations or interactions occurred between CBZ and DGL. Peaks of increased intensity for CBZ can be seen in the diffractograms with

higher CBZ ratios and *vice-versa*. As shown in Fig. 4-8, both CBZ and DGL remained in the crystalline state in all extruded formulations. However, it is evident from the diffactograms of extrudates that bulk CBZ (form III) was transformed to form I during extrusion with characteristic peaks at 7.99°, 9.41°, 12.29°, and 19.91°2θ values, which were consistent with reported studies (Grzesiak et al. 2003).
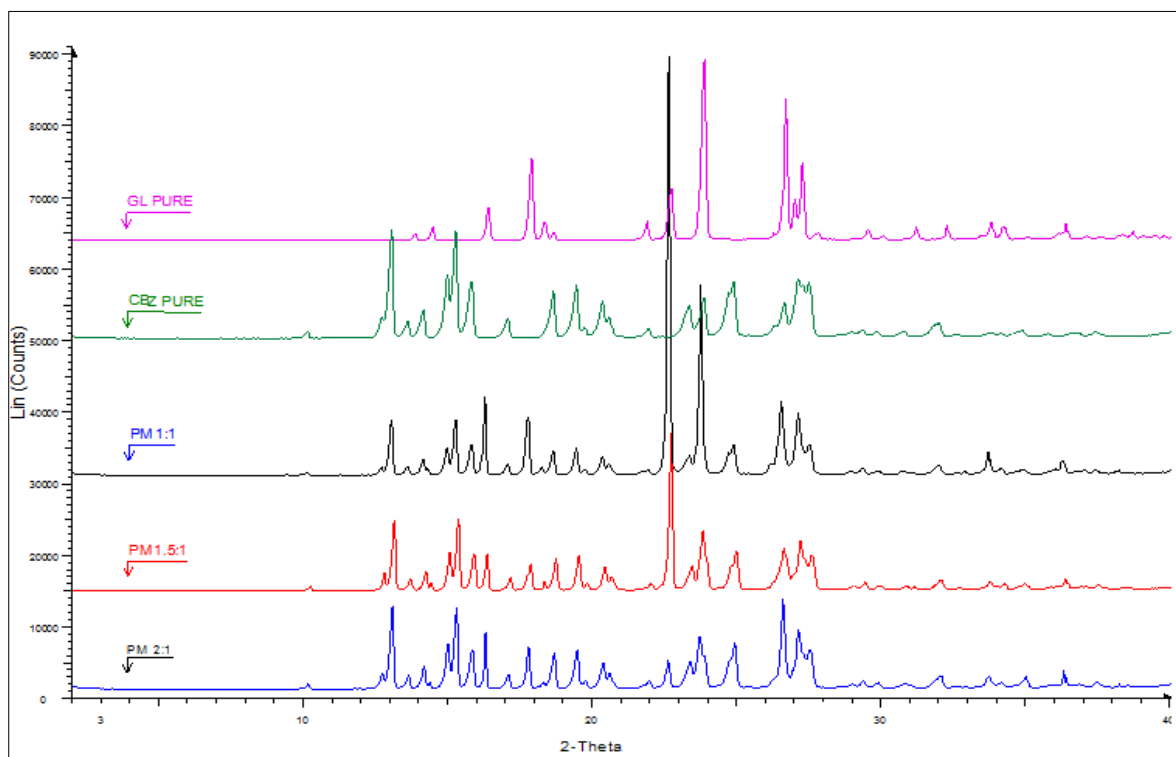
Fig. 4.7. XRPD patterns of bulk CBZ, GNL and PMs at 1:1, 1.5:1 and 2:1 molar ratios of CBZ/ DGL.

The XRPD peak intensities of the extruded samples increased with increasing CBZ ratios. Interestingly some of the XRPD peaks at 14.99°, 15.31° and 15.89° 2θ values corresponding to form III CBZ (indicated with * in Fig. 4.8) could be identified at 1:1 and 2:1 ratios of CBZ-DGL extrudates. These peaks could not be observed at a ratio of 1.5:1 suggesting a complete transformation to form I during HME processing.
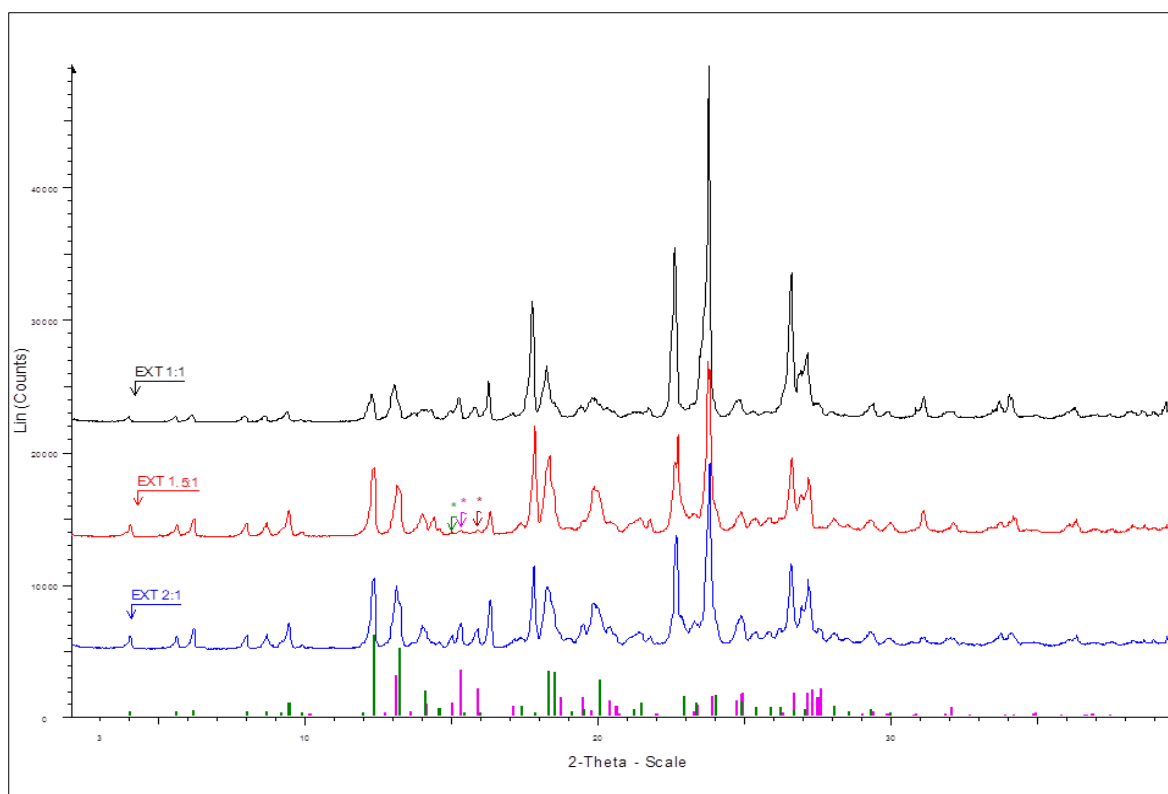
Fig. 4.8. XRPD patterns of extruded CBZ/DGL (1:1, 1.5:1 and 2:1 molar ratios).

4.3.4 Dissolution studies

Dissolution studies revealed interesting results for the dissolution of the PMs and the extruded batches. In Fig. 4.9 it can be seen that bulk CBZ showed slow dissolution rates with only 18% at 60 min and 24% at 120 min, respectively. Interestingly, the PMs - at all CBZ-DGL ratios - showed increased dissolution rates with an ascending order of 2:1<1.5:1<1:1 ratios. These findings indicate a strong effect of DGL on the dissolution rates of the water insoluble drug, CBZ. At low drug ratios (1:1, 1.5:1) dissolution rates for CBZ varied from 63-72% at 120 min. The properties of the hydrophilic carrier DGL has also been reported recently (Al-Hamidi et al. 2014) where PM and solid dispersion of piroxicam obtained by using organic solvents showed increased dissolution rates.
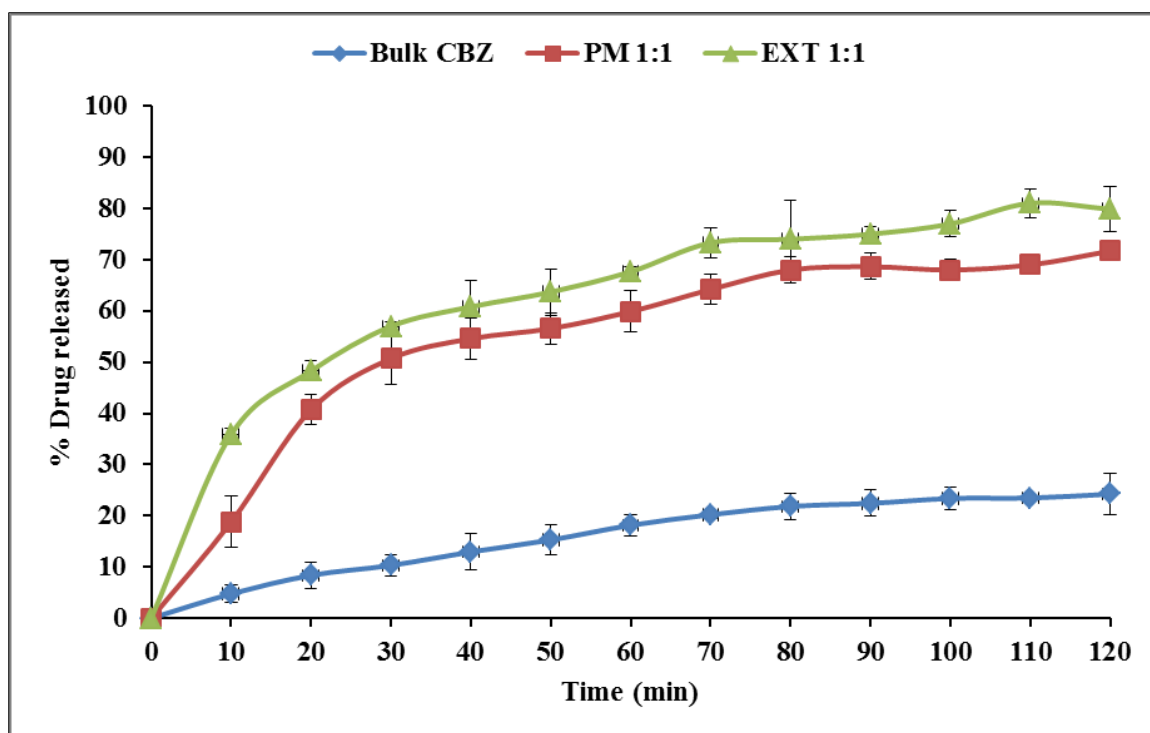
Fig. 4.9. Dissolution profiles of bulk CBZ, PM (1:1) and EXT (1:1).
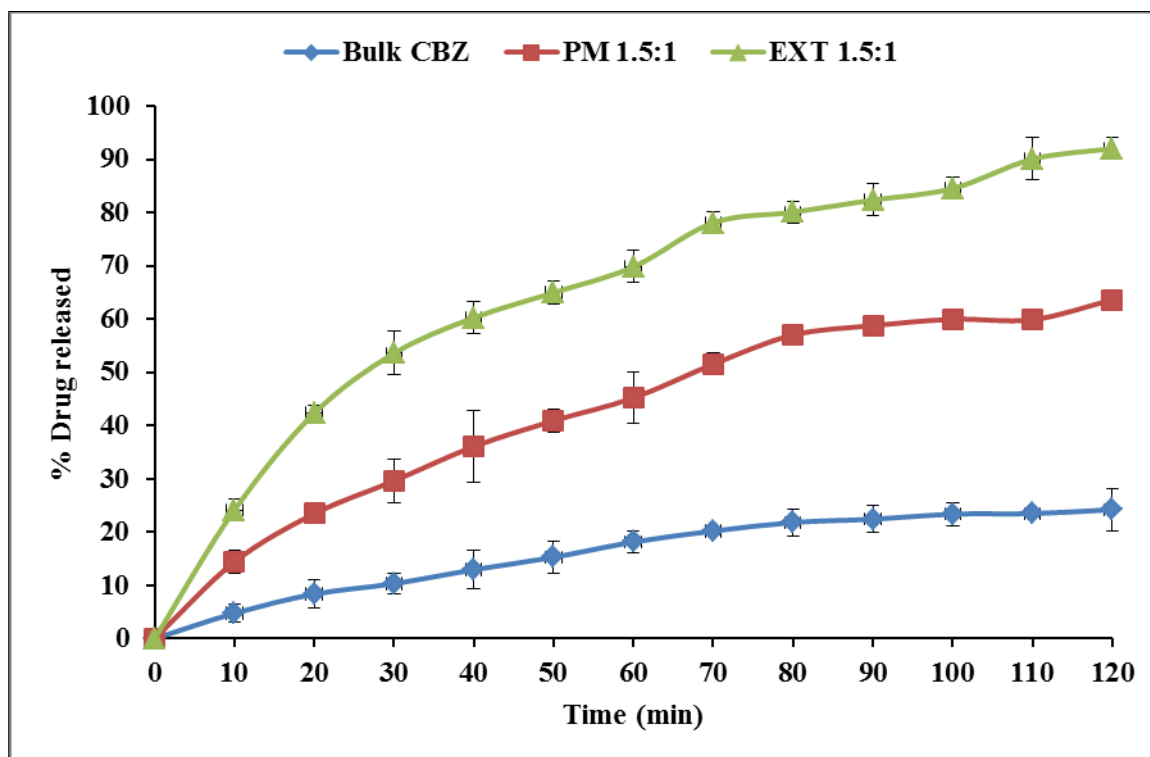
Fig. 4.10. Dissolution profiles of bulk CBZ, PM (1.5:1) and EXT (1.5:1).

71
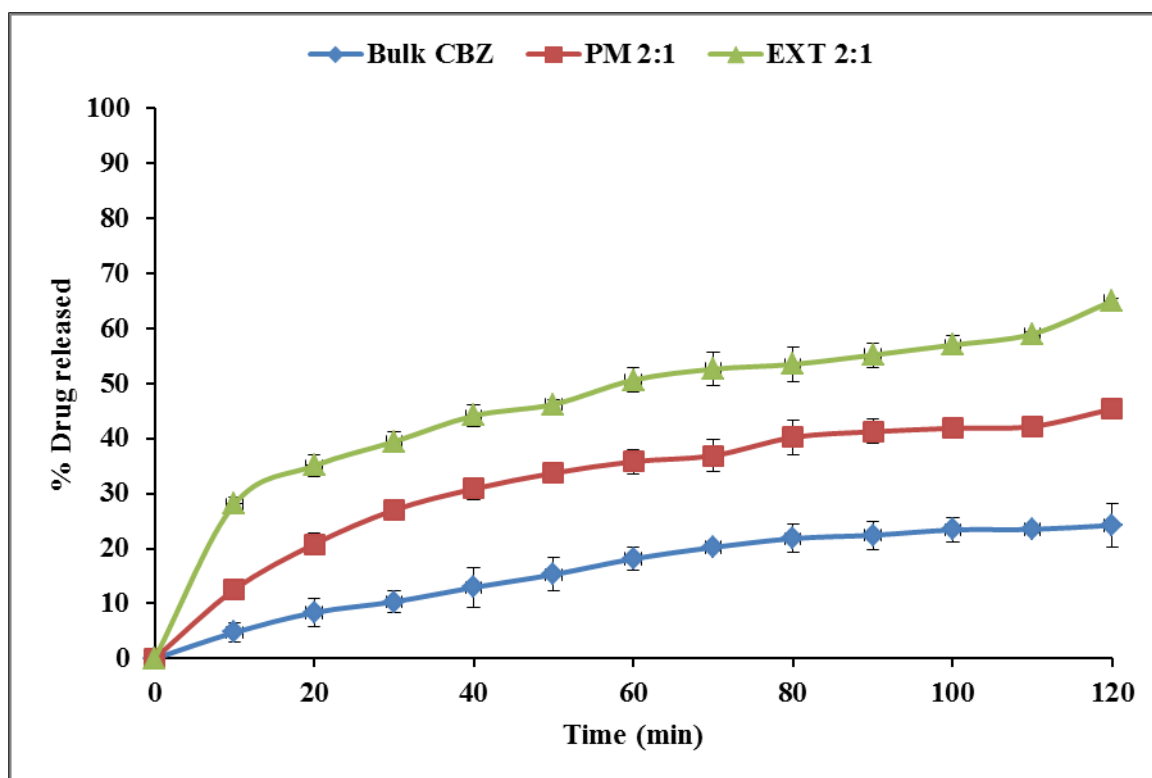
Fig. 4.11. Dissolution profiles of bulk CBZ, PM (2:1) and EXT (2:1).

The hot-melt extruded batches showed a further increase in CBZ dissolution rates-compared to bulk CBZ and PMs with an optimum CBZ-DGL ratio at 1.5:1 and an ascending order of 2:1<1:1<1.5:1 ratios (Figs. 4.9- 4.11). No significant difference was observed between the 1:1 and 1.5:1 extrudates with release rates between 67 − 69% at 60 min. However, at 1.5:1 ratio CBZ showed the highest dissolution rates with 92% being dissolved after 2 h. The reason for the dissolution behaviour of the extruded batches is attributed to the CBZ transformation from polymorph form III to form I. As mentioned previously form I CBZ has been proved to exhibit faster dissolution rates compared to form III.

4.3.5   Particle size distribution

Particle size can have a major influence on dissolution by providing a large surface area. There was no influence of particle size on the dissolution behaviour of any of the processed HME samples (Fig. 4.12). It is evident that extrudates at a molar ratio of 1.5:1 displayed a larger particle size distribution but their dissolution rates where faster. In addition, the particle size of bulk CBZ is much smaller compared to the extruded batches. Thus, if the

72

particle size was crucial for the dissolution rates of the studied formulations then the dissolution of bulk CBZ should be faster.
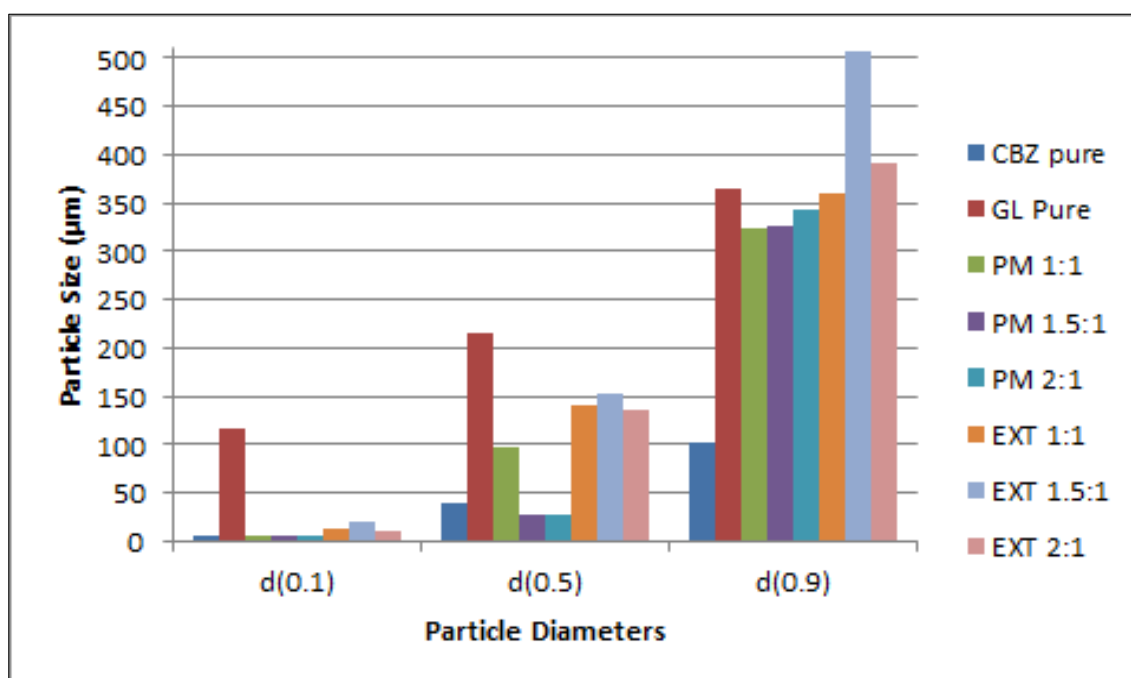
Fig. 4.12. Particle size distribution of bulk CBZ, DGL and PMs and EXTs at molar ratios of 1:1, 1.5:1 and 2:1.

4.4 CONCLUSIONS

DGL was used as a carrier to enhance the dissolution of CBZ when it was physically blended in different molecular ratios (1:1, 1.5:1 and 2:1, CBZ: DGL). Higher drug release was observed for the highest concentration of DGL in the physical mixtures of CBZ-DGL. However, when PMs were processed by using HME, extrudates showed faster rate of dissolution compared to the PMs of the individual components. It was found that the rate of dissolution was not completely related to the amount of DGL but to the polymorphic conversation of bulk CBZ form III to form I into the extruded products. DSC/HSM evaluation of bulk CBZ showed melting (form III), then needle shaped crystals (CBZ form I) which was followed by melting of CBZ form I. DSC could not be used to identify any polymorphic conversionin the extrudates; however, HSM, XRPD and SEM analysis showed polymorphic conversion of bulk CBZ III into CBZ form I which was absent in PMs proved that polymorphic conversion had occurred due to HME processing. XRPD diffractograms of 1.5:1 extrudates showed that some peaks for CBZ III had disappeared but were found to be

present in the rest of the extrudates confirmed that EXT 1.5:1 were more effected by polymorphic effect. Moreover, EXT 1.5:1 had highest dissolution amongst rest of extrudates and PMs. Particle size distribution showed larger particle size for EXT 1.5:1 which had higher rate of dissolution suggested no effect of particle size on the dissolution study. Overall physicochemical analysis suggests that extrudates have higher drug release (compared to the PMs and bulk CBZ) caused by the higher solubility of CBZ form I compared to form III in the presence of DGL.

CHAPTER 5 : PROCESS OPTIMIZATION OF INDOMETHACIN-SACCHARIN COCRYSTALS; THE EFFECT OF PROCESSING PARAMETERS

5.1 INTRODUCTION

HME is a versatile, potentially one step manufacturing process the use of which can result in the enhancement of solubility, dissolution, stability and sometimes bioavailability characteristics of pharmaceutical formulations. By using the appropriate downstream processing equipment it can be used as a continuous process for the development of various solid dosage forms such as granules, tablets, pellets or even implants and medical devices (Douroumis 2012, Maniruzzaman et al. 2012b). HME can be defined as a process where raw materials, undergo blending/kneading and mixing under elevated temperatures through a rotating die to produce extrudates of uniform shape. In the case of extrusion cocrystallisation the HME processing involves the blending of an API and the coformer under high shear and mixing attained by different screw configurations at elevated barrel temperatures for the manufacturing of quality cocrystals (Dhumal et al. 2010). As previously reported, HME can be optimized for cocrystal production by altering the screw geometries which, eventually, enables the formation of cocrystals along the extruder barrel (Moradiya et al. 2014b, Daurio et al. 2011). The barrel temperature, screw speed and feed rate are the extrusion dependent variables (Leister et al. 2012) that can impact on the formation of cocrystals. Therefore the engineering of high quality cocrystals in HME requires optimisation of such processing parameters.

The ability to monitor and control the quality attributes of cocrystals in real-time would be a useful tool, aligning with the current regulatory initiatives towards continuous monitoring (De Beer et al. 2011). In the recent years, process understanding is strongly supported by the FDA through the implementation of quality by design (QbD) and process analytical technology (PAT) tools (FDA 2004). As a result, the scope of the real time data interpretation, continuous quality monitoring and control has led PAT to enjoy a renaissance in continuous manufacturing and product development. To date various PAT tools have been employed to monitor and understand-at the molecular level- HME processing such as UV–visible, NIR and Raman spectroscopic techniques (Saerens et al. 2011, Gryczke 2013).

In particular, NIR has been coupled with HME to successfully monitor the progression of cocrystal formation during HME processing and to identify molecular interactions in the creation of drug-coformer complexes.

The synthesis of indomethacin-saccharin (IND-SCH) cocrystals has been undertaken by using a range of methods such as grinding (Lin et al. 2013b), supercritical fluids (Padrela et al. 2009), anti-solvent (Chun et al. 2013), and solvent evaporation (Basavoju et al. 2008, Jung et al. 2010). The aforementioned techniques suffer from disadvantages such as lack of scalability, multistage processing and the use of organic solvents resulting in their being either complicated or costly in terms of the use and disposal of solvents. Indomethacin is a non-steroidal anti-inflammatory (NSAID) BCS class II drug which displays low aqueous solubility and higher intestinal permeability (Amidon et al. 1995). Cocrystallisation of BCS class II actives with saccharin has been undertaken in order to enhance their aqueous solubility's and dissolution rates. The presence of hydrogen bonding sites in saccharin makes it a highly favourable coformer in the cocrystallisation process.

In the present study, we optimized high quality IND-SCH cocrystals (Fig. 5.1) by altering the process parameters such a temperature, screw speed and feed rate. Further process understanding was achieved by implementing PAT tools such as in-line monitoring and in-line particle size monitoring.
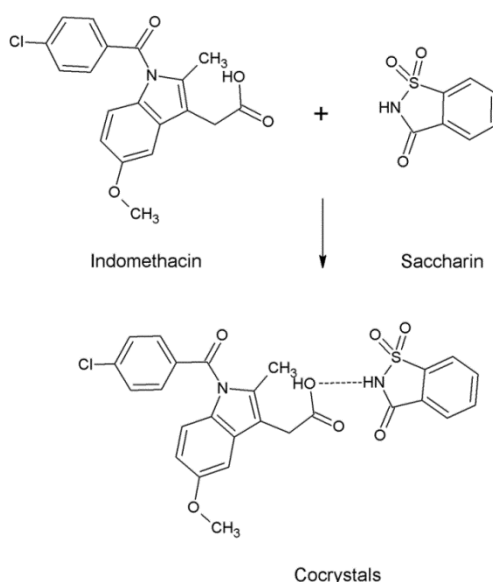
Fig. 5.1. Chemical structures of IND, SCH and H-bonding in the cocrystals of IND-SCH (Basavoju et al. 2008).

5.2   METHODS AND MATERIALS

5.2.1   Materials

Indomethacin (γ-form, IND) and saccharin (SCH) were purchased from Tokyo Chemicals (Tokyo, Japan) and Sigma Aldrich (Gillingham, UK) respectively. All solvent used for HPLC analysis were of analytical grade (Fisher chemical, UK).

5.2.2   HME processing

Equi-molar amounts (1:1) of IND and SCH were accurately weighed and homogenously blended for 10 min using a Turbula mixer. The blend of prepared powder was fed in to a twin-screw extruder (Eurolab 16, Thermo Fisher, Germany) via a DD Flexwall® 18 feeder (Brabender Technology, Germany). The data in Table 5.1 shows the processing parameter settings such as the temperature profiles, screw speed and feed rate used for the optimization of cocrystal synthesis via HME. The HME instrument was operated without the die and the extruded cocrystals collected in powder form.

Micronization of extruded corystals (165°C/30 rpm) was carried out using a cutter mill (Cutting Mill SM 100, Retsch, Uk). A 250 µm sieve was placed at the bottom of the casing holds that control the size of the material discharged from the milling zone.

Table 5.1. HME processing parameters used for the development and scale-up of IND-SCH cocrystals for different formulations.

Formulation (1:1 molar ratio of IND:SCH)	Temperature profile (°C) (Feeder ⟶ Die)	Screw Rate (rpm)	Feed rate (gm/hr)
F1	50/70/95/130/140/140/145/145/145	10	100
F2	70/95/145/150/155/155/155/155/155	10	100
F3	70/95/145/150/155/155/155/155/155	30	300
F4	50/70/95/155/160/165/165/165/165	30	300

5.2.3   Particle size measurements (off-line and in-line)

The particle size distribution of the powder formulations was determined by using sieve analysis (mesh sizes of 63, 125, 250, 500, 1000 and 2000 µm). A collector pan was placed below the sieve with the smallest mesh size. The samples were placed on the top sieve (2000 µm) and a lid was placed on it. The assembly was vibrated on an automatic sieve shaker (VE 1000, Retsch, Germany) for 10 min.

The particle size distribution of all the formulations was conducted using a dry powder dispersion unit (Scirocco 2000) of the Malvern Mastersizer 2000 (Worcestershire, UK) laser diffraction particle size analyser. The three measurements were taken for reproducibility of each batch. Calculations of particle size were received automatically from the Mastersizer 2000 software.

In-line particle size measurements were carried out by using a Parsum® probe (Parsum IPP70; Gesellschaft für Partikel-, Strömungs- und Umweltmesstechnik, Chemnitz, Gemany). D23 disperser attachment with probe was used and operated at Inlet and external pressure was set 15 and 2 L/min. The probe was directly placed at the end of extruder where particles were coming out from the extruder. The data collected by using the IPP software provided with the instrument. The scan rates used were 2-2.5m/s (0.250MHz, free fall), 10-30m/s (5MHz, D23 in-line disperser).

5.2.4   In-line NIR monitoring

Diffuse reflectance near infrared (NIR) spectroscopy was continuously performed in-line and non-invasively during HME processing using an Antaris MX Fourier-Transform NIR spectrometer (Thermo Scientific, UK). A fibre optic NIR probe was fitted for in-line monitoring. Spectra were collected in the 10000-4000 cm^{-1} region with a resolution of 16 cm^{-1}. Each NIR spectrum was an average of 32 scans which took 30 s to obtain. In addition to real-time monitoring, the extruded cocrystal spectra were measured off-line. Data analysis was performed by using RESULT software (version 3.0, Thermo Scientific, UK).

5.2.5   Differential scanning calorimetry (DSC)

DSC analysis was carried out by using a Mettler-Toledo 823e instrument (Greifensee, Switzerland). The accurately weighed samples were crimped in 40 µm aluminium pans and

heated from 25°C to 250°C at a scan rate of 10°C/min using nitrogen as a purge gas. STARe excellence software provided with instrument was used for further data analysis.

5.2.6 XRPD analysis

XRPD was used to determine the solid state of bulk materials, physical mixtures and hot-melt extrudates using a Bruker D8 Advance (Germany) in theta-theta mode. A Cu anode at 40 kV and 40 Ma, parallel beam Goebel mirror, 0.2 mm exit slit, LynxEye Position Sensitive Detector with 3° opening (LynxIris at 6.5 mm) and sample rotation of 15 rpm were used. Each sample was scanned from 2 to 40° 2Θ with a step size of 0.02° 2Θ and a counting time of 0.3 s per step.

5.2.7 Scanning electron microscopy (SEM)

The morphology of bulk IND, SCH and the extruded cocrystals was examined by SEM (Hitachi SU8030, Japan). Samples were placed on a thin layer of Mikrostik non-conductive adhesive (Agar scientific, UK) on an aluminium stub and coated with chromium under an atmosphere of argon at room temperature. SEM images were obtained by using an electron beam accelerating voltage of 2 kV.

5.2.8 Dissolution studies

Dissolution studies were conducted by using a USP II paddle apparatus (Varian 705, US). The amount of extruded powders was equivalent to 25 mg of IND, placed into 900 ml of 1.2 and 6.8 pH in each dissolution vessel (n=3). The temperature of the dissolution media was maintained at 37°C with a paddle rotation of 100 rpm. About 2-3 ml of samples were withdrawn at 15, 30, 60 and 120 min intervals and filtered with a 200 μm filter prior to HPLC analysis.

5.2.9 HPLC analysis

The content of IND in all the samples was confirmed by HPLC. The experiments were performed on an HPLC system (Aligent Technologies, 1200 series) equipped with a quaternary pump. A Hichrom S50DS2-4889 (5 μm×150 mm×4 mm) column was employed. Column temperature and retention time were set at 25°C and 4 min, respectively. The mobile phase used was 70:30:0.2 (v/v/v) methanol: water: acetic acid. The sample volume was 20 μl, injected by using an auto sampler, the flow rate used was 1.5 ml/min and the detector was set

at 260 nm wavelength. The calibration curve for IND was plotted over a concentration range of 10 to 50 μg/ml.

5.3 RESULTS AND DISCUSSION

5.3.1 HME Parameters

The HME processing for the formation and optimization of IND-SCH cocrystals was conducted in the absence of an extrusion die and the extrudates were collected in dry powder form. The studies revealed that the temperature profile and screw speed were the two critical process variables for the engineering of high quality cocrystals. As shown in the data in Table 5.1 the applied extrusion temperatures varied from 145–165°C. The initial maximum extrusion temperature was set at 145°C and a screw speed of 10 rpm was used; however, it was not possible to achieve complete cocrystal formation as small traces of unreacted material were detected by using DSC and XRPD (discussed below). However, batches extruded at 155°C showed cocrystal formation and the absence of unreacted starting materials. The formation of cocrystals at 155°C can be explained by the fact that this is the eutectic temperature of the IND-SCH physical blend (Mohammad et al. 2011). The effect of the screw speed and feed rate was investigated by increasing the rates at 30 rpm and 300 g/hr, respectively for the same temperature profile. Higher screw speeds facilitates the rapid transport of material through the extrusion barrels of the hot-melt extruder with less residence time and it is directly related to the feeding rate (Almeida et al. 2012). It should be noted, however, that higher feeding rates (at a constant screw speed) can cause material blockage in the extruder. Further increase of the screw/feed rates showed again incomplete cocrystal formation and the presence of unreacted material at a barrel temperature of 155°C. At a screw speed of 30 rpm quality cocrystals were obtained when the extrusion temperature was increased to 165°C. This has been previously reported by Dhumal et al. (2010) were temperatures higher than the eutectic point lead to material melting and facilitated mass transfer due to additional degrees of freedom with enhanced molecular collisions. These findings prove that screw speed and temperature play a key role in the development of high quality cocrystals where high screw and feed rates require an increase in the extrusion temperature. The results obtained from these studies will be later used for scale-up of the cocrystal manufacturing process.

5.3.2 Morphology

SEM micrographs of bulk IND showed irregular shape crystals with the particle size varying from 5–10 μm. The SCH coformer crystals presented prismatic shaped crystal morphology with particle size varying from 50-70 μm. The extruded cocrystals revealed cuboid shapes in the form of agglomerates. An increase in the screw speed and the extrusion temperature did not have an effect on the morphology of different batches of cocrystals.
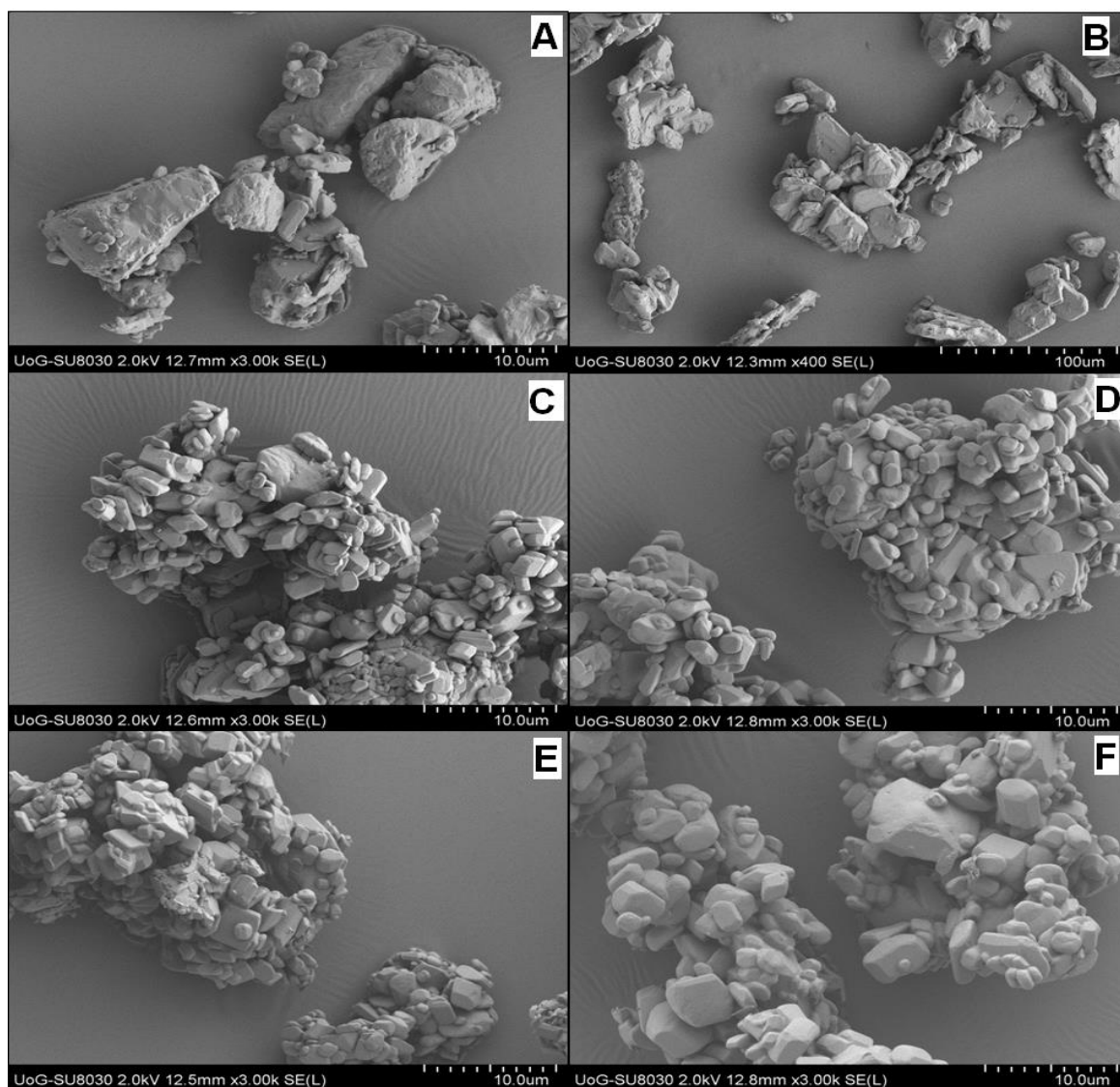
Fig. 5.2. Micrographs of bulk materials (a) indomethacin and (b) saccharin, and HME processed cocrystals (c) 145°C/10 rpm (d) 155°C/10 rpm (e) 155°C/30 rpm and (f)165°C/ 30 rpm

5.3.3 Thermal analysis

DSC analysis was employed to evaluate the solid state thermal properties of the bulk materials, physical mixtures and the extruded cocrystals. As shown in Fig. 5.3 bulk IND presents a sharp endotherm at 160.45°C, which is related to the stable γ polymorphic form (Legendre and Feutelais 2004). Saccharin exhibited a sharp melting endotherm at 226.82°C. The PM of IND-SCH exhibited two endotherms, one at 156.24°C followed by another melting endotherm at 183.05°C which relate to the eutectic melt and the cocrystal melting, respectively (Lu et al. 2008).
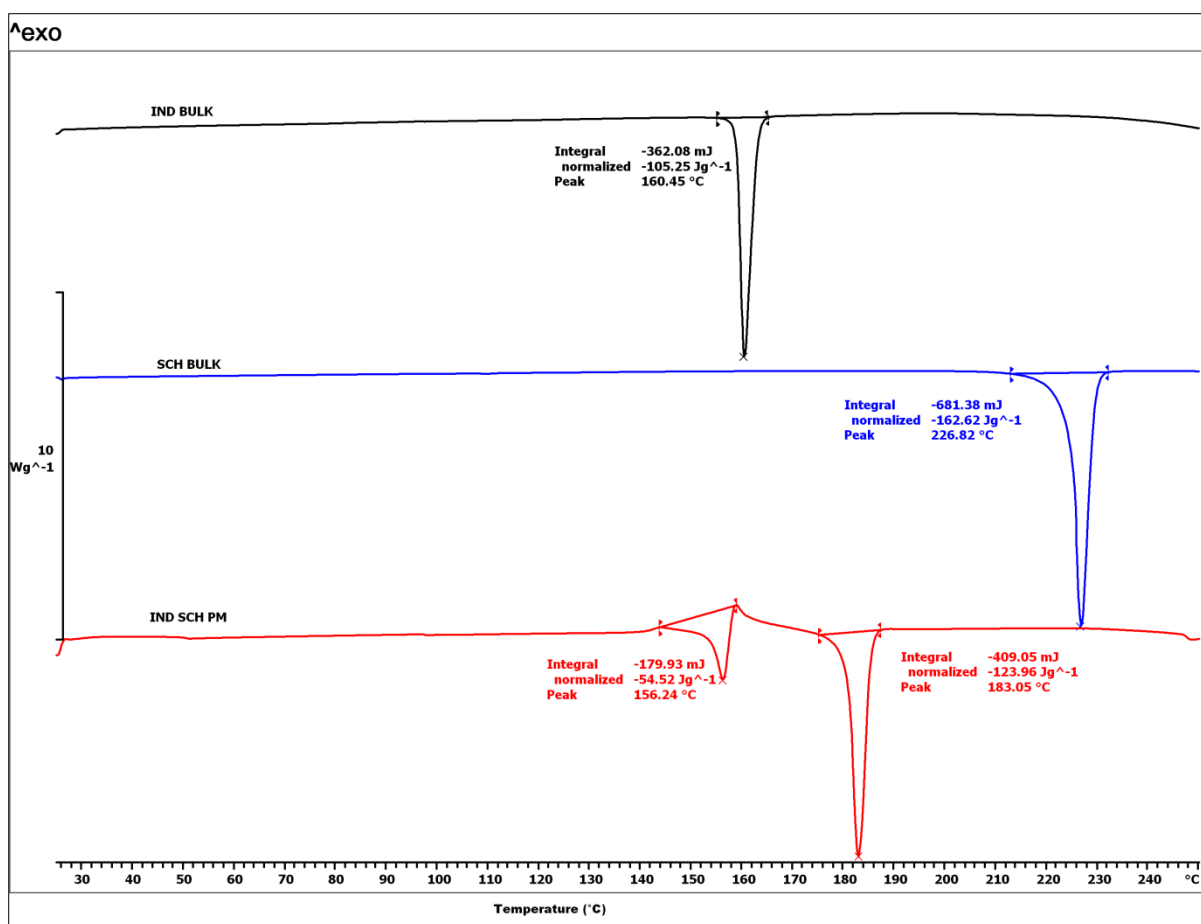
Fig. 5.3. DSC thermograms of bulk IND, SCH and a physical blend (1:1 molar ratio) of IND-SCH.

The DSC thermograms, of IND-SCH processed at 145°C/10 rpm presented two peaks which are similar to those of the PM at 155.73°C and at 182.73°C (Fig. 5.4). However, the melting enthalpy of the first peak appeared very low which suggests undeveloped formation of cocrystals with some trace of unreacted material.

82

An increase in the extrusion temperature to155°C with a constant screw speed (10 rpm) led to the complete formation of cocrystals with a single sharp melting endotherm at 182.97°C. It is obvious that the endothermic peaks of bulk IND and SCH disappeared, as shown in Fig. 5.5.

The next step of the analysis involved a further increase in the screw speed and feed rate using a constant extrusion temperature of 155°C. As shown in the data in Fig. 5.4, the process was incomplete and two melting endothermic peaks appeared at 155.15°C and 183.87°C, respectively. These findings demonstrate the effect of the process variables on the cocrystallisation process indicating that higher screw speeds require higher melt temperatures. Furthermore, an increase of the extrusion temperature to 165°C at 30 rpm extrusion speed again provided cocrystals of high purity. A sharp melting endotherm was observed at 183.23°C without the presence of any melting peak at the eutectic temperature (Fig. 5.5). The DSC analysis provided valuable information relating to the quality of the formed cocrystals and helped to identify the influence of the process variables.
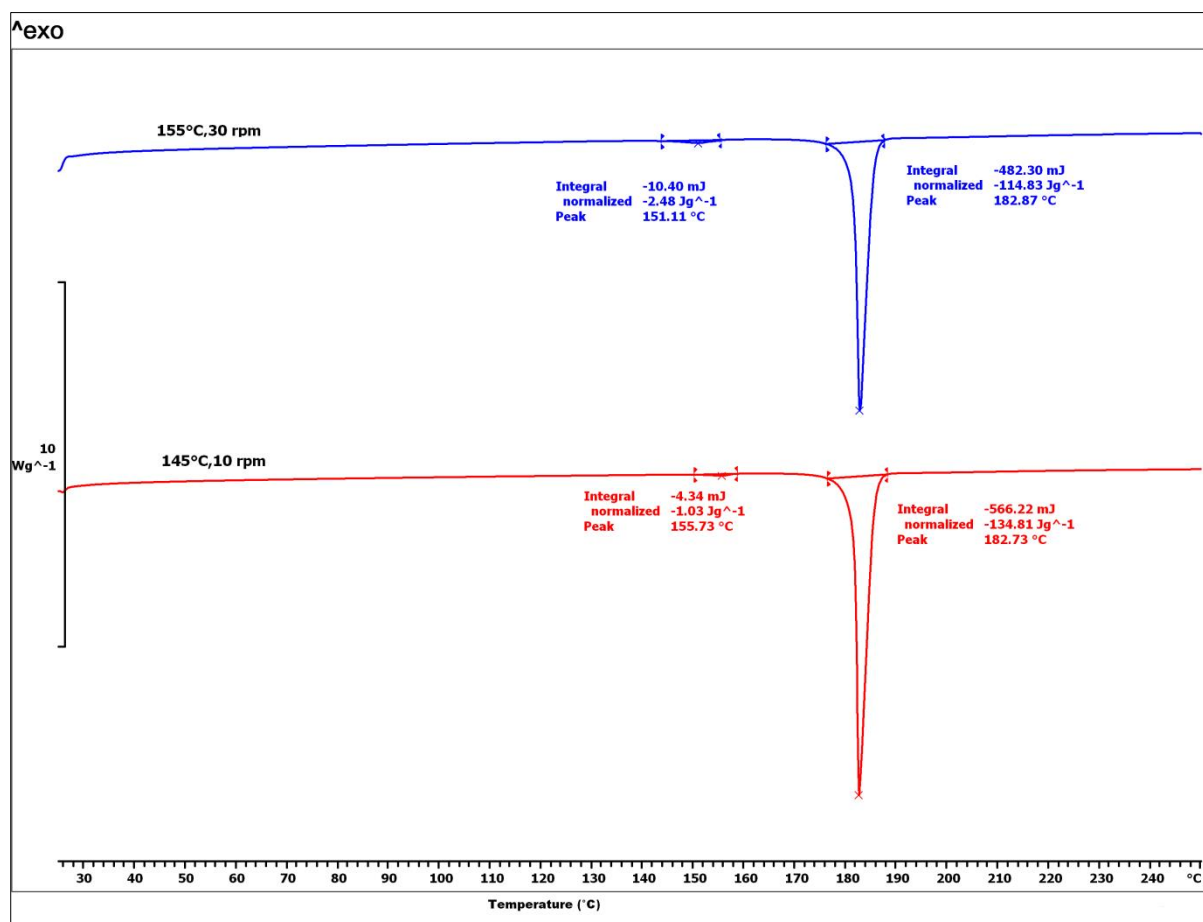
Fig. 5.4. DSC thermograms of hot melt extruded cocrystals, 145°C/10 rpm and 155°C/30 rpm.
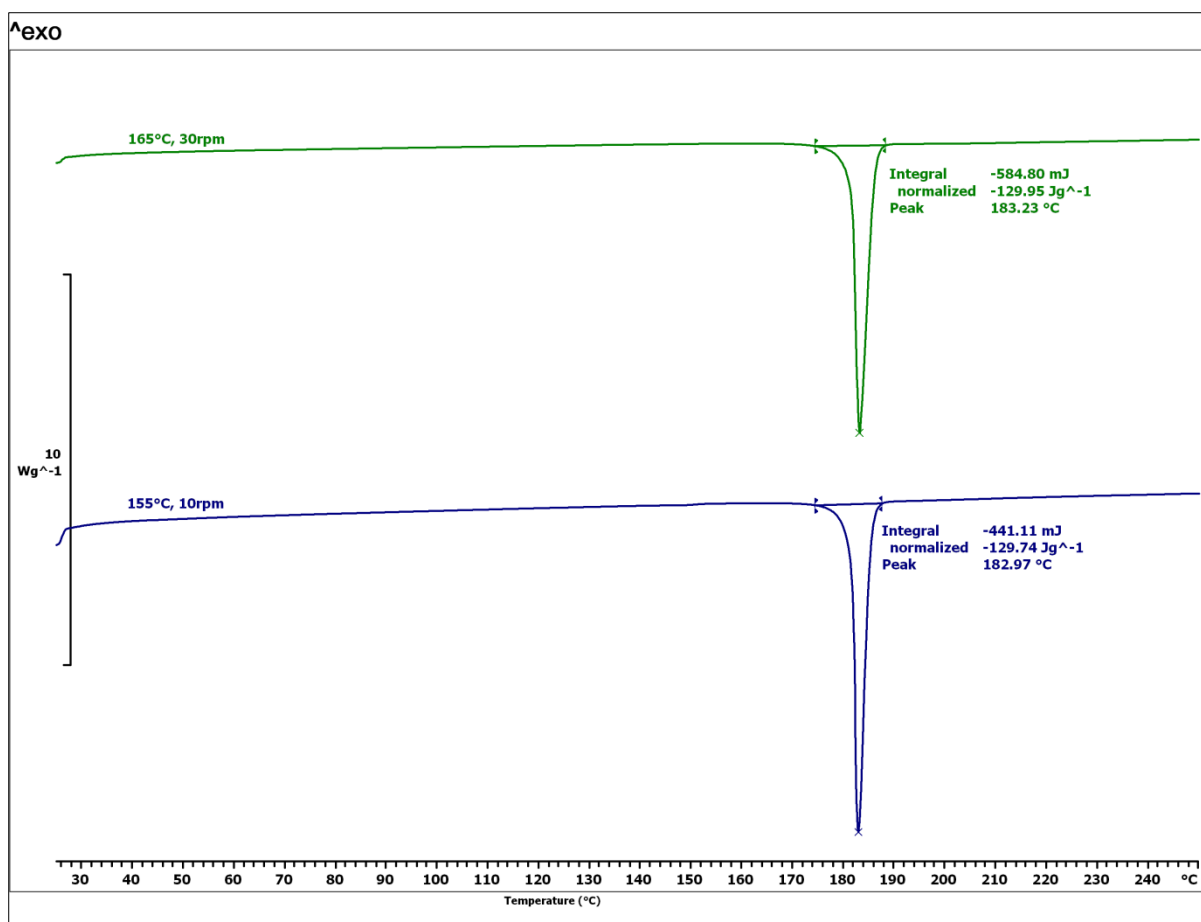
Fig. 5.5. DSC thermograms of hot melt extruded cocrystals (155°C/10 rpm and 165°C/30 rpm).

5.3.4 XRPD

XRPD was used to investigate the purity and the quality of the extruded cocrystals. The X-ray powder diffractograms of the bulk components are illustrated in Fig. 5.6 where IND showed characteristic intensity peaks at 10.25º, 11.67º, 16.77º, 17.02º, 19.68º, 21.87º, 23.99º, 26.61º 2Θ. Intense peaks of bulk SCH were identified at 9.56º, 15.91º, 16.02º, 17.23º, 19.13º, 25.14º 2θ. In the diffractogram of the IND-SCH PM peaks of lower intensities that belong to both IND and SCH were identified.

However, the diffractograms of the extruded cocrystals showed a unique XRPD pattern compared to their parent compounds, which were identical to published data collected from the CCDS (Cambridge Crystallographic Data Centre) (CCDS REF: UFERED). The cocrystals extruded at 145°C/10 rpm and 155°C/30 rpm presented similar XRPD patterns with identical peaks at 10.21° and 14.42° 2Θ, respectively (indicated by an asterisk in

Fig. 5.7). These two peaks are characteristic peaks for IND and suggest the presence of unreacted drug due to incomplete cocrystal formation. High purity cocrystals were obtained when process variables were set at 155°C/10 rpm and 165°C/30 rpm (Fig. 5.7) without any traces of unreacted material. Typical peaks of IND-SCH cocrystals can be identified at 2Ɵ values of 5.43º, 10.89º, 14.42º, 21.22º, 25.45º, and 27.07º.

XRPD analysis confirmed the formation of high quality IND-SCH cocrystals and the findings were in good agreement with the DSC results.
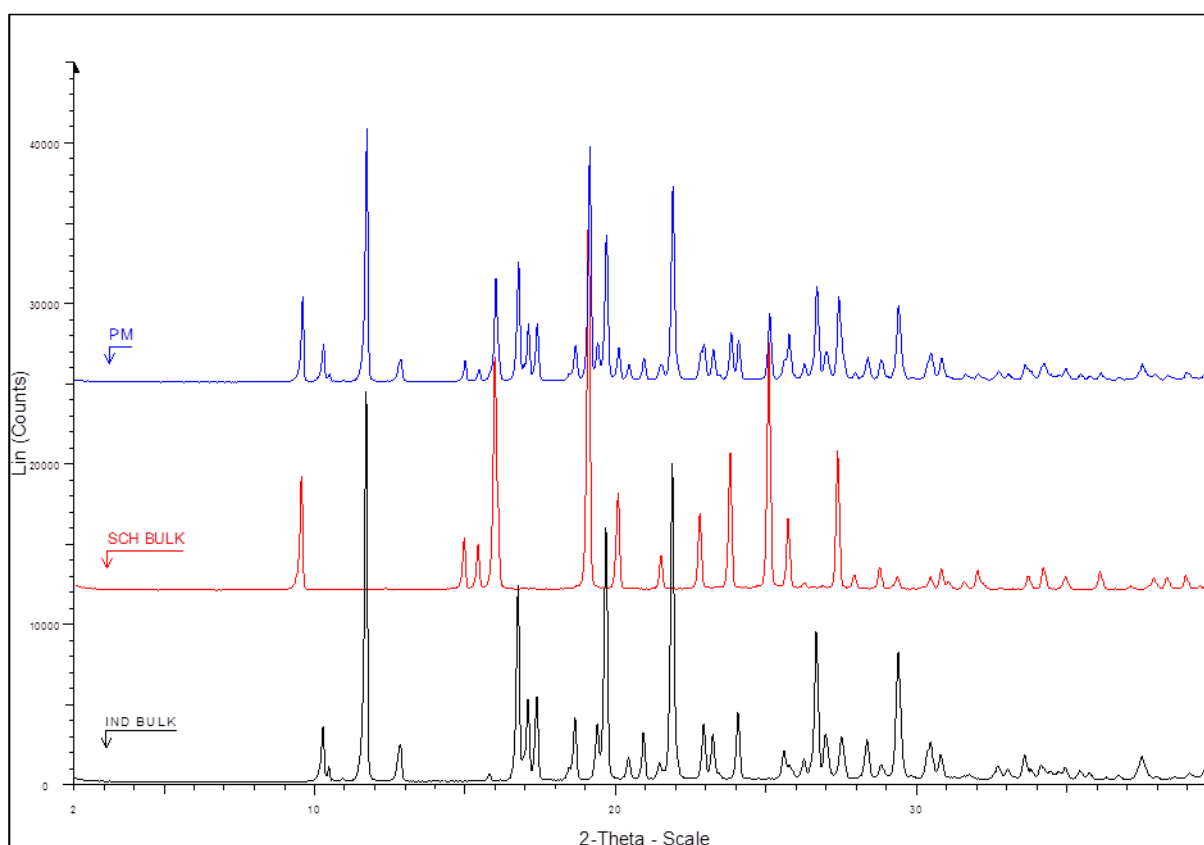
Fig. 5.6. X-ray powder diffractograms of bulk materials and the physical blend of IND SCH (1:1 molar ratio).
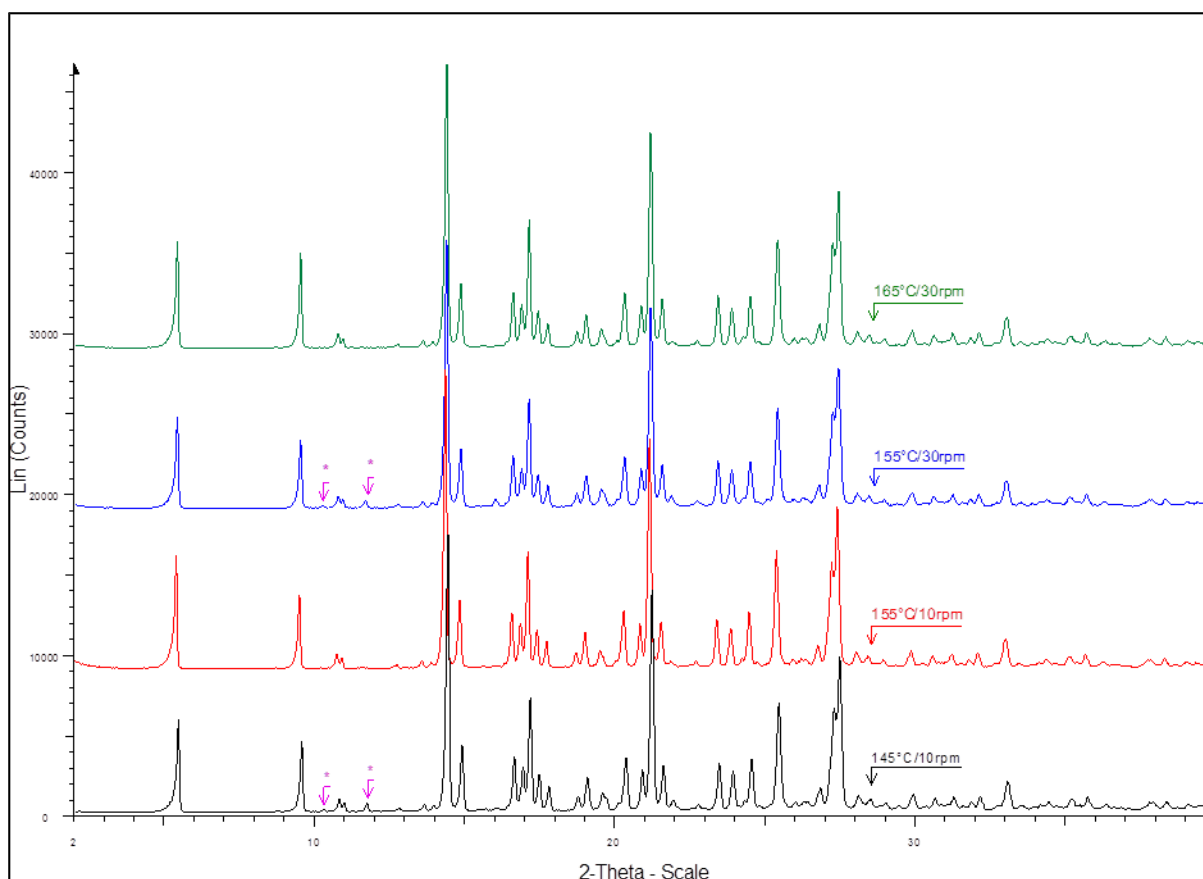
Fig. 5.7. XRPD profiles of HME extruded cocrystals using different process variables.

5.3.5 In-line near infra-red spectroscopy

Off-line NIR spectra of IND, SCH and the physical mixture (PM) were measured to identify the characteristic bands of these materials so that any new bands formed during extrusion could be attributed to the cocrystal. From Fig. 5.8 it can be seen that the NIR spectra of IND and SCH exhibit characteristic peaks at different wavelengths in the 5500-6500 cm-1 region.

The second derivative NIR spectra of IND, SCH and the PM in the 4200-6300 cm^{-1} region are shown in Fig. 5.9. The PM peaks fall between the two component peaks with no shifting indicating no interaction between the components.

Fig. 5.9 depicts the 2nd derivative spectra of bulk components, PM and the extruded cocrystals that show significant differences due to the band shifts. The peak observed in at 5022 cm^{-1} (Fig. 5.9) is due to the OH stretching from the IND molecule. This peak shifted to 4988 cm^{-1} in the spectrum of the extruded cocrystals and it is attributed to the stretching of

OH groups. The peak shifting at lower wavenumber is an occurrence of H- bonding with the –NH group of SCH as a result of the formation of cocrystals between IND and SCH.
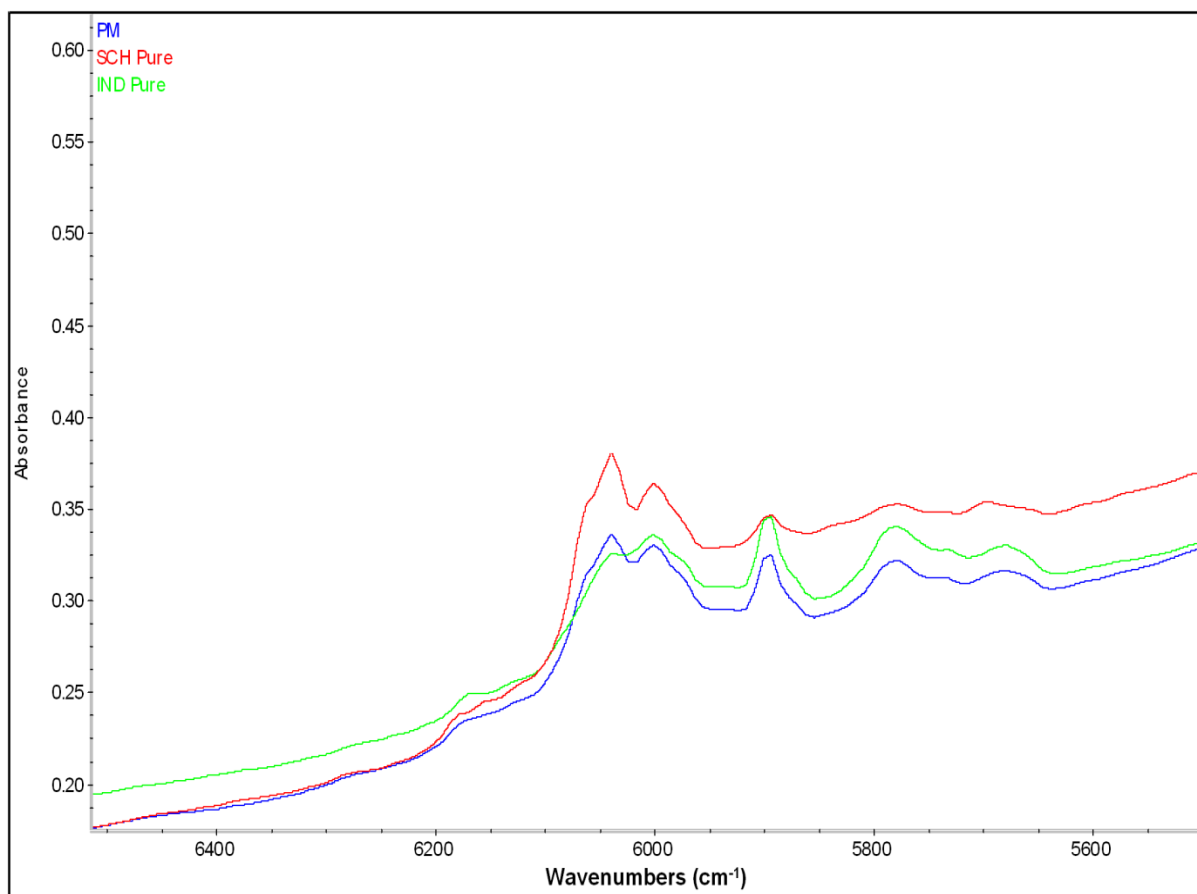
Fig. 5.8. Off-line NIR spectra of bulk IND, SCH and PM in the 5500-6500 cm^{-1} region.

Another distinctive band was detected at 5802 cm^{-1} for hot melt extruded cocrystals which indicates the first overtone of the –CH or –SH stretches and this band is shifted from the band in the physical mixture at 5775 cm^{-1} (Fig. 5.9). This interaction is not due to H-bonding between IND and SCH but is instead an unidentified band in the cocrystals (Allesø et al. 2008).
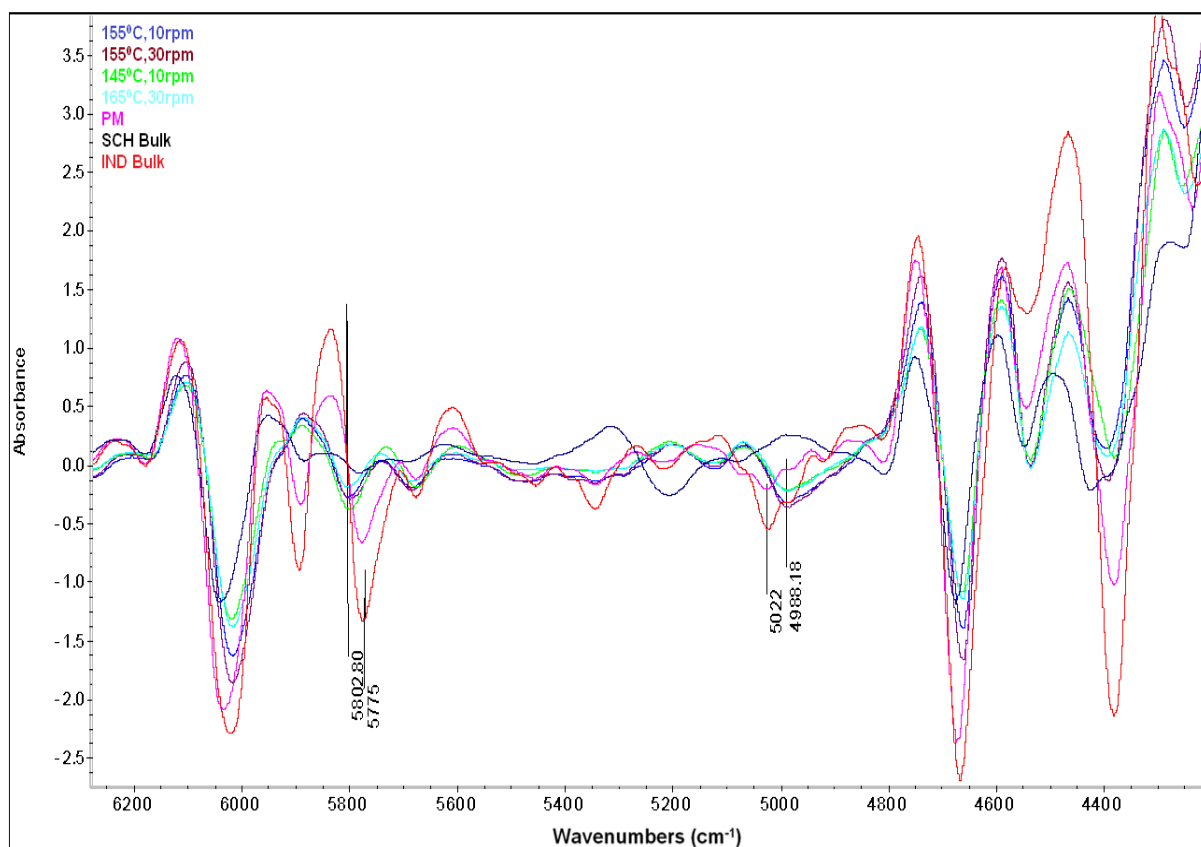
Fig. 5.9. Second derivative spectra of bulk IND, SCH, PM (IND/SCH) and the extruded cocrystals in the 4200-6300 cm^{-1} region.

5.3.6 Dissolution studies

Dissolution testing carried out at pH 1.2 showed no drug release for bulk IND or IND-SCH cocrystals. IND solubility is limited in acidic pH media due to its pKa value (3.5), which make it unable to ionise in acidic media. Additionally, IND-SCH cocrystals present a pH dependent solubility and increase at pH value above the pKa of SCH (1.6) (Alhalaweh et al. 2012).

At pH 6.8 bulk IND (Fig 5.10 (inset)) showed a dissolution rate of 35% followed by 70% at 2 hr. A higher drug release was detected for all extruded batches compared to bulk IND. All extruded cocrystals presented similar release profiles with statistical analysis (t-test) showing no significant differences irrespective of the temperature/screw speed used in the HME processing. As shown in Fig. 5.10 approximately 58% of the IND was released in 30 min and 80% after 2 hr. Interestingly, the two batches (145°C/10 rpm and 155°C/30 rpm) with incomplete cocrystal formation showed similar release profiles to those of the cocrystals

(155°C/10 rpm and 165°C/30 rpm). These release patterns are not uncommon as the traces of unreacted drug-coformer amounts did not affect the overall drug dissolution properties. This can be explained by the higher solubility of IND-SCH cocrystals in buffer solution (Basavoju et al. 2008) compared to bulk IND and, batches of cocrystals contaminated with IND; the rate of dissolution was not affected by the presence of small amounts of IND from the PM.
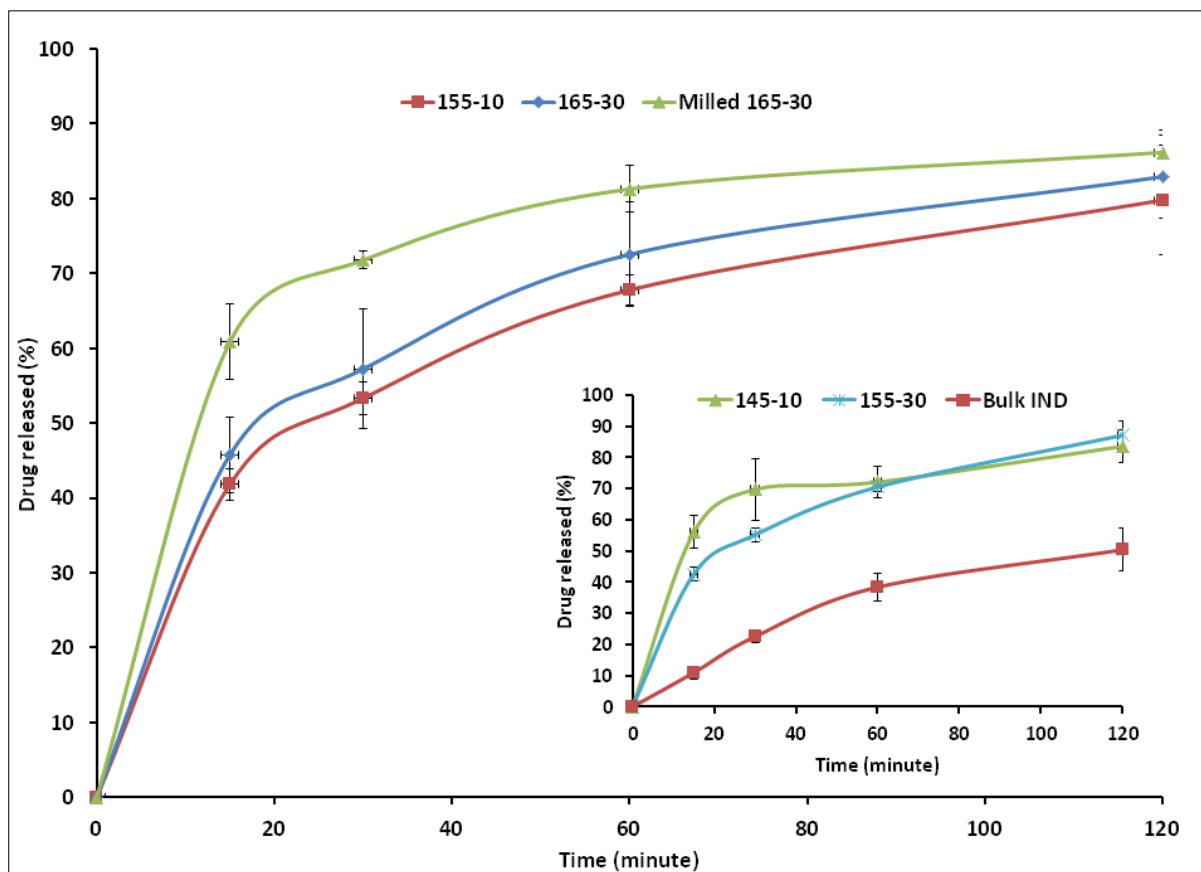
Fig. 5.10. Dissolution profile of pure hot-melt extruded cocrystals (155°C/10 rpm and 165°C/30 rpm) and milled cocrystals of 165°C/30 rpm.(inset: bulk IND and cocrystals with trace of physical mixture).

The particle size of cocrystals can have an influence on their dissolution profiles (Shiraki et al. 2008). The sieve analysis of the extruded cocrystals showed a similar particle size distribution for all the batches of cocrystals. A careful consideration of the cocrystal particle size distribution showed that the increase in the HME extrusion temperature resulted in particle aggregation and the creation of larger particles. As it shown in the data of Fig. 5.11 the fraction of particles above 500 μm diameter increases slightly at higher extrusion temperatures. This small increase in particle size towards larger size of cocrystals did not

affect the dissolution rate of IND. However, milling the cocrystals significantly enhanced IND dissolution rates. As shown in Fig. 5.13 the cocrystal milling produced smaller particles with varying from 63-250 µm. Hence the dissolution rate of IND increased to 60% within the first 15 min and 70% in 30 min.
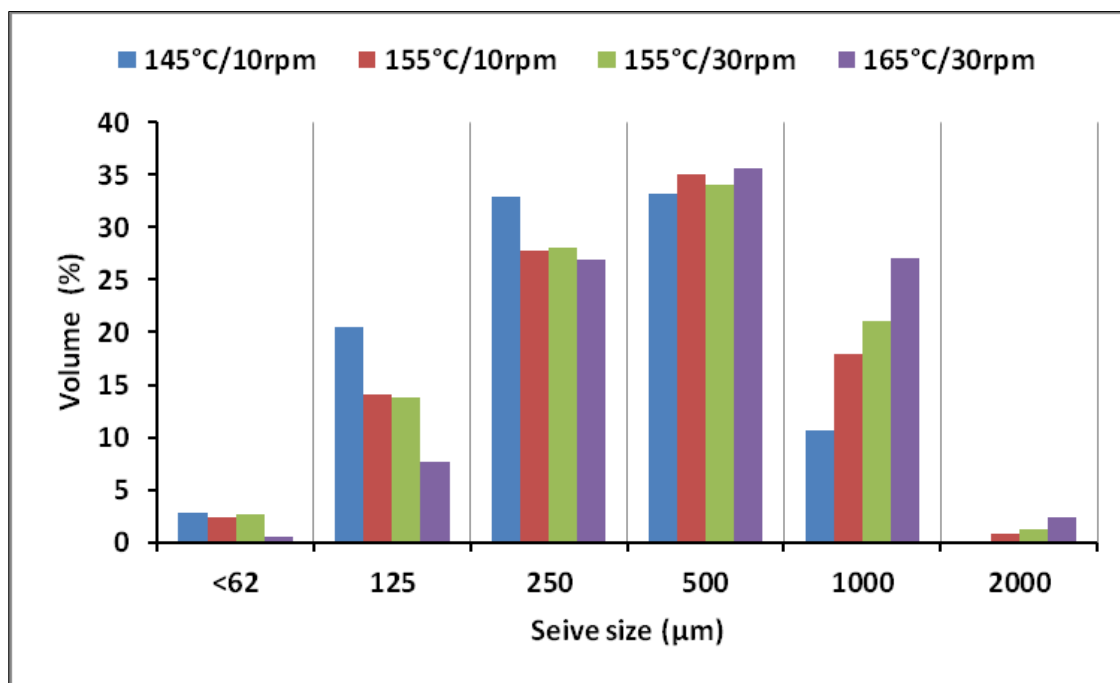
Fig. 5.11. Graphical representation for particle size distribution of extruded cocrystals assessed by using sieve analysis.

5.3.7. In-line particle size measurements

In-line particle size measurements carried out for batches processed at 165°C/30 rpm at two different stages and compared with off-line particle size analysis. The cocrystal particle size was measured at the end of the extruder for the "as made" batches and after milling where the size was further reduced by using a cutter mill. To optimise the process of in-line monitoring two parameters was selected named D23 in-line disperser and free fall. The D23 inductor incorporates a nozzle with air supply which disperses and accelerates particles towards the measuring zone while free fall applies for particles with gravitational flow. It is obvious that both settings of the particle probe are related to the expected average particle velocity.

For the free fall settings of the Parsum probe the "as made" cocrystals showed similar particle size distribution in the range of 250-2000 µm with the off-line sieve analysis. However, the use of the "free fall" setting did not detect smaller particle size (<250 µm) due to the large

agglomerates received at the end of the extrusion process. The use of the D23 in-line disperser did not provide a better size determination as shown in Fig. 5.12. However, asmaller range of particle sizes were obtained but spike in the result was observed at the particle ranges of 1000-2000 μm this could be due to the particle coincidence (Silva et al. 2013). Particle coincidence is considered as false result; if occasionally two particles cross at the same time through the measurement cell, Parsum probe may not able to differentiate that individual particle and believed as a single particle.
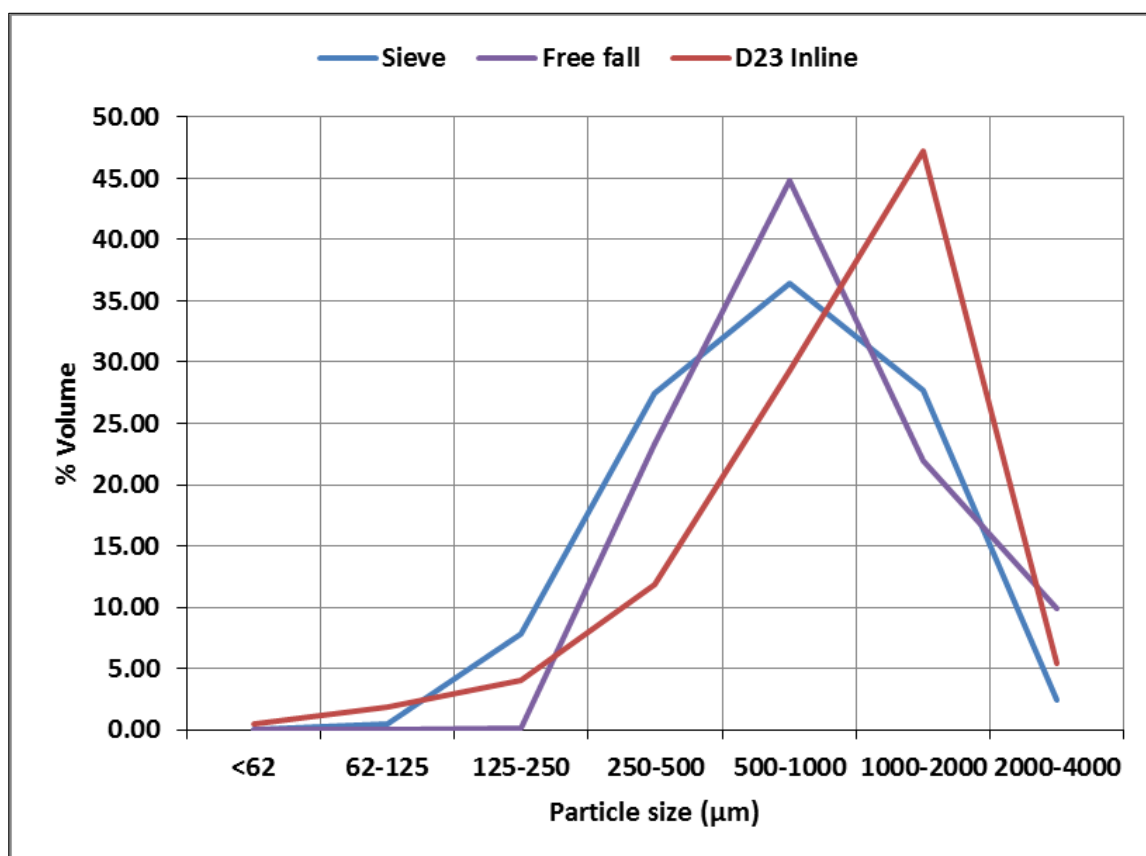
Fig. 5.12. In-line particle size measurements of cocrystals (165°C/30 rpm) in comparison with off-line sieve analysis and two different in-line variables used in Parsum probe.

In-line monitoring of the particle size distribution was also carried out during milling of the extruded cocrystals (165°C/30 rpm) using the D23 in-line setting. The obtained particle size distribution was quite different from that of sieve analysis due to the fact that the smaller cocrystals were "sticky" leading to particle agglomeration in the sieves. As a result, it was not possible to detect particles below 125 μm and obtained uneven size distribution. In this case laser diffraction (Mastersizer) was employed for off-line particle size analysis and the measurement was compared with in-line particle size measurement. As shown in the data in

Fig. 5.13 the size distribution obtained by laser diffraction and Parsum probe were in good agreement. Although both techniques use different theoretical approaches for particle size determination provided accurate particle size measurements for in- and off-line monitoring. In addition, laser diffraction was found to be dependent on the applied pressure (0.1 – 0.5 bars) resulting in slightly different particle size measurements with varying pressure values (see appendix, Fig. S5).

Overall, the use of the Parsum probe was proved efficient for in-line particle size monitoring and an excellent PAT tool for quality control. The tuning of the measuring parameters is a prerequisite for obtaining reliable results.
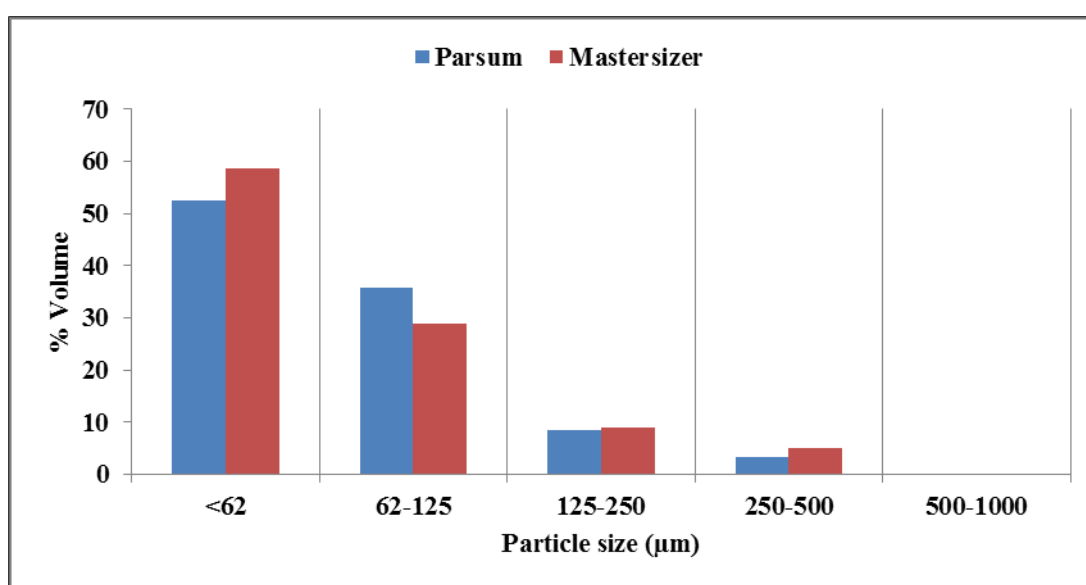
Fig. 5.13. In-line particle size measurements of micronized cocrystals (165°C/30 rpm) in comparison with off-line particle size analysis (Mastersizer).

5.4   CONCLUSIONS

In this study high quality cocrystals of IND-SCH were produced by continuous HME processing. The cocrystals formed were optimized by altering the HME process variables such as extrusion temperature, screw speed and feed rate. It was found that the temperature and screw speed have a significant effect on the quality of the cocrystals. At higher screw/feed rate, an increase in extruder barrel temperature profile was required to obtain complete formation of cocrystals. However, at the desired temperature and higher feed rate an increase in screw speed is essential to avoid any blockage in the barrel during the

extrusion process. Furthermore, untreated traces of PMs were seen in the DSC thermograms of formulations 1 & 3 which was further confirmed as traces of IND by the significant peak observed in XRPD diffractograms. Formulations 2 and 4 showed single endothermic DSC peaks and correlated with published data.

An application of PAT tools to measure in-line particle size or to control cocrystals formation during extrusion was successfully demonstrated without interrupting the process. An in-line NIR probe placed at the last mixing zone of the extruder barrel confirmed the formation of cocrystals during the HME process. Particle size distribution obtained from in-line particle probe was in good agreement with data gathered from off-line methods (laser particle size analyzer or sieve analysis). Cocrystals extruded using different HME processing parameters showed similar dissolution characteristics without having any effects from impurities (trace of bulk IND in cocrystals formulations 1 and 3). A reduction in the particle size of the extrudates has a significant effect on the dissolution rate. Furthermore, an enhancement in in-vitro dissolution was achieved for IND by using the cocrystallisation process.

CHAPTER 6 : CONTINUOUS MANUFACTURING AND SCALE UP OF PHARMACEUTICAL COCRYSTALS BY USING HOT MELT EXTRUSION

6.1   INTRODUCTION

Cocrystals have been extensively studied by using various techniques, including traditional approaches such as solvent evaporation, grinding, melting or ultra-sonication; most recently spray drying, supercritical fluid and thermal-printing approaches have also been employed (Brittain 2012, Steed 2013a, Thakuria et al. 2013, Sun 2012). The engineering of cocrystals involves the theoretical prediction and screening of the supramolecular structures followed by a suitable manufacturing process and *in vitro/in vivo* evaluation (Aitipamula et al. 2012, Babu et al. 2008, Fucke et al. 2012). One of the significant challenges and requirements in the development of cocrystals is to establish a robust, scalable method for industrialisation purposes. Only a few approaches for scale-up of cocrystals have been reported so far using solvent crystallisation (Leung et al. 2012, Sheikh et al. 2009), continuous oscillatory baffled crystallisation (Zhao et al. 2014) and resonant acoustic mixing (Am Ende et al. 2014). However, grinding and extrusion are the only two solvent-free methods hitherto used for the formation of cocrystals. HME has the scope for being a continuous, scalable method and can be used, if necessary, for further downstream processing.

To date, most pharmaceutical processes involve conventional batch production approaches (Wang et al. 2012). However, batch based manufacturing presents several disadvantages such as defined batch size, multiple sequential steps, interruptions, long waiting and throughput times, raw material waste, extensive validation and problems associated with scale-up (Plumb 2005). In order to fulfil the foregoing requirements the regulatory bodies actively encourage the development and implementation of innovative pharmaceutical processes and, very importantly, continuous manufacturing (Scott and Wilcock 2006).

Continuous manufacturing (CM) is well accepted in other industries and it is now gradually being accepted in the pharmaceutical industry. The developments in CM are important, as they will lead, in the future, to sustainable growth in pharmaceutical processing with attendant advantages. There are several reasons why industry should adopt CM that will

eventually increase profitability, and product quality (Proctor et al. 2010). Some of the benefits include saving in space/energy, reduction in raw materials used and waste, less human interference, less complex scale-up and, most importantly, reduced time to market of the finished products (Schaber et al. 2011, Vervaet and Remon 2005).

The operational principles of HME offer the possibility to produce complex dosage forms in a continuous mode coupled with in-line process analytical technology (PAT) tools for process monitoring and quality control. HME scale-up requires a detailed understanding of the process as well as the geometry of the extruder. The scale-up concept in HME can be summarized as follows (Dreiblatt 2012).

a) Case 1: increasing production output in a HME process by increasing the batch size (using the same extruder or multiple extruders of the same size).

b) Case 2: increasing production output in a HME process by increasing the feed rate (with or without changes to other process parameters) using the same extruder

c) Case 3: increasing production output in a HME process by increasing the feed rate (with or without changes to other process parameters) on a different extruder with larger dimensions.

The aim of this study was to optimize HME as a scalable, continuous process for the production of indomethacin-saccharin (IND-SCH) and encapsulation of the cocrystals in gelatine capsules. In addition, the process was coupled with PAT tools using in-line NIR and spatial filter velocimetry (Parsum probe) for real-time monitoring of the formation of cocrystals and particle size distribution, respectively. To our knowledge this the first time that the foregoing has been reported. Scale-up of the production of IND-SCH cocrystals, by using a traditional solvent cooling method, has been previously reported (Jung et al. 2010).

6.2   METHODS AND MATERIALS

6.2.1. Materials

Indomethacin (γ-form, IND) and saccharin (SCH) were purchased from Tokyo Chemicals (Tokyo, Japan) and Sigma Aldrich (Gillingham, UK), respectively. All solvents used for HPLC analysis were of analytical grade (Fisher chemical, UK). All the compounds were used as received.

6.2.2   HME process

IND and SCH in 1:1 molar ratio were accurately weighed and homogenously blended by using a Turbula mixer for 10 min. The blend of prepared powder was fed into a 16 mm twin screw extruder (Eurolab16, Thermo fisher, UK) by using a DD Flexwall® 18 feeder (Brabender Technology, Germany). The temperature profile in the HME barrel was set as 70/95/155/165/175/175/175/175/175°C (feeder to die). The HME instrument was operated without the die and the final extrudates were collected in powder form with some agglomeration.

6.2.3   Downstream process

Capsule preparation was carried out by using a Mini Cap Capsules filling machine, (Karnavati Engineering Limited, India) and was operated in auto mode at a rate of 3000 capsule/hr.

Micronization of extruded corystals was carried out using cutter mill (Cutting Mill SM 100, Retsch, Uk). A sieve (250 μm size) was placed at the bottom of the casing holds that controls the size of the material discharged from the milling zone.

6.2.4   In-line particle size measurements

An in-line particle probe (IP 70 probe, Parsum®, Germany) with a D23 disperser unit, was placed at the end of the extruder and underneath the cutter mill for in-line particle size monitoring. Compressed air was used to stimulate the flow of particles and to keep the probe surface clean. The disperser unit was operated at inlet and external pressures of 15 and 2 L/min, respectively. The particle size distribution data was collected and processed by using INLINE PROBE software provided with the instrument.

6.2.5   Off-line particle size measurements

The particle size distributions of the hot-melt extrudates were found by using a dry powder dispersion unit (Scirocco 2000) of a Mastersizer 2000 (Malvern, Worcestershire, UK) laser diffraction particle size analyser. Samples, post-extrusion, were placed in a vibratory tray, which continuously controls the rate of powder flow, in order to measure the particle size off-line. Three particle size measurements were obtained, in continuous sequence, in order to assess the reproducibility of each batch of extrudates. Particle size distributions were automatically collected by the Mastersizer 2000 software.

Six sieves with mesh sizes of 63, 125, 250, 500, 1000 and 2000 μm were stacked. A collector pan was placed below the sieve with the smallest mesh size. The samples were placed on the top sieve (2000 μm) and a lid was placed on it. The assembly was vibrated on an automatic sieve shaker (VE 1000, Retsch, Germany) for 10 min.

6.2.6 Physicochemical characterisations

The analytical methods used in this Chapter such as DSC, XRPD, in-line NIR, *in vitro* dissolution and HPLC analysis are described in Chapter 5, section 5.2.

Fourier transform infrared (FT-IR) spectroscopy

FT-IR spectra were obtained using a Perkin Elmer spectrophotometer (Spectrum 100, Perkin Elmer, US) equipped with a crystal diamond universal ATR sampling accessory (UATR). Solid sample was placed in contact the universal diamond ATR top-plate and an average spectrum of 4 scans was recorded in the range of 4000-400 cm^{-1}.

6.3   RESULTS AND DISCUSSION

6.3.1   HME Process optimisation

Scale up of HME processing can be achieved by increasing throughput, i.e., by using one of the approaches described above (Dreiblatt 2012). In this study it was decided to increase the throughput from the extruder by increasing the material feed rate by using a 16 mm diameter TSE.

An important criterion was to achieve high throughput rate in a short residence time without compromising the quality of the cocrystals. In addition, a detailed understanding of the effect of the HME process variables such as feed rate, screw speed and temperature profile is required. In Chapter 5 it was revealed that screw speed and temperature played a key role in the cocrystal quality while the feed rate did not appear to have a significant effect. Further to the previous studies the effect of the three process variables was explored by extruding another two formulations (F5 – F6). The reason was that the throughput of the cocrystals for the previous formulations (F1 – F4) was quite low and the process scale-up requires the high throughput rate. The screw speed was increased proportionally to the feed rate in order to achieve constant degree-of-fill for the fed drug and conformer (Table 6.1).

Table 6.1. Processing parameter settings applied for the development and scale-up of IND-SCH cocrystals using a constant degree-of -fill.

	Temperature profile (°C) (Feeder $\longrightarrow$ Die)	Screw rate (rpm)	Feeder rate (Kg/hr)	Residence time (min)	Cocrystals
F1	50-70-95-130-140-140-145-145-145	10	0.10	5.2	X
F2	70-95-145-150-155-155-155-155-155	10	0.10	5.2	✓
F3	70-95-145-150-155-155-155-155-155	30	0.30	2.5	X
F4	50-70-95-155-160-165-165-165-165	30	0.30	2.5	✓
F5	50-70-95-155-160-165-165-165-165	100	1.0	1.0	X
F6	70-95-155-165-175-175-175-175-175	100	1.0	1.0	✓

It is obvious that when changes in extrusion temperature profile and screw speed are made, the feed rate has to be optimised when using an extruder of the same size .The increase in the feed rate and screw speed affected changes in the residence time and extrusion temperature. For extrusion temperatures below the eutectic point of the cocrystals, incomplete conversation to cocrystals was noted, indicated by the presence of small amount of IND in the F1 extrudates. An increase in the processing temperature at the eutectic point provided high quality (i.e. absence of unreacted components) cocrystals. However, the increase in feed rate and screw speed at constant temperature (155°C) did not form quality cocrystals. Thus, the temperature was increased to 165°C in order to eliminate any unreacted material and produce the requisite cocrystals (F4) in which bulk materials could not be detected (the presence of bulk materials, i.e. API and coformer for the synthesis of cocrystals, was ascertained by off-line XRPD and DSC measurements). The same phenomenon was observed for higher feed rates and screw speeds (F5), which eventually led to the use of an extrusion temperature of 175°C (F6). The use of the high extrusion temperatures, above the drug-coformer eutectic melting point, increases the possibility of drug degradation and also

limits the formation of cocrystals. However, extrusion at 175°C did not affect IND and enabled the formation of cocrystals (discussed below). In addition, the residence time for extrusion was significantly reduced from 5.2 min to 1.0 min without having an effect on the resulting product attributes. Fig. 6.1 provides a schematic representation of the process boundary and the melt temperature dependence.
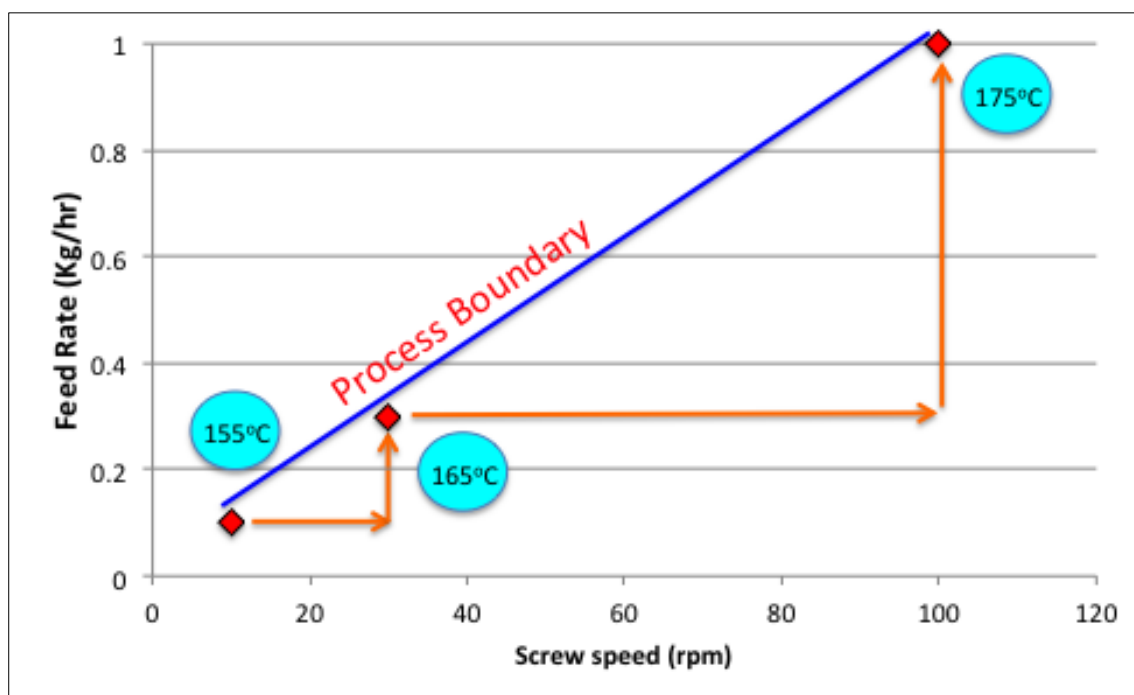
Fig. 6.1. Schematic diagram of the HME process boundaries and melt temperature dependence.

For scale-up purposes, the extrusion settings of F6 at 1.0 kg/hr feed rate; 100 rpm screw speed and 175°C extrusion temperature were used. These processing conditions allowed the extrusion of quality cocrystals at high throughput by using the same extruder.

6.3.2 Continuous downstream process

The goal of the second part of this study was to develop a continuous HME process for the production of IND-SCH cocrystals encapsulated in gelatin capsules. Extrusion processing is among the few suitable/applicable technologies that can be used for continuous manufacturing of solid dosage forms by coupling with the appropriate downstream equipment and PAT tools. Fig. 6.2 shows a schematic diagram of the CM process developed whereby the extruded cocrystals are fed into a cutter mill to reduce the particle size

(downstream equipment) and collected in a volumetric feeder (Brabender Technology, Germany) following blending with an excipient blend from a second volumetric feeder. The blend of cocrystals and excipients are then fed into the hopper of a machine used for the production of capsules in order to produce hard gelatine capsules (size 4); each capsule contains the equivalent of 25 mg IND. Process monitoring and quality control is achieved by using an in-line NIR probe at the end of the extruder and a particle size probe placed underneath the cutter mill. The NIR probe is set to monitor the "as made" IND-SCH cocrystals while the Parsum particle probe is used to continuously measure the size of the micronized particles. The coupling of HME with PAT tools is not limited to these two CM probes; it can involve additional PAT tools such as Raman or ultrasonic probes at different stages of the manufacturing process.

The milled cocrystals were blended with a capsule formulation (feeder 2), which consisted (w/w %) of lactose (31.50%), MCC (microcrystalline cellulose) (28.56%) and silica (0.25%) at a ratio of 39.70:60.30 (w:w) for the cocrystals/excipients. The blending rate of the twin-screw conveyor (Buck Systems Continuous Dry Blender, GEA Pharma system) was calibrated and set at 3.2 kg/hr while the capsule filler was programmed to follow a 10 min lag period prior to capsule filling, in order to allow the transfer of enough material from the conveyor to the capsule machine hopper. The process scale-up allowed the production of capsules at a rate of 3000/hr. The CM of capsules containing cocrystals was allowed to operate successfully for at least 30 min. The cocrystals obtained and the recorded PAT measurements were further evaluated at the end of the CM process. It is important that the process scale-up and the CM operation does not alter the material attributes and provides high quality cocrystals according to the established specifications during the development stage.
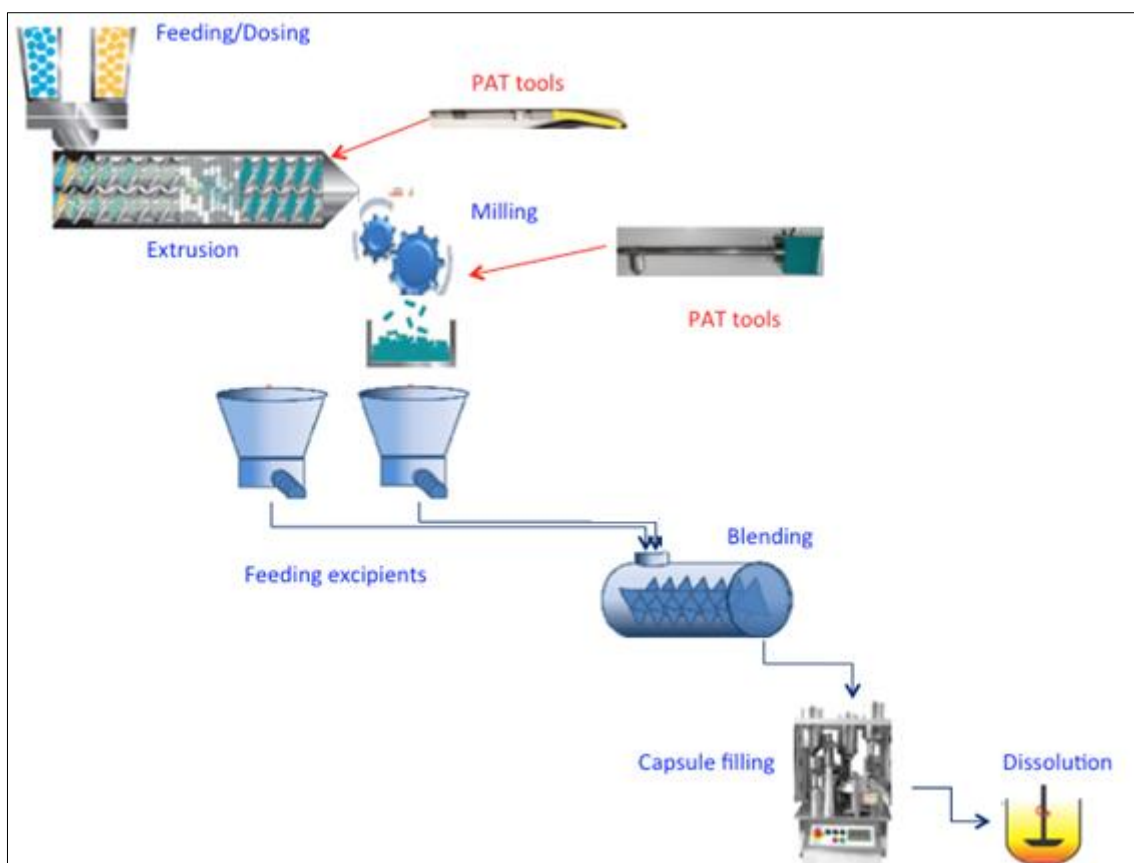
Fig. 6.2. Illustration of continuous downstream manufacturing processes and PAT control points.

6.3.3 In-line particle size monitoring

It was found, using in-line particle size probe, that the IND-SCH cocrystals exit the extruder in the form of agglomerates when the extrusion temperature exceeds 165°C. The agglomerates (which constituted~ 30% of the total particles), produced at an extrusion temperature above 165°C displayed a particle size between 1000 and 2000 μm and thus further micronization was required before capsule filling. The in-line particle size probe equipped with a D23 in-line inductor was placed underneath the cutter mill and the particle size distribution was recorded on-line every 5 min. Samples were collected during the cutter mill process and, for comparative purposes; the particle size was also determined off-line using sieve analysis.

The D23 in-line inductor was used to analyse the "as made" cocrystals extruded at 175°C/100 rpm. In-line particle size distribution measurements showed a good correlation with the results obtained by off-line sieve analysis (Fig.6.3).

101
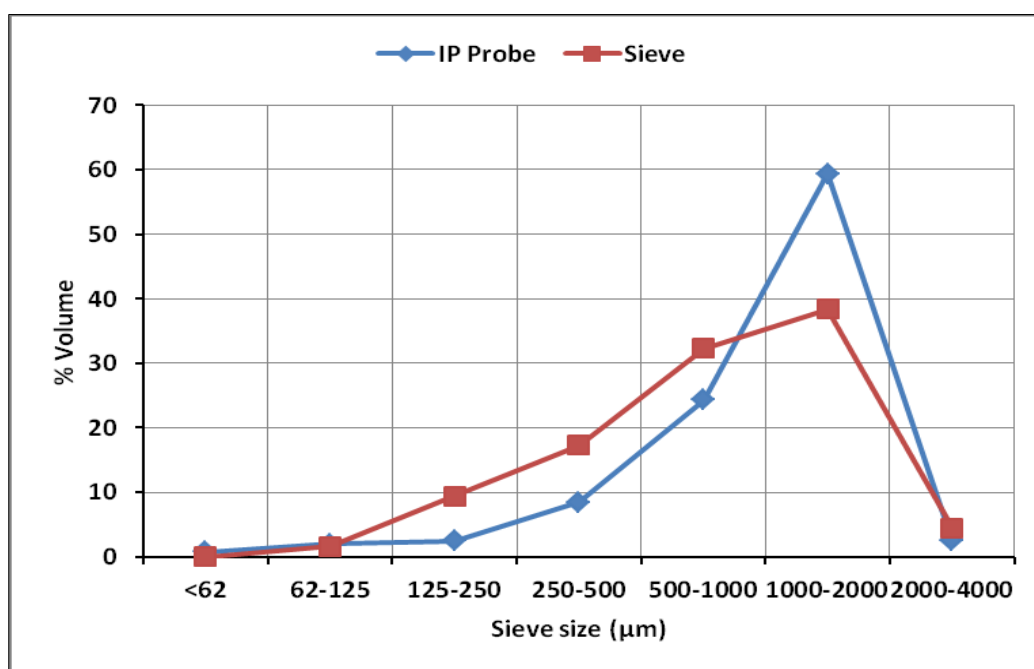
Fig. 6.3. In-line particle measurements during extrusion of cocrystals (175°C/100 rpm) in comparison with off-line sieve analysis.

The milled batches cocrystals, produced at 165°C/30 rpm, were "sticky", and it was difficult to determine the range of particle sizes by sieve analysis. However, cutter milling of IND-SCH cocrystals at 175°C/100 rpm showed no "sticky" behaviour and a free flowing powder was collected. The non-sticky behaviour of the collected powder was assumed to be due to the high extrusion temperature (175°C), i.e. above the eutectic melt of the physical mixture (155°C) and within 5°C of the melting temperature (180°C) of the cocrystals. At this extrusion temperature (175°C) the materials partially melt in the last mixing zone at the end of barrel. The particle size distribution of milled cocrystals (175°C/100 rpm) showed similar results for both in-line and off-line measurements (Fig. 6.4).
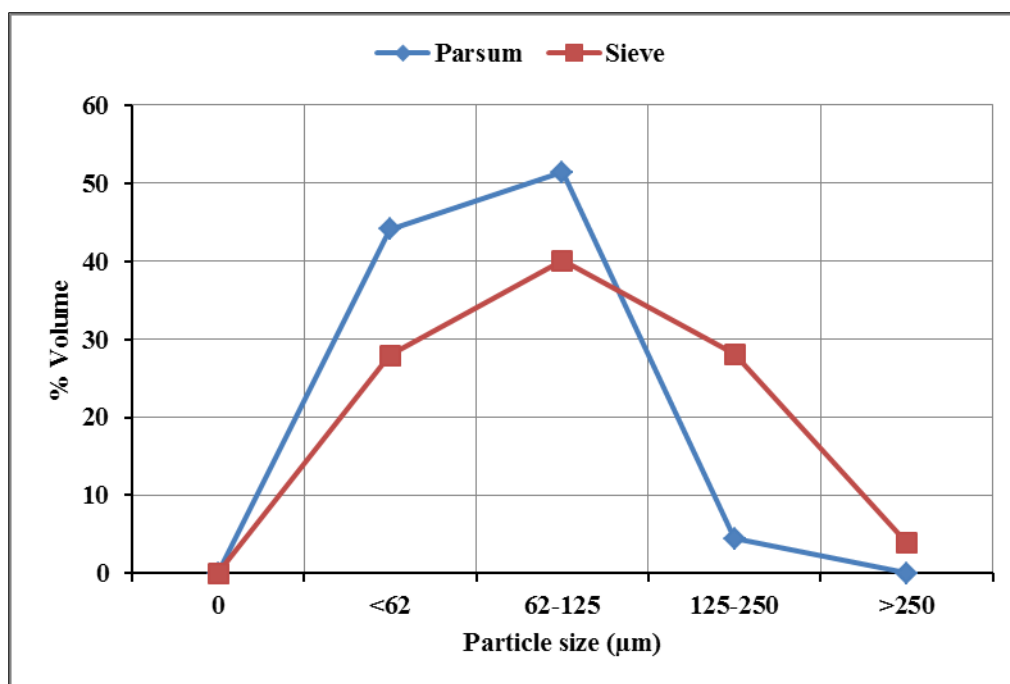
Fig. 6.4. In-line particle size measurements during cutter milling of cocrystals produced by HME (175°C/100 rpm) in comparison with off-line sieve analysis.

6.3.4   In-line NIR monitoring

Prior to extrusion, off-line NIR analysis was performed on bulk IND, SCH and PM to confirm the conversation of cocrystals at a later stage. NIR spectra of the PM showed that there was no molecular interaction between IND and SCH, i.e., the spectra were identical to the bulk materials (Fig. 6.5).

Second derivative spectra of the cocrystals collected from the end of the extruder barrel showed different bands compared to bulk IND, SCH and PM in the 4200-6300 cm^{-1} wavenumber region (Fig. 6.6). The vibrational band at 5022 cm^{-1} in bulk IND, was found to shift towards lower wavenumber, 4988 cm^{-1}, in the cocrystal spectrum; this band is due to OH stretching and is due to hydrogen bonding in the cocrystals. This is a distinct NIR band for the cocrystals and was considered as a reference band; it was continuously monitored throughout the extrusion process to confirm the formation of cocrystals.
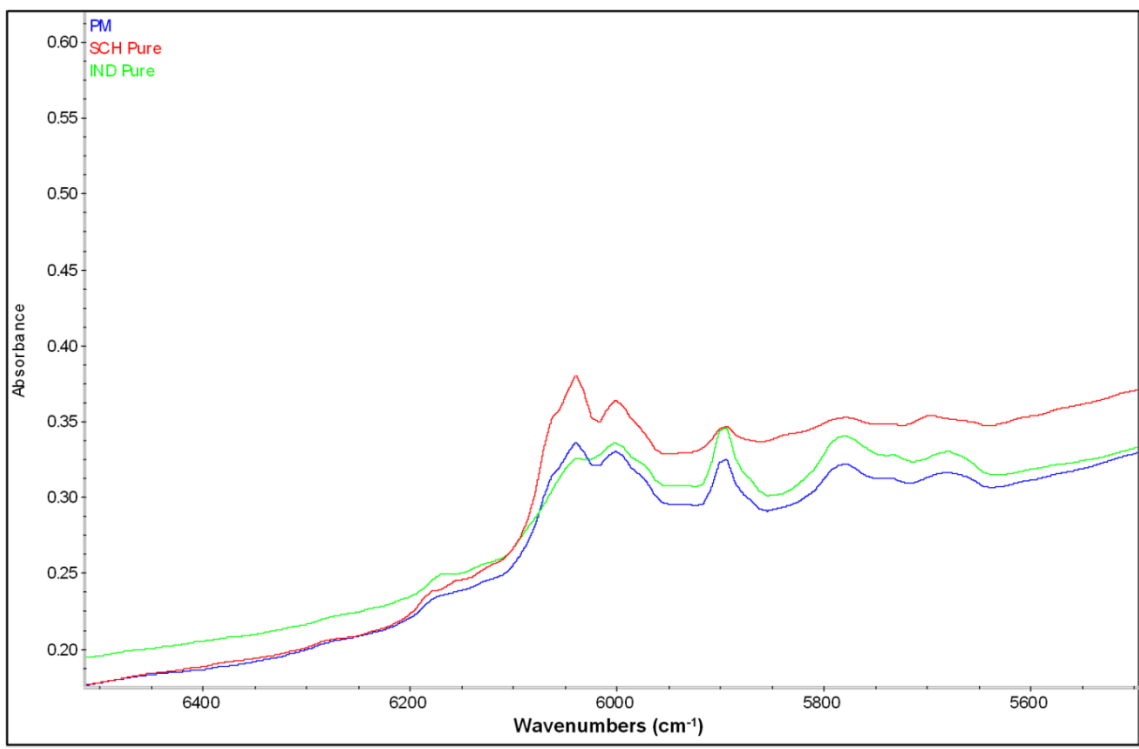
Fig. 6.5. NIR spectra of bulk IND, SCH and the PM of IND: SCH in the 5500-6500 cm^{-1} wavenumber region.
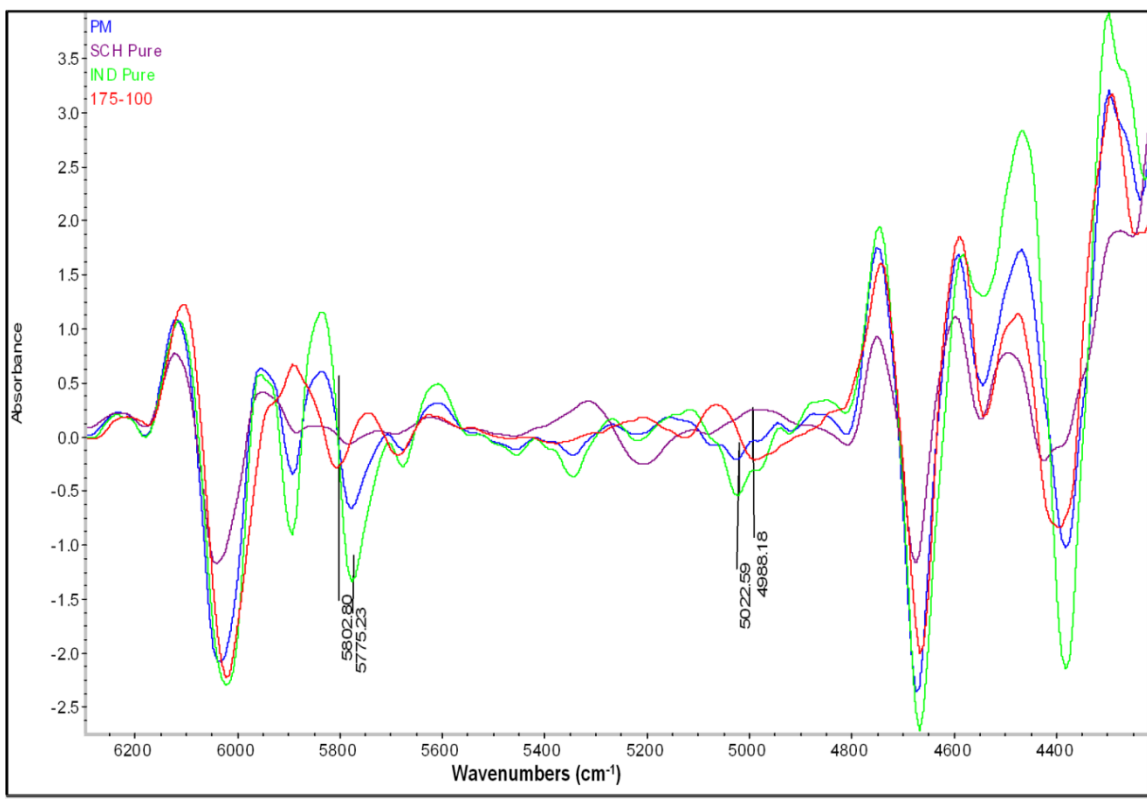
Fig. 6.6. Second derivative NIR spectra of bulk IND, SCH, PM and the hot melt extruded cocrystals at 175°C/100 rpm in the 4200-6300 cm^{-1} wavenumber region.

104

6.3.5 Cocrystal characterisation

DSC and XRPD data of bulk IND, bulk SCH, PM and extruded cocrystals are displayed in Figs. 6.7 and 6.8. Bulk IND and SCH presented single endothermic peaks at 160.45°C and 226.82°C, respectively. The *in situ* melting of the PM showed two endothermic peaks with the first one at 156.24°C related to the eutectic melt of cocrystals (*in-situ* cocrystal formation) while the second peak at 183.05°C is attributed to the melting point of the cocrystals. A single and sharp endothermic peak for extruded cocrystals was observed at 182.85°C which specifies the individuality of the cocrystalline system. The formation of IND-SCH cocrystals was also confirmed by XRPD analysis (Fig. 6.8). IND-SCH cocrystals (175°C/100 rpm) showed unique XRPD pattern compares to bulk components with characteristic diffraction peaks at 5.43°, 10.89°, 14.42°, 21.22°, 25.45°, and 27.07° 2θ. The XRPD diffractograms of the cocrystals were identical to the reference pattern collected from the CCDS database. However, HME processed cocrystals at 165°C/100 rpm showed trace of unreacted IND.
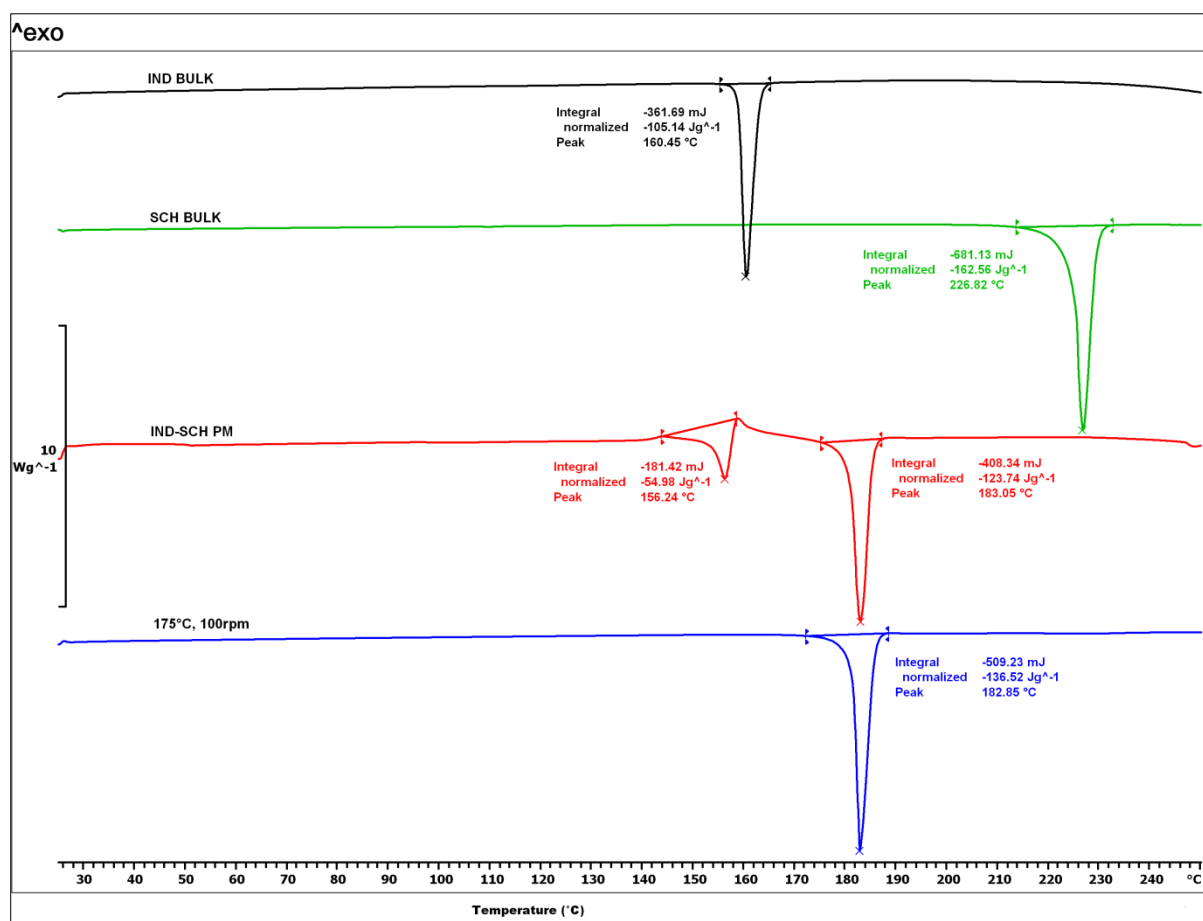
Fig. 6.7. DSC thermograms of bulk IND, bulk SCH, PM and extruded cocrystals (175°C/100 rpm).
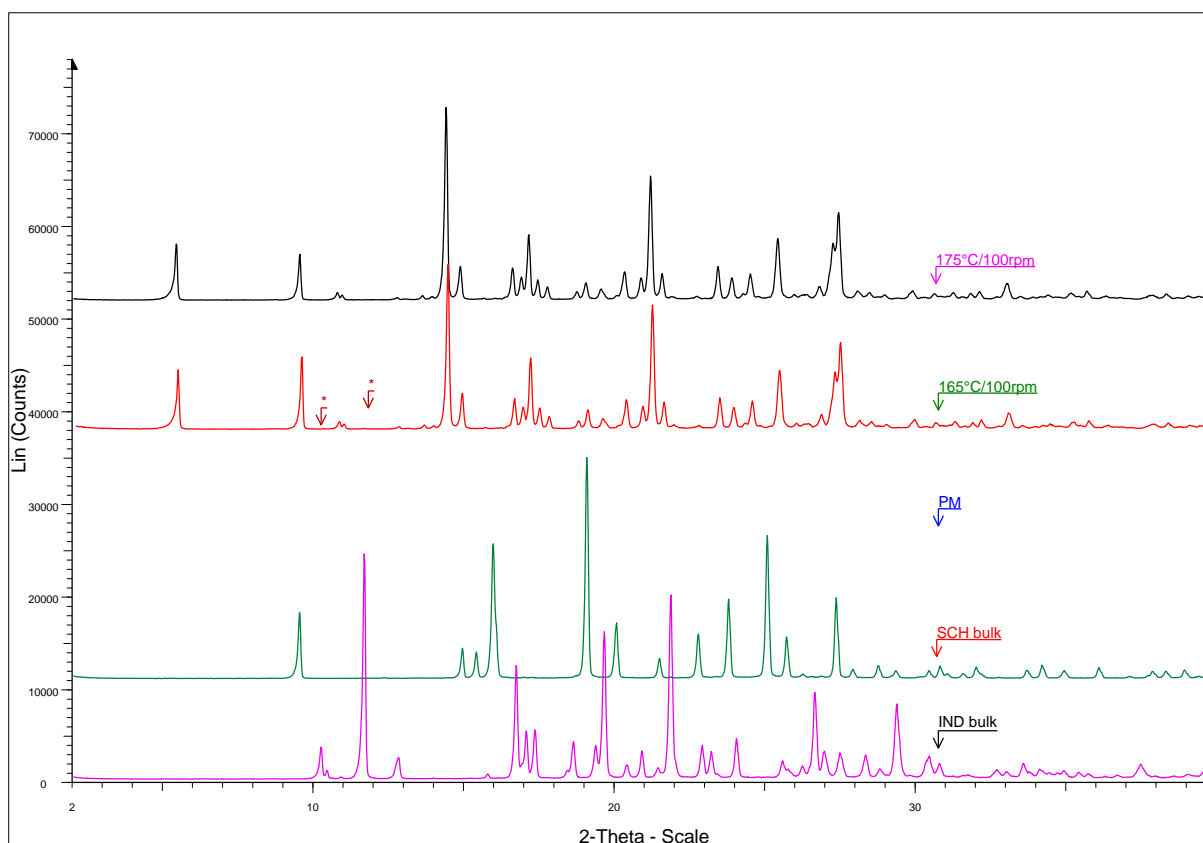
Fig. 6.8. XRPD diffractograms of bulk components (IND, SCH), PM and extruded cocrystals (175°C/100 rpm and 165°C/100 rpm).

6.3.6   FT-IR spectroscopy

The FTIR spectra of IND, SCH and extruded cocrystals are depicted in Fig. 6.9. IR absorption bands at 3093.87 cm^{-1} (-NH stretch), 1716.25 cm^{-1} (secondary -C=O stretch), 1176 cm^{-1} (symmetric -SO$_2$) and 1333 cm^{-1} (asymmetric -SO$_2$) were observed for bulk SCH. Bulk IND displayed IR bands at 3270.3 cm^{-1} for the -OH group and 1713.92cm^{-1} for the carboxylic C=O functional group (Taylor and Zografi 1997).

FT-IR spectra of cocrystals of IND-SCH indicated the presence of the bulk components at 3345.52 cm^{-1} and 3080.7 cm^{-1} related to the -OH and -NH functional groups of IND and SCH, respectively. The broad bands of IND and SCH were shifted towards lower wavenumbers in the IR region of the cocrystals, due to the formation of the -H bond between the hydroxyl group of IND and the -NH group of SCH (Basavoju et al. 2008). Characteristic IR bands related to IND-SCH cocrystals gave bands at 3008.52, 2833.95, 1736.34, 1709.45 and

1315.63 cm^{-1}, which ware in good agreement with previously reported data (Zhang et al. 2012)

The off-line analysis of extrudates by XRPD, DSC and FTIR confirmed the formation of IND-SCH cocrystals.
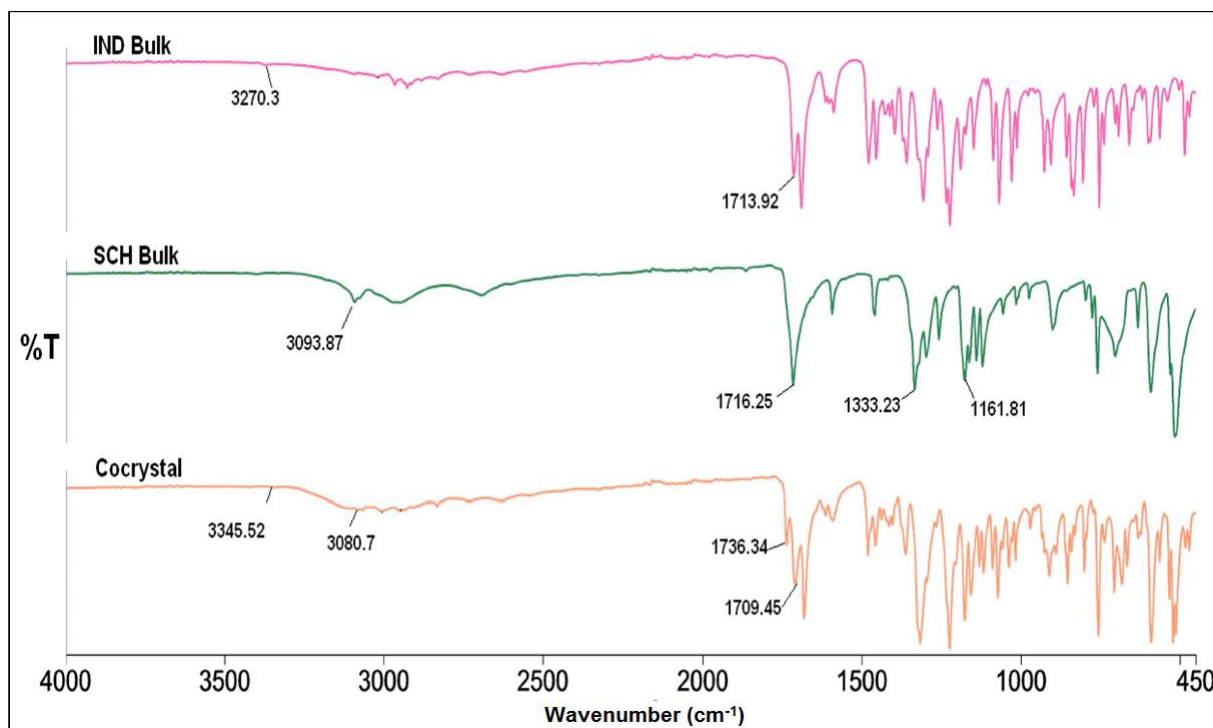
Fig. 6.9. FTIR spectra of bulk IND, bulk SCH and hot-melt extruded cocrystals processed at 175°C/100 rpm.

6.3.7   Dissolution Studies

The dissolution of cocrystals (Fig. 6.10) processed under scale-up conditions (175°C/100 rpm) showed a higher dissolution rate compared to bulk IND. Furthermore, the micronized cocrystals showed even higher dissolution rates compared to the "as made" cocrystals, due to the smaller particle size. In the first 15 min, the dissolution rates were 10%, 40% and 67% for bulk IND, cocrystals (without particle size reduction) and milled cocrystals. The encapsulated cocrystals showed a significant dependence on the selected excipients that were used as fillers in the capsules. The use of MCC and lactose as fillers showed a retardation in the dissolution rates and the dissolution was slightly slower compared to the pure cocrystals. In contrast, when the capsules did not contain fillers the dissolution rates were similar to micronized cocrystals, indicating that the capsule shell had no significant effect on the rate of

dissolution. The dissolution behaviour of the cocrystals encapsulated with excipients is not fully understood and requires further investigation.
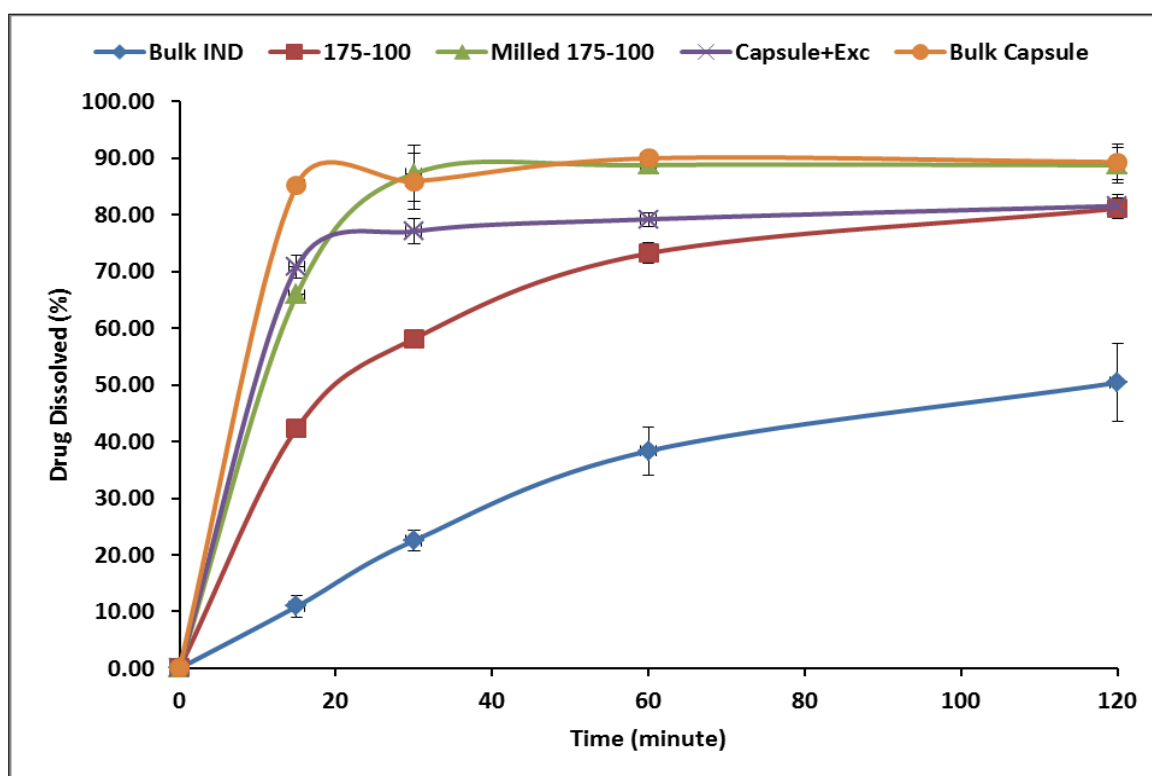
Fig. 6.10. Dissolution profile of bulk IND, extruded cocrystals (175°C/100 rpm, without particle size reduction), milled 175°C-100 rpm cocrystals (<250 μm), capsule + excipients (Exc) (milled cocrystals and excipients) and bulk capsule (milled cocrystals without excipients).

6.4   CONCLUSIONS

Scale-up and continuous downstream process for cocrystallisation of IND-SCH was successfully established by using a laboratory scale twin screw extruder. Screw speed and extrusion temperature with the appropriate choice of feed rate in the hot melt extruder were found to be important processing/scale-up parameters in order to produce cocrystals of the required quality/characteristics. Any throughput can be achieved by varying a combination of feed rate and barrel temperature for the scale-up of the cocrystallisation process. However, an increase in the screw speed is required with an increase in feed rate to avoid any blockage during the extrusion process. In-line monitoring of particle size during extrusion and milling was achieved in the continuous manufacture of cocrystals. Cocrystal formation was confirmed during the extrusion process by using an in-line NIR probe. Off-line FT-IR and

in-line NIR data suggested H-bond formation in the cocrystals produced using IND and SCH. Extruded cocrystals were milled to achieve uniformity in the particle size to prepare the final dosage form. Capsules, as a final dosage form, were prepared in continuous mode by using an auto capsule filler and had a similar dissolution profile to the bulk milled cocrystals when it was encapsulated without any excipients. Milled cocrystals displayed an increase in the rate of dissolution compared to extrudates due to an increase in the surface area of the particles. A more detailed investigation of the effect(s) of excipients on the dissolution characteristics of IND-SCH cocrystals is required.

A continuous process was established from feeding of the PM into the extruder to prepare the final dosage form for cocrystals of IND-SCH and was successfully monitored by using in-line PAT tools.

CHAPTER 7 : SUMMARY

Pharmaceutical cocrystals are a promising way to improve the bioavailability of poorly water soluble drugs resulting in higher aqueous solubility; the solubility and dissolution behaviour of cocrystals has been widely studied. Solvent and grinding are common methods to prepare pharmaceutical cocrystals. The research reported in this thesis attempts to provide scientific insights for the solvent free, continuous cocrystallisation of poorly water soluble drugs and their coformers by using HME.

In this research we have explored the manufacture of cocrystals by using HME to increase the dissolution rate of poorly water soluble drugs. Two types of hot melt extruders (SSE and TSE) were employed in order to assess their effect on the formation and quality of cocrystals produced. Cocrystallisation was performed on the low aqueous soluble BCS class II active, carbamazepine, and GRAS approved coformers (saccharin and *trans*-cinnamic acid) by screening the processing temperatures when using SSE. Comparisons of TSE and SSE extruded cocrystals, showed that SSE could be used to form cocrystals; but the lack of mixing screw elements resulted in a decrease in the crystallinity of the cocrystals, caused by the presence of unreacted materials from the physical mixture used. DSC analysis performed on SSE extruded cocrystals exhibited a single, low intensity peak compare to the TSE and prototype cocrystals and less intense peaks in the XRPD diffractograms indicated different applied temperatures during SSE had an effect on the quality of the cocrystals. Moreover, TSE could be used to produce high quality of cocrystals when the optimum screened temperature was applied from SSE experiments. Off-line XRPD and DSC analysis of the samples collected from the three different mixing zones of the TSE barrel during CBZ-TCA extrusion showed the important role of the mixing elements, along the length of the extrusion barrel, in the cocrystallisation process. All the cocrystals, including those processed by both SSE and TSE showed higher dissolution rates when compared to bulk carbamazepine. The dissolution rate of extruded cocrystals was significantly affected by the purity (i.e., the presence of unreacted materials) of the final product and the dissolution rates were found to be in the order: SSE cocrystals $\leq$ prototype $<$ TSE cocrystals. TSE extrudates were found to have a single, sharp endotherm similar to prototype cocrystals which were synthesized by using the solvent method. Interestingly, XRPD studies and stability testing could not be used to differentiate TSE cocrystals from the prototype cocrystals. The TSE was employed at a

constant HME processing temperature and screw speed for the production of binary mixtures of CBZ-DGL at three different molar ratios. DSC analysis could not be used to identify any transformations in the extrudates; however, hot stage microscopy (HSM) and XRPD studies of the extrudates revealed the conversation of CBZ form III into polymorphic form I in the extrudates. Furthermore, SEM analysis of extrudates showed needle shaped crystals (CBZ Polymorph form I) present in extrudates which was absent in PMs. All HME treated samples (extrudates) exhibited a higher rate of drug dissolution compared to the bulk CBZ and the PMs of CBZ and DGL. For PMs, the rate of dissolution was higher according to the amount of GL present in each PM which was not the case for extrudates. Differences between the dissolution rates of PMs and extrudates confirmed the effect of polymorphism on the dissolution rate which was higher for the 1.5:1 molar ratio of CBZ: DGL extrudates compared to the other ratios of extrudates (i.e. 1:1 and 2:1).

Cocrystals of IND-SCH were produced by using TSE. The HME processing parameters were examined in order to optimise the cocrystallisation process. It was evident that screw speed and extrusion temperature have a significant influence on the quality of the cocrystals, and thus need to be optimised. An increased dissolution rate was found for this cocrystal system compared to bulk IND. The particle size of the IND-SCH cocrystals, produced by HME, had a significant effect on the dissolution rate due to an increase in the surface area of the milled compared to the non-milled cocrystals. An in-line NIR probe was sucessfully used to detect cocrystal formation during HME processing. In-line particle size distribution was monitored during the extrusion and at the cutter mill, which was in good agreement with the particle size distribution obtained from off-line laser particle size analyser or sieve analysis.

Scale-up of the production of IND-SCH cocrystals was achieved by increasing the throughput rate of the reactants, i.e., by increasing the feed rate. An optimisation of the extrusion temperature and the screw speed was required with increase in feed rate to optimise cocrystal formation. Furthermore, PAT tools, in-line NIR and Parsum® (in-line particle measurement) probe, were used during the extrusion process. Off-line XRPD, DSC and FTIR analyses were performed on extruded cocrystals to support the in-line NIR results. In-line NIR data suggested H-bond formation between IND and SCH. It was found, by in-line particle size distribution measurements that the extruded cocrystals consisted of a range of particle sizes, including agglomerates, which was in agreement with off-line sieve analysis and required a reduction in particle size (milling). During the scale-up further processing was continued in

order to make the final dosage form. Capsules of IND-SCH cocrystals were successfully produced in continuous mode via HME processing. An effective practice for in-line particle measurement was established for the HME process.

Overall, cocrystallisation of poorly water soluble drugs was found to increase their dissolution performance. A solvent free, continuous, one step HME environment is an ideal process for formulating and scale-up for the production of cocrystals.

CHAPTER 8 : FUTURE WORK

In the scientific literature there are various reports of the use of HME for the manufacture and engineering of various pharmaceutical dosage forms. Herein the production of cocrystals by continuous HME methodologies has been reported. The scope of any future work in relation to process optimisation and advanced applications of pharmaceutical cocrystallisation via HME processing would include (but is not limited to) the following.

(i)   Continuous cocrystallisation, of API's and coformers, by HME was shown to increase the solubity and dissolution of poorly water soluble drugs. However, in aquesous media the API, after drug release, tends to crystallise in to the less soluble and more stable form. A small amount of surfactant/ polymer has proven to inhibit the transformation of the metastable form (less soluble form) of an API (e.g. carbamazepine or indomethacin) in aqueous dissolution media (Alhalaweh et al. 2013). This can be further studied by adding low concentrations of surfactants and/or polymers during extrusion in order to produce matrices containing cocrystals. The presence of a surfactant and/or polymer can have an effect on the solubility, stability and dissolution rates of cocrystals in media differing in pH.

(ii)   One of the advantages of TSE is that the mixing elements can be placed at different angles in order to achieve the required shear and mixing, according to specific requirements. The screw configuration of the TSE could be modified to achieve more efficient mixing, which may have an effect on cocrystal formation. A mixing zone could be created by using a combination of mixing and conveying elements followed by a second mixing zone made only of mixing elements placed at different angles to achive maxium mixing efficiency of TSE.

(iii)   Salt forms of APIs (an acid-base reaction between the API and an acidic or basic substance) are commonly used in pharmaceutical drug development (Elder et al. 2013). However, HME has never (to our knowledge) been used for forming salts. For comparative purposes cocrystals and salts of poorly water soluble drugs could be processed via HME and then examined using different analytical techniques, including dissolution studies.

New trends in the synthesis of cocrystals include "ionic cocrystals" which involve a salt and another neutral molecule or salt (Smith et al. 2013). Ionic cocrystals

have been synthesized by solution crystallization, slurry or mechanochemistry (grinding) methods; however, it would be interesting to examine whether the high shear and mixing environment used in HME can be used to form ionic cocrystals. HME can offer a new way to formulate ionic cocrystals or pharmaceutical salt formation via contionous, one step, solvent free processing offers enhancement in physicochemical properties of pharmaceutical molecules and development of patents.

CHAPTER 9 : REFERENCES

Aakeroy, C. B., Champness, N. R. and Janiak, C. (2010) 'Recent advances in crystal engineering', *CrystEngComm,* 12(1), 22-43.

Aher, S., Dhumal, R., Mahadik, K., Paradkar, A. and York, P. (2010) 'Ultrasound assisted cocrystallization from solution (USSC) containing a non-congruently soluble cocrystal component pair: Caffeine/maleic acid', *European Journal of Pharmaceutical Sciences,* 41(5), 597-602.

Aina, A. T. (2012) *In situ monitoring of pharmaceutical crystallisation*, (Doctoral Thesis), University of Nottingham.

Aitipamula, S., Banerjee, R., Bansal, A. K., Biradha, K., Cheney, M. L., Choudhury, A. R., Desiraju, G. R., Dikundwar, A. G., Dubey, R. and Duggirala, N. (2012) 'Polymorphs, Salts, and Cocrystals: What's in a Name?', *Crystal Growth & Design,* 12(5), 2147-2152.

Aitipamula, S., Chow, P. S. and Tan, R. B. H. (2009) 'Dimorphs of a 1 : 1 cocrystal of ethenzamide and saccharin: solid-state grinding methods result in metastable polymorph', *CrystEngComm,* 11(5), 889-895.

Aitipamula, S., Chow, P. S. and Tan, R. B. H. (2014) 'Polymorphism in cocrystals: a review and assessment of its significance', *CrystEngComm,* 16(17), 3451-3465.

Al-Hamidi, H., A., E. A., Mohammad, M. A. and Nokhodchi, A. (2010) 'UK-PharmSci 2010 - The Science of Medicines. Abstracts from the UK-PharmSci Conference, 1-3 September 2010', *Journal of Pharmacy and Pharmacology,* 62(10), 1201-1516.

Al-Hamidi, H., Obeidat, W. M. and Nokhodchi, A. (2014) 'The dissolution enhancement of piroxicam in its physical mixtures and solid dispersion formulations using gluconolactone and glucosamine hydrochloride as potential carriers', *Pharmaceutical Development and Technology,* DOI: 10.3109/10837450.2013.871029.

Alhalaweh, A., Ali, H. R. H. and Velaga, S. P. (2013) 'Effects of polymer and surfactant on the dissolution and transformation profiles of cocrystals in aqueous media', *Crystal Growth & Design,* 14(2), 643-648.

Alhalaweh, A., Roy, L., Rodriguez-Hornedo, N. and Velaga, S. P. (2012) 'pH-dependent solubility of indomethacin-saccharin and carbamazepine-saccharin cocrystals in aqueous media', *Molecular Pharmaceutics,* 9(9), 2605-2612.

Alhalaweh, A., Sokolowski, A., Rodriguez-Hornedo, N. and Velaga, S. P. (2011) 'Solubility Behavior and Solution Chemistry of Indomethacin Cocrystals in Organic Solvents', *Crystal Growth & Design,* 11(9), 3923-3929.

Alhalaweh, A. and Velaga, S. P. (2010) 'Formation of Cocrystals from Stoichiometric Solutions of Incongruently Saturating Systems by Spray Drying', *Crystal Growth & Design,* 10(8), 3302-3305.

Allen, L. V., Popovich, N. G. and Ansen, H. C. (2009) 'Pharmaceutical and formulation considerations' in *Ansel's Pharmaceutical dosage forms and drug delivery systems*, 9th ed., New York: Lippincott Williams & Wilkins, 90-142.

Allesø, M., Velaga, S., Alhalaweh, A., Cornett, C., Rasmussen, M. A., Berg, F. v. d., Diego, H. L. d. and Rantanen, J. (2008) 'Near-Infrared Spectroscopy for Cocrystal Screening. A Comparative Study with Raman Spectroscopy', *Analytical Chemistry,* 80(20), 7755-7764.

Almarsson, O. and Zaworotko, M. J. (2004) 'Crystal engineering of the composition of pharmaceutical phases. Do pharmaceutical cocrystals represent a new path to improved medicines?', *Chemical Communications*, 1889-1896.

Almeida, A., Claeys, B., Remon, J. P. and Vervaet, C. (2012) 'Hot-Melt Extrusion Developments in the Pharmaceutical Industry' in Douroumis, D., ed., *Hot-Melt Extrusion: Pharmaceutical Applications*, John Wiley & Sons Ltd UK, 43-69.

Am Ende, D. J., Anderson, S. R. and Salan, J. S. (2014) 'Development and Scale-Up of Cocrystals Using Resonant Acoustic Mixing', *Organic Process Research & Development,* 18(2), 331-341.

Amidon, G. L., Lennernas, H., Shah, V. P. and Crison, J. R. (1995) 'A theoretical basis for a biopharmaceutic drug classification: the correlation of in vitro drug product dissolution and in vivo bioavailability', *Pharmaceutical Research,* 12(3), 413-420.

Andrews, G. P., Jones, D. S., Abu Diak, O., McCoy, C. P., Watts, A. B. and McGinity, J. W. (2008) 'The manufacture and characterisation of hot-melt extruded enteric tablets', *European Journal of Pharmaceutics and Biopharmaceutics,* 69(1), 264-273.

Andrews, G. P., Jones, D. S., Diak, O. A., Margetson, D. N. and McAllister, M. S. (2009) 'Hot-melt extrusion: an emerging drug delivery technology', 2(1), 24-27, [online] available: http://www.pharmtech.com/pharmtech/Manufacturing+%26+Processing/Hot-melt-extrusion-an-emerging-drug-delivery-techn/ArticleStandard/Article/detail/574856

Babu, N. J., Reddy, L. S., Aitipamula, S. and Nangia, A. (2008) 'Polymorphs and Polymorphic Cocrystals of Temozolomide', *Chemistry – An Asian Journal,* 3(7), 1122-1133.

Bak, A., Gore, A., Yanez, E., Stanton, M., Tufekcic, S., Syed, R., Akrami, A., Rose, M., Surapaneni, S., Bostick, T., King, A., Neervannan, S., Ostovic, D. and Koparkar, A. (2008) 'The cocrystal approach to improve the exposure of a water-insoluble compound: AMG 517 sorbic acid cocrystal characterization and pharmacokinetics', *Journal of Pharmaceutical Science,* 97(9), 3942-3956.

Basavoju, S., Bostrom, D. and Velaga, S. P. (2008) 'Indomethacin-saccharin cocrystal: design, synthesis and preliminary pharmaceutical characterization', *Pharmaceutical Research,* 25(3), 530-541.

Behme, R. J. and Brooke, D. (1991) 'Heat of Fusion Measurement of a Low Melting Polymorph of Carbamazepine That Undergoes Multiple-Phase Changes during Differential Scanning Calorimetry Analysis', *Journal of Pharmaceutical Science,* 80(10), 986-990.

Berry, D. J., Seaton, C. C., Clegg, W., Harrington, R. W., Coles, S. J., Horton, P. N., Hursthouse, M. B., Storey, R., Jones, W., Friščić, T. and Blagden, N. (2008) 'Applying Hot-Stage Microscopy to Cocrystal Screening: A Study of Nicotinamide with Seven Active Pharmaceutical Ingredients', *Crystal Growth & Design,* 8(5), 1697-1712.

Bhatt, P. M., Azim, Y., Thakur, T. S. and Desiraju, G. R. (2008) 'Cocrystals of the Anti-HIV Drugs Lamivudine and Zidovudine', *Crystal Growth & Design,* 9(2), 951-957.

Blagden, N., Berry, D. J., Parkin, A., Javed, H., Ibrahim, A., Gavan, P. T., De Matos, L. L. and Seaton, C. C. (2008) 'Current directions in cocrystal growth', *New Journal of Chemistry,* 32(10), 1659-1672.

Blagden, N., Coles, S. J. and Berry, D. J. (2014) 'Pharmaceutical cocrystals - are we there yet?', *CrystEngComm,* 16(26), 5753-5761.

Blagden, N., de Matas, M., Gavan, P. T. and York, P. (2007) 'Crystal engineering of active pharmaceutical ingredients to improve solubility and dissolution rates', *Advanced Drug Delivery Reviews,* 59(7), 617-630.

Boksa, K., Otte, A. and Pinal, R. (2014) 'Matrix-Assisted Cocrystallization (MAC) Simultaneous Production and Formulation of Pharmaceutical Cocrystals by Hot-Melt Extrusion', *Journal of Pharmaceutical Science,* 103(9), 2904-2910.

Bond, A. D. (2009) 'Polymorphism in molecular crystals', *Current Opinion in Solid State and Materials Science,* 13(3), 91-97.

Braga, D., Maini, L. and Grepioni, F. (2013) 'Mechanochemical preparation of cocrystals', *Chemical Society Reviews,* 42(18), 7638-7648.

Brittain, H. G. (2012) 'Cocrystal Systems of Pharmaceutical Interest: 2011', *Crystal Growth & Design,* 12(11), 5823-5832.

Buanz, A. B. M., Telford, R., Scowen, I. J. and Gaisford, S. (2013) 'Rapid preparation of pharmaceutical cocrystals with thermal ink-jet printing', *CrystEngComm,* 15(6), 1031-1035.

Carino, S. R., Sperry, D. C. and Hawley, M. (2006) 'Relative bioavailability estimation of carbamazepine crystal forms using an artificial stomach-duodenum model', *Journal of Pharmaceutical Science,* 95(1), 116-125.

Chadha, R., Arora, P., Bhandari, S. and Bala, M. (2012) 'Thermomicroscopy and its pharmaceuticals applications', *Current Microscopy Contributions to Advances in Science and Technology (A. Mendez-Vilas, Ed.).*

Chattoraj, S., Shi, L. and Sun, C. C. (2010) 'Understanding the relationship between crystal structure, plasticity and compaction behaviour of theophylline, methyl gallate, and their 1 : 1 cocrystal', *CrystEngComm,* 12(8), 2466-2472.

Childs, S. L., Chyall, L. J., Dunlap, J. T., Smolenskaya, V. N., Stahly, B. C. and Stahly, G. P. (2004) 'Crystal Engineering Approach To Forming Cocrystals of Amine Hydrochlorides with Organic Acids. Molecular Complexes of Fluoxetine Hydrochloride with Benzoic, Succinic, and Fumaric Acids', *Journal of the American Chemical Society,* 126(41), 13335-13342.

Chokshi, R. and Zia, H. (2010) 'Hot-melt extrusion technique: a review', *Iranian Journal of Pharmaceutical Research*, 3, 3-16.

Chow, S., Chen, M., Shi, L., Chow, A. L. and Sun, C. (2012) 'Simultaneously Improving the Mechanical Properties, Dissolution Performance, and Hygroscopicity of Ibuprofen and Flurbiprofen by Cocrystallization with Nicotinamide', *Pharmaceutical Research,* 29(7), 1854-1865.

Chun, N. H., Wang, I. C., Lee, M. J., Jung, Y. T., Lee, S., Kim, W. S. and Choi, G. J. (2013) 'Characteristics of indomethacin-saccharin (IMC-SAC) cocrystals prepared by an anti-solvent crystallization process', *European Journal Of Pharmaceutics and Biopharmaceutics,* 85(3 Pt B), 854-861.

Crowley, M. M., Zhang, F., Repka, M. A., Thumma, S., Upadhye, S. B., Battu, S. K., McGinity, J. W. and Martin, C. (2007) 'Pharmaceutical applications of hot-melt extrusion: Part I', *Drug Development and Industrial Pharmacy,* 33(9), 909-926.

Daurio, D., Medina, C., Saw, R., Nagapudi, K. and Alvarez-Núñez, F. (2011) 'Application of Twin Screw Extrusion in the Manufacture of Cocrystals, Part I: Four Case Studies', *Pharmaceutics,* 3(3), 582-600.

Davis, T. D., Peck, G. E., Stowell, J. G., Morris, K. R. and Byrn, S. R. (2004) 'Modeling and monitoring of polymorphic transformations during the drying phase of wet granulation', *Pharmaceutical Research,* 21(5), 860-866.

De Beer, T., Burggraeve, A., Fonteyne, M., Saerens, L., Remon, J. P. and Vervaet, C. (2011) 'Near infrared and Raman spectroscopy for the in-process monitoring of pharmaceutical production processes', *International Journal of Pharmaceutics,* 417(1), 32-47.

Desiraju, G. R. (1995) 'Supramolecular Synthons in Crystal Engineering—A New Organic Synthesis', *Angewandte Chemie International Edition in English,* 34(21), 2311-2327.

Dhumal, R. S., Kelly, A. L., York, P., Coates, P. D. and Paradkar, A. (2010) 'Cocrystalization and simultaneous agglomeration using hot melt extrusion', *Pharmaceutical Research,* 27(12), 2725-2733.

Dierickx, L., Saerens, L., Almeida, A., De Beer, T., Remon, J. P. and Vervaet, C. (2012) 'Co-extrusion as manufacturing technique for fixed-dose combination mini-matrices', *European Journal of Pharmaceutics and Biopharmaceutics,* 81(3), 683-689.

DiNunzio, J. C., Brough, C., Hughey, J. R., Miller, D. A., Williams Iii, R. O. and McGinity, J. W. (2010) 'Fusion production of solid dispersions containing a heat-sensitive active ingredient by hot melt extrusion and Kinetisol® dispersing', *European Journal of Pharmaceutics and Biopharmaceutics,* 74(2), 340-351.

Douroumis, D. (2012) *Hot-Melt Extrusion: Pharmaceutical Applications,* John Wiley & Sons, UK.

Douroumis, D. D., Gryczke, A. and Schminke, S. (2011) 'Development and evaluation of cetirizine HCl taste-masked oral disintegrating tablets', *AAPS PharmSciTech,* 12(1), 141-151.

Dreiblatt, A. (2012) 'Technological Considerations Relates to Scale-up of Hot-melt Extrusion Processes' in Douroumis, D., ed. *Hot-Melt Extrusion: Pharmaceutical Applications*, John Wiley & Sons UK.

Eddleston, M. D., Patel, B., Day, G. M. and Jones, W. (2013) 'Cocrystallization by Freeze-Drying: Preparation of Novel Multicomponent Crystal Forms', *Crystal Growth & Design,* 13(10), 4599-4606.

Elder, D. P., Holm, R. and Diego, H. L. (2013) 'Use of pharmaceutical salts and cocrystals to address the issue of poor solubility', *International Journal of Pharmaceutics,* 453(1), 88-100.

Elqidra, R., Unlu, N., Capan, Y., Sahin, G., Dalkara, T. and Hincal, A. A. (2004) 'Effect of polymorphism on in vitro in vivo properties of carbamazepine conventional tablets', *Journal of Drug Delivery Science and Technology,* 14(2), 147-153.

'Esteve R&D Portfolio', (2013) *E-58425 : Increased magnitude of efficacy without increasing side effects.* [online] Availbale from: http://www.esteve.es/EsteveFront/CargarPagina.do?pagina=idi_rd_portfolio_E-58425.jsp&div=idi&lng=en

FDA (2004) 'Guidance for Industry PAT — A Framework for Innovative Pharmaceutical Development, Manufacturing, and Quality Assurance. [online] Available from: http://www.fda.gov/downloads/Drugs/Guidances/ucm070305.pdf

FDA (2013) 'Guidance for Industry: Regulatory Classification of Pharmaceutical Cocrystals. [online] Available from: www.fda.gov/downloads/drugs/guidancecomplianceregulatoryinformation/guidances/ucm281764.pdf

Fleischman, S. G., Kuduva, S. S., McMahon, J. A., Moulton, B., Bailey Walsh, R. D., Rodríguez-Hornedo, N. and Zaworotko, M. J. (2003) 'Crystal Engineering of the Composition of Pharmaceutical Phases: Multiple-Component Crystalline Solids Involving Carbamazepine', *Crystal Growth & Design,* 3(6), 909-919.

Friscic, T. and Jones, W. (2007) 'Cocrystal architecture and properties: design and building of chiral and racemic structures by solid-solid reactions', *Faraday Discussions,* 136(0), 167-178.

Friščić, T. and Jones, W. (2009) 'Recent Advances in Understanding the Mechanism of Cocrystal Formation via Grinding', *Crystal Growth & Design,* 9(3), 1621-1637.

FSA (2013) Current EU approved additives and their E Numbers. [online] Available from: https://www.food.gov.uk/science/additives/enumberlist.

Fucke, K., Myz, S. A., Shakhtshneider, T. P., Boldyreva, E. V. and Griesser, U. J. (2012) 'How good are the crystallisation methods for cocrystals? A comparative study of piroxicam', *New Journal of Chemistry,* 36(10), 1969-1977.

Fukuda, M., Miller, D. A., Peppas, N. A. and McGinity, J. W. (2008) 'Influence of sulfobutyl ether β-cyclodextrin (Captisol®) on the dissolution properties of a poorly soluble drug from extrudates prepared by hot-melt extrusion', *International Journal of Pharmaceutics,* 350(1–2), 188-196.

Fukuda, M., Peppas, N. A. and McGinity, J. W. (2006) 'Properties of sustained release hot-melt extruded tablets containing chitosan and xanthan gum', *International Journal of Pharmaceutics,* 310(1-2), 90-100.

Ghalanbor, Z., Körber, M. and Bodmeier, R. (2012) 'Protein release from poly(lactide-co-glycolide) implants prepared by hot-melt extrusion: Thioester formation as a reason for incomplete release', *International Journal of Pharmaceutics,* 438(1–2), 302-306.

Good, D. J. and Rodríguez-Hornedo, N. r. (2009) 'Solubility Advantage of Pharmaceutical Cocrystals', *Crystal Growth & Design,* 9(5), 2252-2264.

Gryczke, A. (2013) 'Hot-Melt Extrusion Process Design Using Process Analytical Technology' in Repka, M. A., Langley, N. and DiNunzio, J., eds., *Melt Extrusion*, Springer New York, 397-431.

Gryczke, A., Schminke, S., Maniruzzaman, M., Beck, J. and Douroumis, D. (2011) 'Development and evaluation of orally disintegrating tablets (ODTs) containing Ibuprofen granules prepared by hot melt extrusion', *Colloids and Surfaces B: Biointerfaces,* 86(2), 275-284.

Grzesiak, A. L., Lang, M. D., Kim, K. and Matzger, A. J. (2003) 'Comparison of the four anhydrous polymorphs of carbamazepine and the crystal structure of form I', *Journal of Pharmaceutical Science,* 92(11), 2260-2271.

Guo, Z., Ma, M., Wang, T., Chang, D., Jiang, T. and Wang, S. (2011) 'A Kinetic Study of the Polymorphic Transformation of Nimodipine and Indomethacin during High Shear Granulation', *AAPS PharmSciTech,* 12(2), 610-619.

Hickey, M. B., Peterson, M. L., Scoppettuolo, L. A., Morrisette, S. L., Vetter, A., Guzman, H., Remenar, J. F., Zhang, Z., Tawa, M. D., Haley, S., Zaworotko, M. J. and Almarsson, O. (2007) 'Performance comparison of a cocrystal of carbamazepine with

marketed product', *European Journal of Pharmaceutics and Biopharmaceutics,* 67(1), 112-119.

Islam, M. T., Maniruzzaman, M., Halsey, S. A., Chowdhry, B. Z. and Douroumis, D. (2014) 'Development of sustained-release formulations processed by hot-melt extrusion by using a quality-by-design approach', *Drug Delivery and Translational Research*, 4, 377-387.

Javadzadeh, Y., Jafari-Navimipour, B. and Nokhodchi, A. (2007) 'Liquisolid technique for dissolution rate enhancement of a high dose water-insoluble drug (carbamazepine)', *International Journal of Pharmaceutics,* 341(1-2), 26-34.

Jones, W., Motherwell, W. and Trask, A. V. (2006) 'Pharmaceutical cocrystals: an emerging approach to physical property enhancement', *Materials Research Society Bulletin,* 31(11), 875-879.

Jung, M. S., Kim, J. S., Kim, M. S., Alhalaweh, A., Cho, W., Hwang, S. J. and Velaga, S. P. (2010) 'Bioavailability of indomethacin-saccharin cocrystals', *Journal of Pharmacy and Pharmacology,* 62(11), 1560-1568.

Kanzer, J., Hupfeld, S., Vasskog, T., Tho, I., Hölig, P., Mägerlein, M., Fricker, G. and Brandl, M. (2010) 'In situ formation of nanoparticles upon dispersion of melt extrudate formulations in aqueous medium assessed by asymmetrical flow field-flow fractionation', *Journal of Pharmaceutical and Biomedical Analysis,* 53(3), 359-365.

Karki, S., Friščić, T., Fábián, L., Laity, P. R., Day, G. M. and Jones, W. (2009) 'Improving Mechanical Properties of Crystalline Solids by Cocrystal Formation: New Compressible Forms of Paracetamol', *Advanced Materials,* 21(38-39), 3905-3909.

Kobayashi, Y., Ito, S., Itai, S. and Yamamoto, K. (2000) 'Physicochemical properties and bioavailability of carbamazepine polymorphs and dihydrate', *International Journal of Pharmaceutics,* 193(2), 137-146.

Kolter, K., Karl, M, Gryczke, A. 'Hot-Melt Extruion with BASF pharma polymers' (2012), *Extrusion compendium* , BASF Germany.

Kou, W., Cai, C., Xu, S., Wang, H., Liu, J., Yang, D. and Zhang, T. (2011) 'In vitro and in vivo evaluation of novel immediate release carbamazepine tablets: Complexation with hydroxypropyl-beta-cyclodextrin in the presence of HPMC', *International Journal of Pharmaceutics,* 409(1-2), 75-80.

Kulkarni, C., Kelly, A., Kendrick, J., Gough, T. and Paradkar, A. (2013a) 'Mechanism for Polymorphic Transformation of Artemisinin during High Temperature Extrusion', *Crystal Growth & Design,* 13(12), 5157-5161.

Kulkarni, C., Kendrick, J., Kelly, A., Gough, T., Dash, R. C. and Paradkar, A. (2013b) 'Polymorphic transformation of artemisinin by high temperature extrusion', *CrystEngComm,* 15(32), 6297-6300.

Lang, B., McGinity, J. W. and Williams, R. O. (2014) 'Hot-melt extrusion – basic principles and pharmaceutical applications', *Drug Development and Industrial Pharmacy,* 10.3109/03639045.2013.838577, 1-23.

Lee, H. G., Zhang, G. G. Z. and Flanagan, D. R. (2011) 'Cocrystal intrinsic dissolution behavior using a rotating disk', *Journal of Pharmaceutical Science,* 100(5), 1736-1744.

Lefebvre, C. and Guyot-Herman, A. M. (1986) 'Polymorphic Transitions of Carbamazepine During Grinding and Compression', *Drug Development and Industrial Pharmacy,* 12(11-13), 1913-1927.

Legendre, B. and Feutelais, Y. (2004) 'Polymorphic and Thermodynamic Study of Indomethacin', *Journal of Thermal Analysis and Calorimetry,* 76(1), 255-264.

Leister, D., Geilen, T. and Geissler, T. (2012) 'Twin-screw Extruders for Pharmaceutical Hot-melt Extrusion:Technology, Techniques and Practices' in Douroumis, D., ed. *Hot-melt extrusion: Pharmaceutical applications*, John Wiley & Sons UK, 28-42.

Leung, D. H., Lohani, S., Ball, R. G., Canfield, N., Wang, Y., Rhodes, T. and Bak, A. (2012) 'Two Novel Pharmaceutical Cocrystals of a Development Compound – Screening, Scale-up, and Characterization', *Crystal Growth & Design,* 12(3), 1254-1262.

Lin, H.-L., Hsu, P.-C. and Lin, S.-Y. (2013a) 'Theophylline–citric acid cocrystals easily induced by DSC–FTIR microspectroscopy or different storage conditions', *Asian Journal of Pharmaceutical Sciences,* 8(1), 19-27.

Lin, H.-L., Zhang, G.-C., Hsu, P.-C. and Lin, S.-Y. (2013b) 'A portable fiber-optic Raman analyzer for fast real-time screening and identifying cocrystal formation of drug-coformer via grinding process', *Microchemical Journal,* 110(0), 15-20.

Liu, J., Cao, F., Zhang, C. and Ping, Q. (2013) 'Use of polymer combinations in the preparation of solid dispersions of a thermally unstable drug by hot-melt extrusion', *Acta Pharmaceutica Sinica B,* 3(4), 263-272.

Liu, X., Lu, M., Guo, Z., Huang, L., Feng, X. and Wu, C. (2012) 'Improving the Chemical Stability of Amorphous Solid Dispersion with Cocrystal Technique by Hot Melt Extrusion', *Pharmaceutical Research,* 29(3), 806-817.

Loreti, G., Maroni, A., Del Curto, M. D., Melocchi, A., Gazzaniga, A. and Zema, L. (2014) 'Evaluation of hot-melt extrusion technique in the preparation of HPC matrices for prolonged release', *European Journal of Pharmaceutical Sciences,* 52(0), 77-85.

Lu, E., Rodriguez-Hornedo, N. and Suryanarayanan, R. (2008) 'A rapid thermal method for cocrystal screening', *CrystEngComm,* 10(6), 665-668.

Luker, K. (2012) 'Single-screw Extrusion: Principles' in Douroumis, D., ed. *Hot-melt extrusion: Pharmaceutical applications*, John Wiley & Sons UK.

Madan, S. and Madan, S. (2012) 'Hot melt extrusion and its pharmaceutical applications', *Asian Journal of Pharmaceutical Sciences,* 7(2), 123-133.

Maniruzzaman, M. (2012) *Development of hot-melt extrusion as a novel technique for the formulation of oral solid dosage forms*, (PhD Thesis), University of Greenwich UK.

Maniruzzaman, M., Boateng, J. S., Bonnefille, M., Aranyos, A., Mitchell, J. C. and Douroumis, D. (2012a) 'Taste masking of paracetamol by hot-melt extrusion: An in vitro and in vivo evaluation', *European Journal of Pharmaceutics and Biopharmaceutics,* 80(2), 433-442.

Maniruzzaman, M., Boateng, J. S., Snowden, M. J. and Douroumis, D. (2012b) 'A review of hot-melt extrusion: process technology to pharmaceutical products', *International Scholarly Research Notices,* 2012.

Mcmohan, J. A. (2006) *Crystal engineering of novel pharmaceutical forms*, (Master of Science Thesis), University of South Florida.

McNamara, D., Childs, S., Giordano, J., Iarriccio, A., Cassidy, J., Shet, M., Mannion, R., O'Donnell, E. and Park, A. (2006) 'Use of a Glutaric Acid Cocrystal to Improve Oral Bioavailability of a Low Solubility API', *Pharmaceutical Research,* 23(8), 1888-1897.

Medina, C., Daurio, D., Nagapudi, K. and Alvarez-Nunez, F. (2010) 'Manufacture of pharmaceutical cocrystals using twin screw extrusion: A solvent-less and scalable process', *Journal of Pharmaceutical Science,* 99(4), 1693-1696.

Merisko-Liversidge, E., Liversidge, G. G. and Cooper, E. R. (2003) 'Nanosizing: a formulation approach for poorly-water-soluble compounds', *European Journal of Pharmaceutical Sciences,* 18(2), 113-120.

Mididoddi, P. K. and Repka, M. A. (2007) 'Characterization of hot-melt extruded drug delivery systems for onychomycosis', *European Journal of Pharmaceutics and Biopharmaceutics,* 66(1), 95-105.

Miroshnyk, I., Mirza, S. and Sandler, N. (2009) 'Pharmaceutical cocrystals–an opportunity for drug product enhancement', *Expert Opinion on Drug Delivery,* 6(4), 333-341.

Mohammad, M. A., Alhalaweh, A. and Velaga, S. P. (2011) 'Hansen solubility parameter as a tool to predict cocrystal formation', *International Journal of Pharmaceutics,* 407(1-2), 63-71.

Mollan, M. (2003) 'Historical Overview' in Ghebre-Sellassie, I. and Charles, M., eds., *Pharmaceutical extrusion technology*, CRC Press.

Moneghini, M., Voinovich, D., Perissutti, B. and Princivalle, F. (2002) 'Action of carriers on carbamazepine dissolution', *Pharmaceutical Development and Technology,* 7(3), 289-296.

Moradiya, H., Islam, M. T., Woollam, G. R., Slipper, I. J., Halsey, S., Snowden, M. J. and Douroumis, D. (2014a) 'Continuous Cocrystallization for Dissolution Rate Optimization of a Poorly Water-Soluble Drug', *Crystal Growth & Design,* 14(1), 189-198.

Moradiya, H. G. and Douroumis, D. (2014) *Continuous solidification of L-SMEDDS by using a twin screw extruder,* presented at the APS PharmSci conference, University of Hertfordshire.

Moradiya, H. G., Islam, M. T., Halsey, S., Maniruzzaman, M., Chowdhry, B. Z., Snowden, M. J. and Douroumis, D. (2014b) 'Continuous cocrystallisation of carbamazepine and trans-cinnamic acid via melt extrusion processing', *CrystEngComm,* 16(17), 3573-3583.

Nair, R., Gonen, S. and Hoag, S. W. (2002) 'Influence of polyethylene glycol and povidone on the polymorphic transformation and solubility of carbamazepine', *International Journal of Pharmaceutics,* 240(1-2), 11-22.

Nokhodchi, A., Bolourtchian, N. and Dinarvand, R. (2005) 'Dissolution and mechanical behaviors of recrystallized carbamazepine from alcohol solution in the presence of additives', *Journal of Crystal Growth,* 274(3–4), 573-584.

Noyes, A. A. and Whitney, W. R. (1897) 'The rate of solution of solid substances in their own solutions', *Journal of the American Chemical Society,* 19(12), 930-934.

O'Donnell, K. and Williams, R., III (2012) 'Optimizing the Formulation of Poorly Water-Soluble Drugs' in Williams Iii, R. O., Watts, A. B. and Miller, D. A., eds., *Formulating Poorly Water Soluble Drugs*, Springer New York, 27-93.

Otsuka, M., Hasegawa, H. and Matsuda, Y. (1997) 'Effect of polymorphic transformation during the extrusion-granulation process on the pharmaceutical properties of carbamazepine granules', *Chemical & Pharmaceutical Bulletin,* 45(5), 894-898.

Otsuka, M., Hasegawa, H. and Matsuda, Y. (1999) 'Effect of polymorphic forms of bulk powders on pharmaceutical properties of carbamazepine granules', *Chemical & Pharmaceutical Bulletin,* 47(6), 852-856.

Otun, S. O. (2011) *Characterisation and performance assessment of semi-solid dispersions using surface active lipidic carriers*, (PhD Thesis) University of East Anglia.

Padrela, L., Rodrigues, M. A., Velaga, S. P., Fernandes, A. C., Matos, H. A. and de Azevedo, E. G. (2010) 'Screening for pharmaceutical cocrystals using the supercritical fluid enhanced atomization process', *The Journal of Supercritical Fluids,* 53(1–3), 156-164.

Padrela, L., Rodrigues, M. A., Velaga, S. P., Matos, H. A. and de Azevedo, E. G. (2009) 'Formation of indomethacin-saccharin cocrystals using supercritical fluid technology', *European Journal of Pharmaceutical Sciences,* 38(1), 9-17.

Patil, H., Kulkarni, V., Majumdar, S. and Repka, M. A. (2014) 'Continuous manufacturing of solid lipid nanoparticles by hot melt extrusion', *International Journal of Pharmaceutics,* 471(1–2), 153-156.

Plumb, K. (2005) 'Continuous Processing in the Pharmaceutical Industry: Changing the Mind Set', *Chemical Engineering Research and Design,* 83(6), 730-738.

Porter III, W. W., Elie, S. C. and Matzger, A. J. (2008) 'Polymorphism in Carbamazepine Cocrystals', *Crystal Growth & Design,* 8(1), 14-16.

Prajapati, S. T., Gohel, M. C. and Patel, L. D. (2007) 'Studies to enhance dissolution properties of carbamazepine', *Indian Journal of Pharmaceutical Sciences,* 69(3), 427.

Proctor, L., Dunn, P. J., Hawkins, J. M., Wells, A. S. and Williams, M. T. (2010) 'Continuous processing in the pharmaceutical industry', *Green Chemistry in the Pharmaceutical Industry*, 221-242.

Qiu, Y. (2009) *Developing Solid Oral Dosage Forms: Pharmaceutical Theory and Practice, Developing Solid Oral Dosage Forms: Pharmaceutical Theory and Practice.* Academic Press USA.

Quinten, T., Beer, T. D., Vervaet, C. and Remon, J. P. (2009) 'Evaluation of injection moulding as a pharmaceutical technology to produce matrix tablets', *European Journal of Pharmaceutics and Biopharmaceutics,* 71(1), 145-154.

Rane, Y., Mashru, R., Sankalia, M. and Sankalia, J. (2007) 'Effect of hydrophilic swellable polymers on dissolution enhancement of carbamazepine solid dispersions studied using response surface methodology', *AAPS PharmSciTech,* 8(2), E1 -E11.

Reboul, J. P., Cristau, B., Soyfer, J. C. and Astier, J. P. (1981) '5H-Dibenz[b,f]azepinecarboxamide-5 (carbamazepine)', *Acta Crystallographica Section B,* 37(10), 1844-1848.

Repka, M. A., Battu, S. K., Upadhye, S. B., Thumma, S., Crowley, M. M., Zhang, F., Martin, C. and McGinity, J. W. (2007) 'Pharmaceutical applications of hot-melt extrusion: Part II', *Drug Development and Industrial Pharmacy,* 33(10), 1043-1057.

Rubinstein, A. (2010) 'Gastrointestinal anatomy, physiology and permeation pathways', *Enhancement in drug delivery,* 4-28.

Rustichelli, C., Gamberini, G., Ferioli, V., Gamberini, M. C., Ficarra, R. and Tommasini, S. (2000) 'Solid-state study of polymorphic drugs: carbamazepine', *Journal of Pharmaceutical and Biomedical Analysis,* 23(1), 41-54.

Saerens, L., Dierickx, L., Lenain, B., Vervaet, C., Remon, J. P. and De Beer, T. (2011) 'Raman spectroscopy for the in-line polymer-drug quantification and solid state characterization during a pharmaceutical hot-melt extrusion process', *European Journal of Pharmaceutics and Biopharmaceutics,* 77(1), 158-163.

Saharan, V., Kukkar, V., Kataria, M., Gera, M. and Choudhury, P. K. (2009) 'Dissolution enhancement of drugs. Part I: technologies and effect of carriers', *International Journal of Health Research,* 2(2), 107-124.

Sanphui, P., Goud, N. R., Khandavilli, U. B. R. and Nangia, A. (2011) 'Fast Dissolving Curcumin Cocrystals', *Crystal Growth & Design,* 11(9), 4135-4145.

Schaber, S. D., Gerogiorgis, D. I., Ramachandran, R., Evans, J. M. B., Barton, P. I. and Trout, B. L. (2011) 'Economic Analysis of Integrated Continuous and Batch Pharmaceutical Manufacturing: A Case Study', *Industrial & Engineering Chemistry Research,* 50(17), 10083-10092.

Schultheiss, N. and Newman, A. (2009) 'Pharmaceutical Cocrystals and Their Physicochemical Properties', *Crystal Growth & Design,* 9(6), 2950-2967.

Scott, B. and Wilcock, A. (2006) 'Process Analytical Technology in the Pharmaceutical Industry: A Toolkit for Continuous Improvement', *PDA Journal of Pharmaceutical Science and Technology,* 60(1), 17-53.

Sekhon, B. (2009) 'Pharmaceutical cocrystals - a review', *ARS Pharmaceutica,* 50(3), 99-117.

Sekhon, B. S. (2012) 'Drug-drug cocrystals', *DARU Journal of Pharmaceutical Sciences,* 20(1), 45.

Serajuddin, A. T. M. (2007) 'Salt formation to improve drug solubility', *Advanced Drug Delivery Reviews,* 59(7), 603-616.

Shayanfar, A., Asadpour-Zeynali, K. and Jouyban, A. (2013) 'Solubility and dissolution rate of a carbamazepine–cinnamic acid cocrystal', *Journal of Molecular Liquids,* 187, 171-176.

Sheikh, A. Y., Rahim, S. A., Hammond, R. B. and Roberts, K. J. (2009) 'Scalable solution cocrystallization: case of carbamazepine-nicotinamide I', *CrystEngComm,* 11(3), 501-509.

Shiraki, K., Takata, N., Takano, R., Hayashi, Y. and Terada, K. (2008) 'Dissolution improvement and the mechanism of the improvement from cocrystallization of poorly water-soluble compounds', *Pharmaceutical Research,* 25(11), 2581-2592.

Silva, A. F., Burggraeve, A., Denon, Q., Van der Meeren, P., Sandler, N., Van Den Kerkhof, T., Hellings, M., Vervaet, C., Remon, J. P., Lopes, J. A. and De Beer, T. (2013) 'Particle sizing measurements in pharmaceutical applications: comparison of in-process methods versus off-line methods', *European Journal of Pharmaceutical Sciences,* 85(3 Pt B), 1006-1018.

Singhal, S., Lohar, V. and Arora, V. (2011) 'Hot melt extrusion technique', *WebmedCentralPharmaceutical Sciences* 2011;2(1): WMC001459, DOI: 10.9754/journal.wmc.2011.001459

Sreekanth, B. R., Vishweshwar, P. and Vyas, K. (2007) 'Supramolecular synthon polymorphism in 2 : 1 cocrystal of 4-hydroxybenzoic acid and 2,3,5,6-tetramethylpyrazine', *Chemical Communications,* (23), 2375-2377.

Smith, A. J., Kim, S.-H., Duggirala, N. K., Jin, J., Wojtas, L., Ehrhart, J., Giunta, B., Tan, J., Zaworotko, M. J. and Shytle, R. D. (2013) 'Improving Lithium Therapeutics by Crystal Engineering of Novel Ionic Cocrystals', *Molecular Pharmaceutics,* 10(12), 4728-4738.

Stahly, G. P. (2009) 'A Survey of Cocrystals Reported Prior to 2000', *Crystal Growth & Design,* 9(10), 4212-4229.

Stanton, M. K. and Bak, A. (2008) 'Physicochemical Properties of Pharmaceutical Cocrystals: A Case Study of Ten AMG 517 Cocrystals', *Crystal Growth & Design,* 8(10), 3856-3862.

Steed, J. W. (2013) 'The role of cocrystals in pharmaceutical design', *Trends in Pharmacological Sciences,* 34(3), 185-193.

Sun, C. C. (2012) 'Cocrystallization for successful drug delivery', *Expert Opinion on Drug Delivery,* 10(2), 201-213.

Sun, C. C. and Hou, H. (2008) 'Improving Mechanical Properties of Caffeine and Methyl Gallate Crystals by Cocrystallization', *Crystal Growth & Design,* 8(5), 1575-1579.

Sun, C. Q. and Grant, D. J. W. (2001) 'Influence of crystal structure on the tableting properties of sulfamerazine polymorphs', *Pharmaceutical Research,* 18(3), 274-280.

Talukder, R., Reed, C., Durig, T. and Hussain, M. (2011) 'Dissolution and solid-state characterization of poorly water-soluble drugs in the presence of a hydrophilic carrier', *AAPS PharmSciTech,* 12(4), 1227-1233.

Taylor, L. S. and Zografi, G. (1997) 'Spectroscopic characterization of interactions between PVP and indomethacin in amorphous molecular dispersions', *Pharmaceutical Research,* 14(12), 1691-1698.

Thakuria, R., Delori, A., Jones, W., Lipert, M. P., Roy, L. and Rodríguez-Hornedo, N. (2013) 'Pharmaceutical cocrystals and poorly soluble drugs', *International Journal of Pharmaceutics,* 453(1), 101-125.

Tian, F., Sandler, N., Aaltonen, J., Lang, C., Saville, D. J., Gordon, K. C., Strachan, C. J., Rantanen, J. and Rades, T. (2007) 'Influence of polymorphic form, morphology, and excipient interactions on the dissolution of carbamazepine compacts', *Journal of Pharmaceutical Science,* 96(3), 584-594.

Tian, F., Saville, D. J., Gordon, K. C., Strachan, C. J., Zeitler, J. A., Sandler, N. and Rades, T. (2007) 'The influence of various excipients on the conversion kinetics of

carbamazepine polymorphs in aqueous suspension', *Journal of Pharmacology and Pharmacotherapeutics,* 59(2), 193-201.

Tomaszewska, I., Karki, S., Shur, J., Price, R. and Fotaki, N. (2013) 'Pharmaceutical characterisation and evaluation of cocrystals: Importance of in vitro dissolution conditions and type of coformer', *International Journal of Pharmaceutics,* 453(2), 380-388.

Trask, A. V. and Jones, W. (2005) 'Crystal engineering of organic cocrystals by the solid-state grinding approach', *Organic Solid State Reactions,* 254, 41-70.

Trask, A. V., Motherwell, W. D. S. and Jones, W. (2004) 'Solvent-drop grinding: green polymorph control of cocrystallisation', *Chemical Communications,* (7), 890-891.

Trask, A. V., Motherwell, W. D. S. and Jones, W. (2005) 'Pharmaceutical Cocrystallization: Engineering a Remedy for Caffeine Hydration', *Crystal Growth & Design,* 5(3), 1013-1021.

Trask, A. V., Motherwell, W. D. S. and Jones, W. (2006) 'Physical stability enhancement of theophylline via cocrystallization', *International Journal of Pharmaceutics,* 320(1–2), 114-123.

Trey, S. M., Wicks, D. A., Mididoddi, P. K. and Repka, M. A. (2007) 'Delivery of itraconazole from extruded HPC films', *Drug Development and Industrial Pharmacy,* 33(7), 727-735.

Verreck, G. (2012) 'The influence of plasticezers in hot-melt extrusion' in Douroumis, D., ed. *Hot-Melt Extrusion: Pharmaceutical Applications*, John Wiley & Sons UK, 93-107.

Verreck, G., Decorte, A., Li, H., Tomasko, D., Arien, A., Peeters, J., Rombaut, P., Van den Mooter, G. and Brewster, M. E. (2006) 'The effect of pressurized carbon dioxide as a plasticizer and foaming agent on the hot melt extrusion process and extrudate properties of pharmaceutical polymers', *The Journal of Supercritical Fluids,* 38(3), 383-391.

Vervaet, C. and Remon, J. P. (2005) 'Continuous granulation in the pharmaceutical industry', *Chemical Engineering Science,* 60(14), 3949-3957.

Vippagunta, S. R., Brittain, H. G. and Grant, D. J. (2001) 'Crystalline solids', *Advanced Drug Delivery Reviews,* 48(1), 3-26.

Vishweshwar, P., McMahon, J. A., Bis, J. A. and Zaworotko, M. J. (2006) 'Pharmaceutical cocrystals', *Journal of Pharmaceutical Science,* 95(3), 499-516.

Vithani, K., Maniruzzaman, M., Slipper, I. J., Mostafa, S., Miolane, C., Cuppok, Y., Marchaud, D. and Douroumis, D. (2013) 'Sustained release solid lipid matrices processed by hot-melt extrusion (HME)', *Colloids and Surfaces B-Biointerfaces,* 110, 403-410.

Vynckier, A. K., Dierickx, L., Saerens, L., Voorspoels, J., Gonnissen, Y., De Beer, T., Vervaet, C. and Remon, J. P. (2014) 'Hot-melt co-extrusion for the production of fixed-dose combination products with a controlled release ethylcellulose matrix core', *International Journal of Pharmaceutics,* 464(1–2), 65-74.

Wang, M., Rutledge, G. C., Myerson, A. S. and Trout, B. L. (2012) 'Production and characterization of carbamazepine nanocrystals by electrospraying for continuous pharmaceutical manufacturing', *Journal of Pharmaceutical Science,* 101(3), 1178-1188.

Wildi, R. H. and Maier, C. (1998) *Understanding compounding,* Hanser Publishers USA.

Wöhler, F. (1844) 'Untersuchungen über das chinon', *Annalen der Chemie und Pharmacie,* 51, 145-163.

Yadav, A. V., Shete, A. S., Dabke, A. P., Kulkarni, P. V. and Sakhare, S. S. (2009) 'Cocrystals: a novel approach to modify physicochemical properties of active pharmaceutical ingredients', *Indian Journal of Pharmaceutical Sciences,* 71(4), 359-370.

Zegarac, M., Leksic, E., Sket, P., Plavec, J., Devcic Bogdanovic, M., Bucar, D.-K., Dumic, M. and Mestrovic, E. (2014) 'A sildenafil cocrystal based on acetylsalicylic acid exhibits an enhanced intrinsic dissolution rate', *CrystEngComm,* 16(1), 32-35.

Zhang, F. and McGinity, J. W. (1999) 'Properties of sustained-release tablets prepared by hot-melt extrusion', *Pharmaceutical Development and Technology,* 4(2), 241-250.

Zhang, G. C., Lin, H. L. and Lin, S. Y. (2012) 'Thermal analysis and FTIR spectral curve-fitting investigation of formation mechanism and stability of indomethacin-saccharin cocrystals via solid-state grinding process', *Journal of Pharmaceutical and Biomedical Analysis,* 66, 162-169.

Zhao, L., Raval, V., Briggs, N. E. B., Bhardwaj, R. M., McGlone, T., Oswald, I. D. H. and Florence, A. J. (2014) 'From discovery to scale-up: α-lipoic acid∶nicotinamide cocrystals in a continuous oscillatory baffled crystalliser', *CrystEngComm,* 16(26), 5769.

APPENDIX
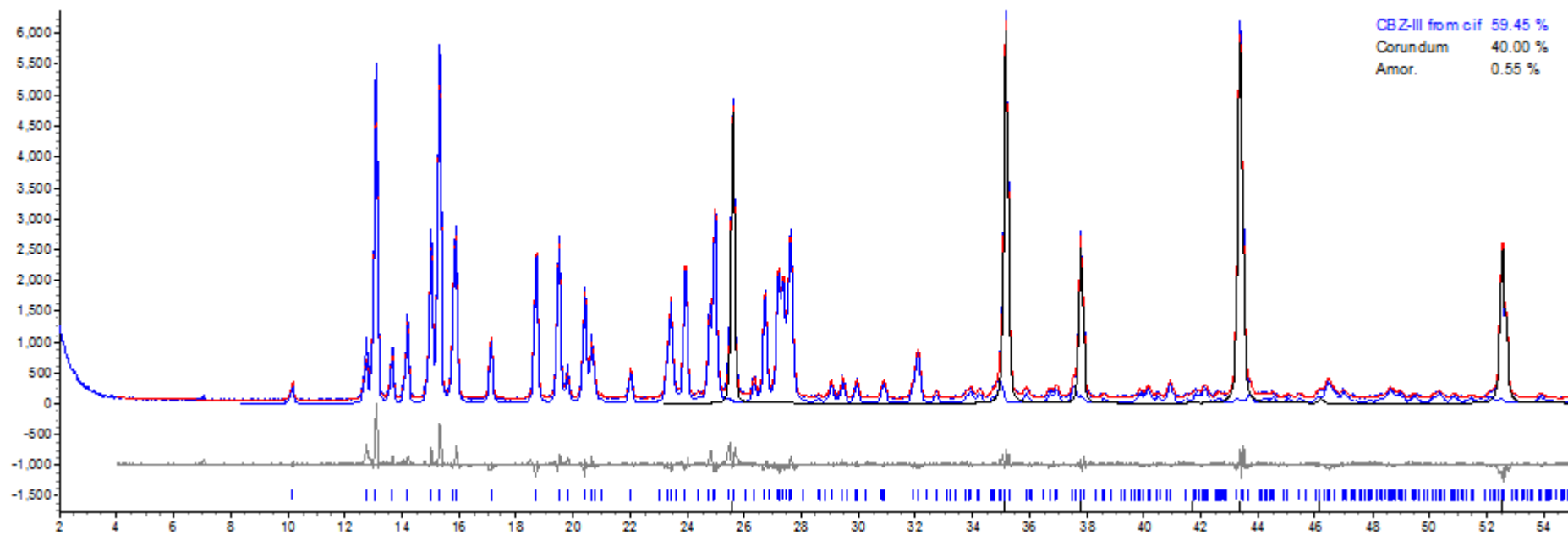
Fig. S1. Rietveld refinement result for the spiked sample of Pure CBZ-III (CCDS Ref: CBMZPNO1; Reboul et al., 1981).
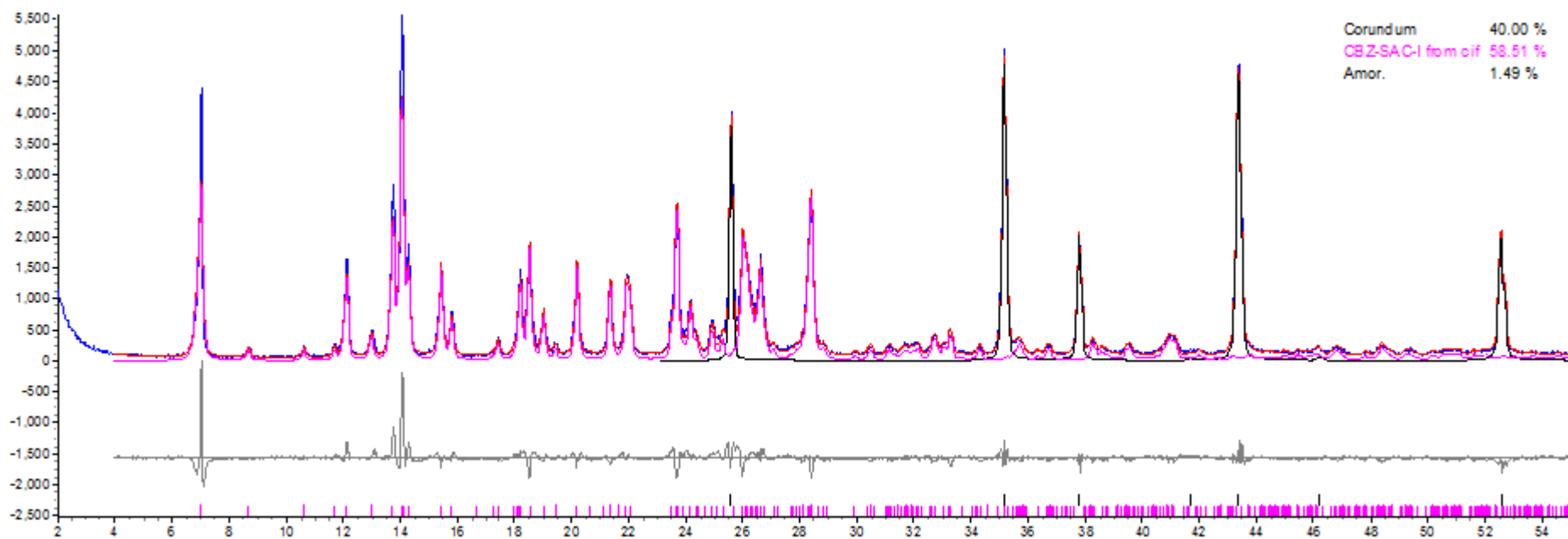
Fig. S2. Rietveld refinement result for the spiked sample of CBZ-SCH cocrystals processed at 135°C, 10 rpm by using TSE.(CIF file CCDS Ref: UNEZAO; Fleischmann et al., 2003).
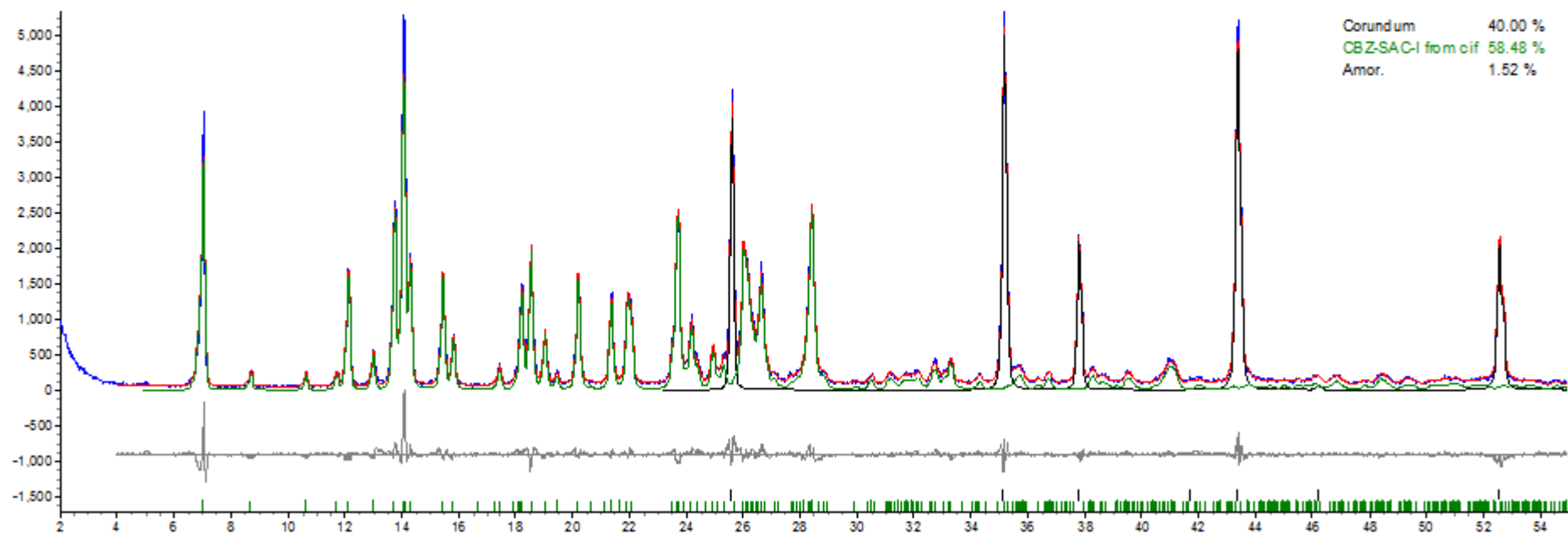
Fig. S3. Rietveld refinement result for the spiked sample of CBZ-SCH cocrystals processed at 135°C, 5 rpm by using TSE.
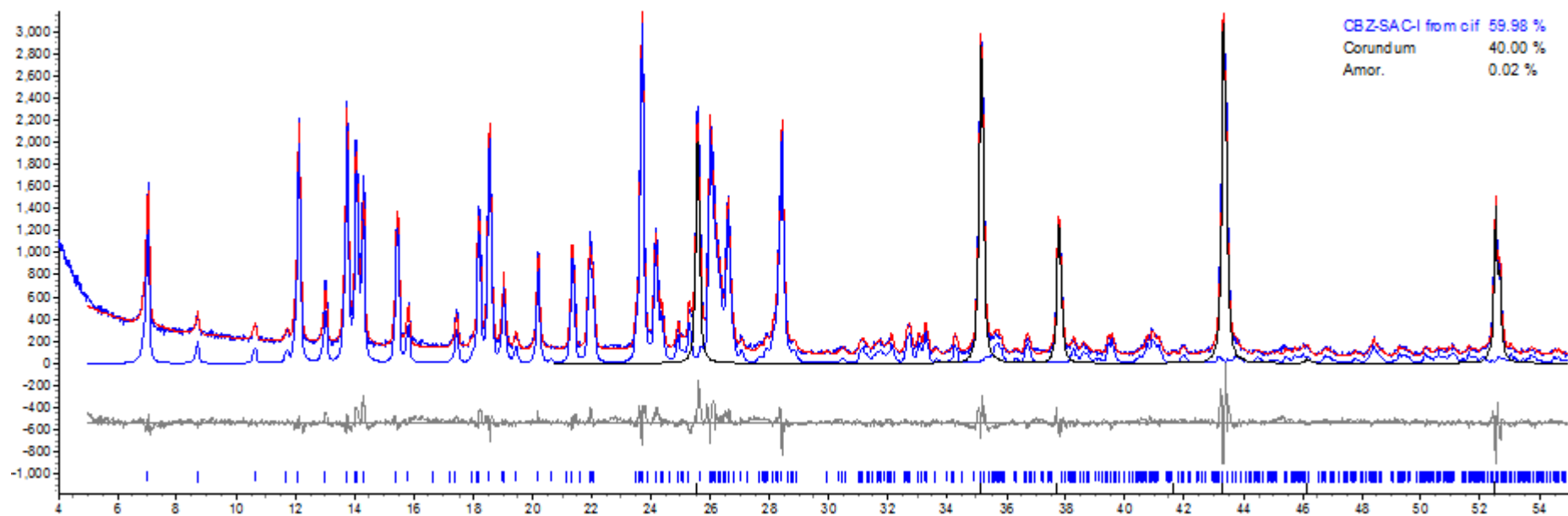
Fig. S4. Rietveld refinement result for the spiked sample of CBZ-SCH Prototype cocrystals prepared by solvent method.
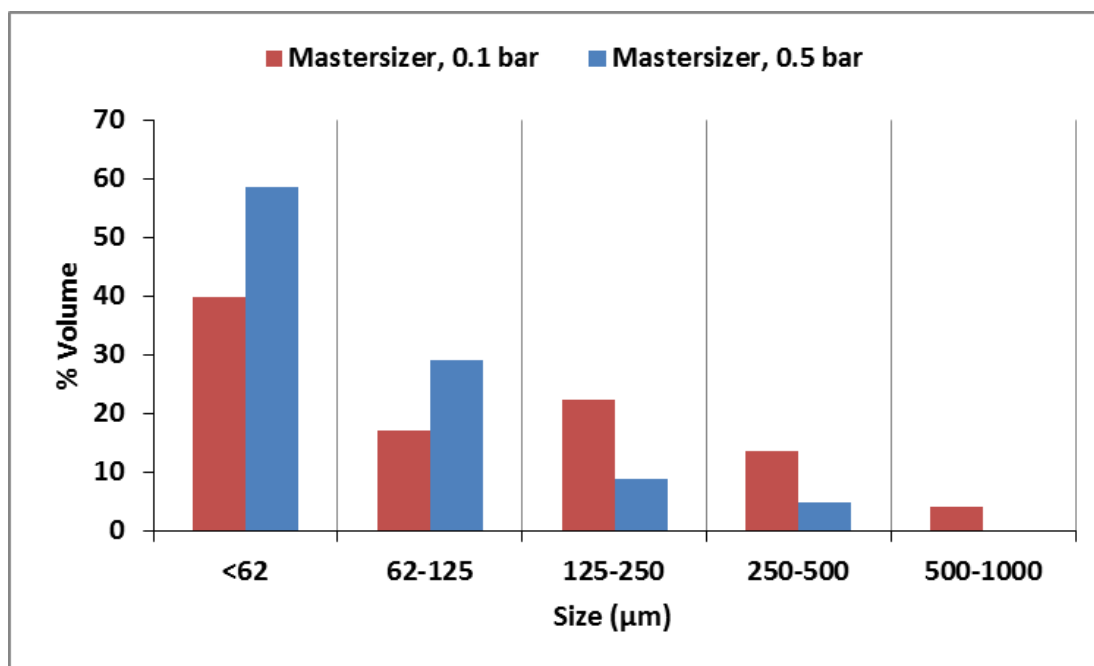
Fig. S5. Particle size distribution by using off-line Mastersizer (at 0.1 and 0.5 bar pressure) for milled cocrystals of 165°C-30 rpm.